

# The Development and Implementation of a Localised Position Location Strategy

by  
Willem Petrus Francois Schonken

*Thesis presented in partial fulfilment of the requirements  
for the degree of Master of Science in Engineering  
at the University of Stellenbosch*



Supervisor: Prof. Johann B. de Swardt  
Faculty of Engineering  
Department of Electrical and Electronic Engineering

December 2010

## **Declaration**

By submitting this thesis electronically, I declare that the work contained therein is my own original work and that I have not previously in its entirety or in part submitted it at any university for a degree.

December 2010

Copyright ©2010 Stellenbosch University

All rights reserved

## **Abstract**

Location and tracking of personnel and assets is a lucrative enterprise that has seen much expansion in the last decade or two. This expansion is coupled with the rise in popularity of GPS-based technologies. It has become common practice for businesses to track and manage vehicle fleets with GPS enabled devices. We use GPS to navigate while driving our cars, to keep track of our loved ones and we even have GPS receivers in our cell phones.

Unfortunately, GPS technology has a few limitations. It can only be used in areas with a clear view of the sky, as line-of-sight must be maintained with at least four satellites at all times. This precludes the use of GPS indoors or in heavily built-up areas. GPS receivers are also still quite expensive.

This thesis developed and implemented a strategy for Localised Position Location. Several possible solutions were investigated. Spread Spectrum was selected as the best method to develop into a working example. The characteristics of Spread Spectrum signals and Pseudo-Noise Codes were investigated in some detail, which led to the proposal of several simulation models. These simulations suggested that a simple configuration consisting of a transmitter, sliding correlator, bandpass filter and RF power detector can effectively track a stationary target.

A transmitter was designed and implemented and was then used in a simplified measurement to corroborate the predictions made by earlier simulations. With results looking positive it was decided to continue with the design and implementation of a receiver. A complete transmitter/receiver system allowed for extensive measurements to be made. The physical measurements agreed with simulated predictions, confirming that the proposed position location strategy is effective.

## Opsomming

Die toenemende gewildheid en toeganklikheid van GPS-gebaseerde opsporingstegnologie het gelei tot 'n geweldige toename in die verkope van toerusting om die beweging van besigheidsbates te monitor en bestuur. Selfs op die persoonlike ontspanningsmark vind GPS-tegnologie toenemend aanklank met vervaardigers van selfone en voertuignavigasietoerusting.

GPS-gebaseerde opsporingstegnologie het egter beperkinge, omdat dit te alle tye direkte oogkontak moet behou met minstens vier satelliete. Gevolglik kan GPS-gebaseerde opsporingstegnologie nie binnenshuis of in erg beboude gebiede gebruik word nie. GPS ontvangers is ook redelik duur.

Hierdie tesis het 'n strategie vir Gelokaliseerde Posisie Bepaling ontwikkel en geïmplementeer. Ondersoek is ingestel na 'n verskeidenheid van moontlike oplossings. Strek Spektrum is gekies as die beste metode om verder in 'n werkende voorbeeld te ontwikkel. Die eienskappe van Strek Spektrum seine en Pseudo-Ruis Kodes is in detail bestudeer, wat gelei het na die opstelling van 'n aantal simulasiemodelle. Hierdie modelle dui aan dat 'n eenvoudige opstelling, bestaande uit 'n sender, glykorellator, banddeurlaat filter en 'n RF drywingsmeter doeltreffend aangewend kan word om 'n stilstande teiken te monitor.

'n Sender, wat in 'n vereenvoudigde meetopstelling gebruik kon word om van die voorspellings wat vroeër gemaak is te staaf, is hierna ontwerp en gebou. Met positiewe resultate is daar besluit om voort te gaan met die ontwerp en bou van 'n ontvanger. Met 'n volledige sender/ontvanger stelsel was dit moontlik om uitgebreide meetings te neem. Die fisiese meetings stem ooreen met die simulasiestoelvoorspellings, wat dien as bevestiging dat die voorgestelde strategie vir posisie bepaling doeltreffend aangewend kan word.

## **Acknowledgements**

I would like to express my sincerest gratitude towards Prof. J.B. de Swardt. Your guidance, experience and especially your patience has been invaluable to me.

I would also like to thank my parents. Your support, both financial and emotional, made this thesis a reality.

*I must not fear.*

Fear is the mind-killer.

Fear is the little-death that brings total obliteration.

I will face my fear.

I will permit it to pass over me and through me.

And when it has gone past I will turn the inner eye to see its path.

Where the fear has gone there will be nothing.

Only I will remain

- *The Litany against Fear*

(from the novel *Dune*, by Frank Herbert)

# Contents

List of Figures .....	ix
List of Tables .....	xi
List of Abbreviations .....	xii
Chapter 1:	
Introduction .....	1
1.1    A Short History of Navigation .....	1
1.2    Problem Statement .....	2
1.3    Proposed Solution .....	2
1.4    Layout of this Thesis .....	3
Chapter 2:	
Literature Study .....	5
2.1    Terminology .....	5
2.2    Possible solutions .....	9
2.2.1    Measured Signal Strength as an Indication of Distance .....	9
2.2.2    Difference in Phase as an Indication of Distance .....	10
2.2.3    Using Spread Spectrum Signals to Determine Distance .....	10
2.2.4    Other techniques .....	12
2.3    Conclusion .....	13
Chapter 3:	
Strategy Development .....	14
3.1    System Configuration .....	14
3.2    Ranging Signal Characteristics .....	15
3.3    Strategy Proposal .....	20
3.4    Basic Layout .....	23
3.4.1    Transmitter .....	23
3.4.2    Receiver .....	24
Chapter 4:	
Transmitter Design .....	26
4.1    PN Code Generator .....	26

4.1.1	Shift Register Sequences.....	27
4.1.2	Design Parameters for MLSR Configurations.....	29
4.1.3	Implementation.....	32
4.2	RF Interface and Peripheral Circuits.....	33
4.2.1	Peripheral Circuits .....	33
4.2.2	RF Interface.....	33
4.3	Experimental Measurements .....	34
4.3.1	PN Code Signal Characteristics.....	34
4.3.2	Corroborating Measurements .....	38
Chapter 5:		
Receiver Design.....		42
5.1	Basic Layout .....	42
5.2	RF Frontend .....	43
5.2.1	Antenna .....	45
5.2.2	LNA .....	46
5.2.3	Mixer.....	48
5.2.4	Local Oscillator .....	49
5.2.5	Amplifiers and Filters.....	52
5.3	PN Code Generator .....	54
5.3.1	Frequency Divider .....	55
5.3.2	PN Code Generator .....	57
5.4	Mixer, Filter and Power Detector .....	58
5.4.1	Mixer.....	58
5.4.2	Filter.....	58
5.4.3	RF Power Detector .....	60
5.4.4	Summary.....	61
5.5	Digital Processor and Peripheral Circuits .....	61
5.5.1	Power Supply .....	61
5.5.2	Oscillator.....	62
5.5.3	Serial Communication.....	62
5.5.4	Central Processor .....	63
5.6	Embedded Software.....	65



5.6.1	Setup Procedures .....	66
5.6.2	Measurement Algorithms.....	66
Chapter 6:		
System Measurements.....		70
6.1	Basic Correlation Measurement .....	70
6.2	PN Code Tracking Measurement .....	72
6.3	Cable Length Measurement .....	75
6.4	Time-Difference-of-Arrival Measurement.....	78
6.5	Discussion of Results .....	80
6.6	Evaluation of Project Success .....	81
Chapter 7:		
Conclusion and Recommendations.....		83
7.1	Conclusion .....	83
7.2	Recommendations and Further Study .....	83
Appendix A:		
Additional ADF7011 Information .....		85
A.1	Power Supply and Microprocessor .....	85
A.2	Crystal Resonator.....	86
A.3	Loop Filter.....	86
A.4	Matching Circuit.....	87
A.5	Additional Components.....	88
A.6	Register Setup.....	88
Appendix B:		
Receiver Schematics and PCB Layout .....		91
B.1	Receiver Schematics.....	91
B.2	PCB Layout: Top Layer.....	93
B.3	PCB Layout: Bottom Layer.....	94
Bibliography.....		95

## List of Figures

Figure 2.1 A basic diagram describing Triangulation.....	5
Figure 2.2 A basic diagram describing Trilateration.....	6
Figure 2.3 A basic diagram describing Multilateration.....	7
Figure 2.4 Graph showing the autocorrelation function of a PN Code sequence .....	11
Figure 3.1 A diagram illustrating system configuration.....	15
Figure 3.2 A graph showing an example of a PN Code signal's structure .....	16
Figure 3.3 The Simulink model used to generate the signal shown in Figure 3.2.....	16
Figure 3.4 An example of a PN Code signal modulated by a sinusoid carrier.....	17
Figure 3.5 The Simulink model used to generate the signal in Figure 3.4.....	17
Figure 3.6 A graph showing the FFT of a modulated PN Code signal.....	18
Figure 3.7 A graph showing the FFT of a signal produced by multiplying two PN Code signals (not to scale).....	19
Figure 3.8 A graph showing the FFT of a signal produced by multiplying two PN Code signals (not to scale).....	20
Figure 3.9 A Simulink model representing the proposed transmitter .....	21
Figure 3.10 A Simulink model representing the proposed receiver.....	21
Figure 3.11 A Simulink model representing the proposed detector.....	22
Figure 3.12 A graph showing the output power measured by combining the models proposed in Figures 3.9, 3.10 and 3.11.....	22
Figure 3.13 A diagram illustrating the proposed layout of the transmitter .....	24
Figure 3.14 A diagram illustrating the proposed layout of the receiver .....	24
Figure 4.1 A diagram illustrating a general shift register feedback configuration.....	27
Figure 4.2 A diagram illustrating an example of a Linear Shift Register.....	28
Figure 4.3 A diagram showing the layout of the shift register feedback configuration that will be used to generate the PN Code .....	32
Figure 4.4 A diagram showing the circuit that will force the PN Code Generator into a consistent state at startup .....	33
Figure 4.5 A diagram illustrating the layout for the RF Interface .....	34
Figure 4.6 A graph showing the measured output for the PN Code Generator .....	35
Figure 4.7 A graph showing the modulated output signal produced by the transmitter. The baseband PN Code signal is also shown for comparison .....	35
Figure 4.8 A graph showing the measured spectrum of a modulated PN Code signal .....	36
Figures 4.9 (a) and (b) illustrate the sampled nature of the frequency-domain PN Code signal. ....	37
Figure 4.10 A graph showing a practical measurement of two PN Codes after multiplication.....	38
Figure 4.11 A graph showing a practical measurement of two PN Code signals after multiplication .....	39
Figure 4.12 A diagram illustrating the setup for the measurement that will confirm the simulated results from Chapter 3.....	40
Figure 4.13 A graph of the output power measured by the configuration in Figure 4.12 .....	40
Figure 5.1 A diagram illustrating the basic layout for the receiver .....	43

Figure 5.2 A photograph of the completed receiver board.....	44
Figure 5.3 A diagram of the RF Frontend's layout .....	45
Figure 5.4 A graph illustrating the Return Loss of the antenna .....	46
Figure 5.5 Application circuit for the MAR6+ amplifier.....	47
Figure 5.6 A diagram illustrating the application circuit for the SA602 mixer.....	48
Figure 5.7 A diagram illustrating the basic layout for a Fractional-N PLL.....	50
Figure 5.8 A diagram of the internal connections of the ADF7011 component.....	51
Figure 5.9 A graph showing the measured spectrum of the LO .....	52
Figure 5.10 A circuit diagram of the lowpass filter .....	53
Figure 5.11 A graph showing the lowpass filter's frequency response.....	53
Figure 5.12 A diagram illustrating the Delay Control Mechanism .....	54
Figure 5.13 A diagram illustrating the Frequency Divider.....	55
Figure 5.14 A circuit diagram for the Frequency Divider.....	56
Figure 5.15 A circuit diagram for the PN Code Generator.....	57
Figure 5.16 A circuit diagram for the bandpass filter.....	59
Figure 5.17 A graph of the bandpass filter's frequency response .....	59
Figure 5.18 A circuit diagram for the RF Power Detector.....	60
Figure 5.19 A diagram showing the gain for the different components of the receiver board.....	61
Figure 5.20 A diagram illustrating how multiple receiver boards will be synchronised .....	62
Figure 5.21 A diagram showing the connectivity of the various receiver modules.....	63
Figure 5.22 A diagram of the PIC's various pin connections.....	64
Figure 5.23 A flow-diagram showing the setup procedure for the microprocessor.....	65
Figure 5.24 A flow-diagram showing the most basic measurement algorithm.....	66
Figure 5.25 A flow-diagram of the brute force algorithm .....	67
Figure 5.26 A flow-diagram of the efficient measurement algorithm .....	68
Figure 6.1 A diagram illustrating the basic correlation measurement setup .....	70
Figure 6.2 A photograph of the physical measurement setup in section 6.1.....	71
Figure 6.3 A graph of the basic correlation measurement.....	72
Figure 6.4 A diagram of the setup for the PN Code tracking measurement .....	73
Figure 6.5 A photograph of the physical measurement setup in section 6.2.....	73
Figure 6.6 A graph showing the result of the PN Code tracking measurement .....	74
Figure 6.7 A diagram that illustrates the setup for the cable length measurement.....	75
Figure 6.8 A photograph of the physical setup for the measurement in section 6.3 .....	76
Figure 6.9 A diagram illustrating the setup for the TDOA measurement.....	78
Figure 6.10 A photograph of the physical setup for the TDOA measurement .....	79
Figure A.1.....	85
Figure A.2.....	86
Figure A.3.....	87
Figure A.4.....	87
Figure A.5.....	88

## List of Tables

Table 5.1 .....	47
Table 5.2 .....	49
Table 6.1 .....	71
Table 6.2 .....	74
Table 6.3 .....	76
Table 6.4 .....	77
Table 6.5 .....	77
Table 6.6 .....	79
Table 6.7 .....	80
Table 6.8 .....	82
Table A.1 .....	89
Table A.2 .....	89
Table A.3 .....	90
Table A.4 .....	90

## List of Abbreviations

ADC	- Analogue-to-Digital Converter
AWGN	- Add White Gaussian Noise (Simulink Building Block)
BPSK	- Binary Phase Shift Keying
CDMA	- Code Division Multiple Access
DSSS	- Direct Sequence Spread Spectrum
FFT	- Fast Fourier Transform
GPS/NAVSTAR	- Global Positioning System
IC	- Integrated Circuit
LNA	-Low Noise Amplifier
LO	- Local Oscillator
LSR	- Linear Shift Register (Feedback Configuration)
MLSR	- Maximum Length Linear Shift Register (Feedback Configuration)
OFDM	- Orthogonal Frequency Division Multiplexing
PIC	- Programmable Interrupt Controller
PLL	- Phase Locked Loop
PN	- Pseudo Noise
PR	- Pseudo Random
PRN	- Pseudo Random Noise
RF	- Radio Frequency
SA	- Spectrum Analyser
SAW	- Surface Acoustic Wave
SS	- Spread Spectrum
TDOA	- Time-Difference-of-Arrival
TOA	- Time-of-Arrival

VCO - Voltage Controlled Oscillator

# Chapter 1

---

## Introduction

Location and tracking of personnel and assets has become more important and lucrative in recent years, especially with GPS technology becoming a widespread application. Most current generation cellular phones have a GPS module installed. We use it to manage motor vehicle and transportation fleets, drive our cars and even keep track of our loved ones.

However, there are a few drawbacks when using GPS technology though. Receivers are still on the expensive side and generally require additional hardware for remote operation. The simplest option is to attach a wireless communication module, which incurs additional service costs. The other major drawback is that any GPS receiver must maintain line-of-sight with at least four satellites. This precludes the use of GPS indoors or in other places where a view of the sky is obstructed.

The question that this project asked is whether there are any other options. How difficult would it be to develop an alternative system, given a more localised set of parameters?

### 1.1 A Short History of Navigation

Since the beginning of civilisation humankind has used some form of navigation. It is navigation that allows us to explore our surroundings and not only return safely home, but enables us to explain to others where we have been. One of the most basic methods is to use landmarks. This works reasonably well for slow, land-based travel. Eventually, however, this method will become insufficient.

Explorers set sail on the open oceans, where there simply are no landmarks. Other methods begin to emerge, most notably the use of celestial bodies. This makes navigation at sea possible, if still somewhat unreliable and dangerous. It is only after the arrival of certain navigational tools, such as the compass, sextant and especially robust chronometers that navigation a sea becomes more reliable [1].

The next big step came when it was discovered that radio waves can be used for navigational purposes. World War II saw the advent of new ground-based radio navigation systems [1]. These were used to guide bombers deep into enemy territory. After the war systems like Decca, Omega and LORAN were very successful. These were also land-based, but it soon became apparent that space was a better option. Transit was America's first satellite navigation system, designed and constructed by the US Navy [2]. Transit was eventually replaced by NAVSTAR GPS, the Global Positioning System in widespread use today.

## 1.2 Problem Statement

This section will now define more precisely the problem that will be addressed by this project, as well as the constraints under which it has to solve that problem.

There exists a need for locating and tracking certain targets, such as personnel. A cost-effective radio location system is required that can be deployed in a localised area, for example a shopping complex or an industrial installation. An effective radio location method is needed for such a system to be realised, which is what this project aims to develop. This project will briefly investigate several radio location techniques, select a suitable method, develop that method into a viable solution and then design and implement a working device to confirm the theory.

As mentioned before, there are several constraints placed on this project from the very beginning. Most of these are due to the nature of the problem itself, while others are added for academic purposes:

- The end solution must be extendable to multiple targets.
- These targets may not be burdened in any way with bulky equipment. RF tags the size of credit cards (or smaller) may be used if necessary.
- The system must be cost effective. Any tags placed on targets must be low-cost; receivers can be more expensive.
- Simple, omnidirectional antennas should be used. This excludes methods that rely on direction finding antennas.
- All the receivers may be synchronised by using a single clock frequency source.
- It was assumed that targets are slow-moving or stationary, which eliminates the need to correct for Doppler effects.

## 1.3 Proposed Solution

A number of radio location techniques will be investigated, of which the Spread Spectrum method will be chosen for further development. It will be proposed that a system consisting of three or four synchronised receivers monitoring several RF tags can be effective.

Synchronised receivers allow for accurate measurement of differences in ranging signal arrival times between the various receivers. With this in mind a strategy will be developed for measuring these time differences, which will lead to the design and implementation of a transmitter and a receiver.



## **1.4 Layout of this Thesis**

### **Chapter 2: Literature Study**

Chapter 2 will explore some of the basic theory that is used in this project, as well as some general concepts that may be encountered in radio location literature. After discussing basic theory a number of possible solutions are briefly investigated. The chapter ends with the selection of one particular method for further investigation.

### **Chapter 3: Strategy Development**

Chapter 3 takes the method proposed in Chapter 2 and re-examines it in more depth. The basic structure of the ranging signal is analysed to find a way of extracting a relative time-of-arrival measurement. From this analysis a strategy is formed, which is used to construct a Simulink model. Simulations show that this method can work.

With results looking positive it is decided to continue with this technique. A basic layout is proposed for both the transmitter and the receiver.

### **Chapter 4: Transmitter Design**

Chapter 3 has already proposed a basic layout for the transmitter. This is used to create a detailed transmitter design in Chapter 4. Much of Chapter 4 is used to find an economical method for generating the ranging signal. Various aspects of shift register feedback configurations are studied until a suitable method is found.

As soon as a working transmitter is implemented, the chapter will look at some basic measurements of the PN Code signal. The last measurement for this chapter will confirm the simulation results from Chapter 3.

### **Chapter 5: Receiver Design**

Chapter 5 takes the basic layout from Chapter 3 and creates a detailed receiver design. The receiver is far more complex than the transmitter and can be broken down into several modules:

- RF Frontend
- Pseudo Noise Generator
- Correlator/Detector
- Central Processor

Each of these modules will be discussed in detail.

### **Chapter 6: System Measurements**

This chapter will test the system as whole. Several experiments will be proposed and executed, in order to prove that the strategy developed in Chapter 3 is feasible. The results from these measurements will be compared to the predictions made in previous chapters.

### **Chapter 7: Conclusions and Recommendations**

With the results from previous chapters a conclusion can now be reached. Recommendations will also be made regarding some research aspects that fell outside the scope of this project.

# Chapter 2

---

## Literature Study

This chapter will look at some basic theory. Various concepts that are often encountered when discussing radio location in general will be examined. Once the basic theory has been covered the focus will shift to possible radio location techniques. Each method will be discussed briefly, after which a single technique will be selected for further study in Chapter 3.

### 2.1 Terminology

Some of the terminology used in this thesis, as well as some of the terminology encountered in radiolocation literature, will be discussed here.

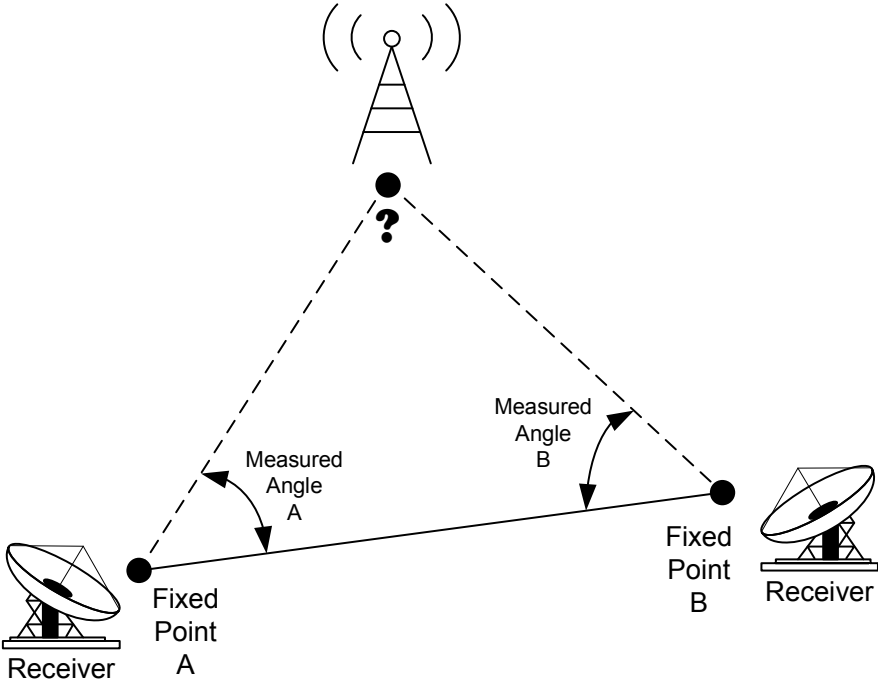


Figure 2.1

A basic diagram describing Triangulation.

- **Triangulation:** Triangulation in Euclidean geometry is the determination of the third point of a triangle when the length of the opposite side and the angles at the opposite two points are known. This can be applied to navigation when the location of two or more points is known and the direction from each of these points to an unknown point can be measured. Figure 2.1 illustrates this concept.
- **Trilateration:** Trilateration is the determination of the point of intersection of three spheres. This is the technique used by GPS, since GPS receivers measure the distance between the user and the orbiting satellites, which can then be interpreted as the radii of three (or more) spheres. Figure 2.2 provides a two-dimensional illustration of this:

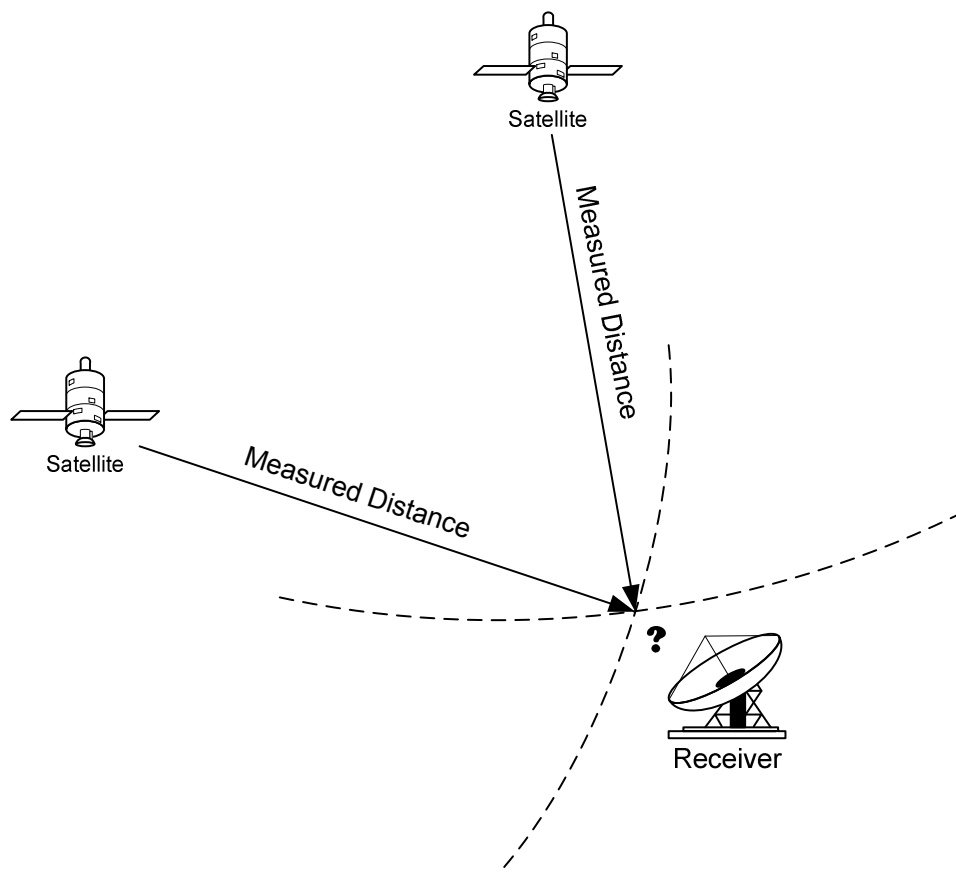


Figure 2.2

A basic diagram describing Trilateration.

- **Multilateration:** This method is somewhat trickier than Trilateration. Instead of measuring the direct travel time or distance between an unknown point of interest and a fixed reference point, the difference in arrival times is measured for a signal that is transmitted from an unknown point and received at two (or more) fixed references. From these differences in arrival times hyperboloids may be drawn, which represent possible locations for the unknown point of interest. If more measurements are made using other reference points, more hyperboloids may be drawn, the intersection of which will determine the location of the unknown point of interest [3]. This technique is also known as **Hyperbolic Position Location**, as Figure 2.3 illustrates.

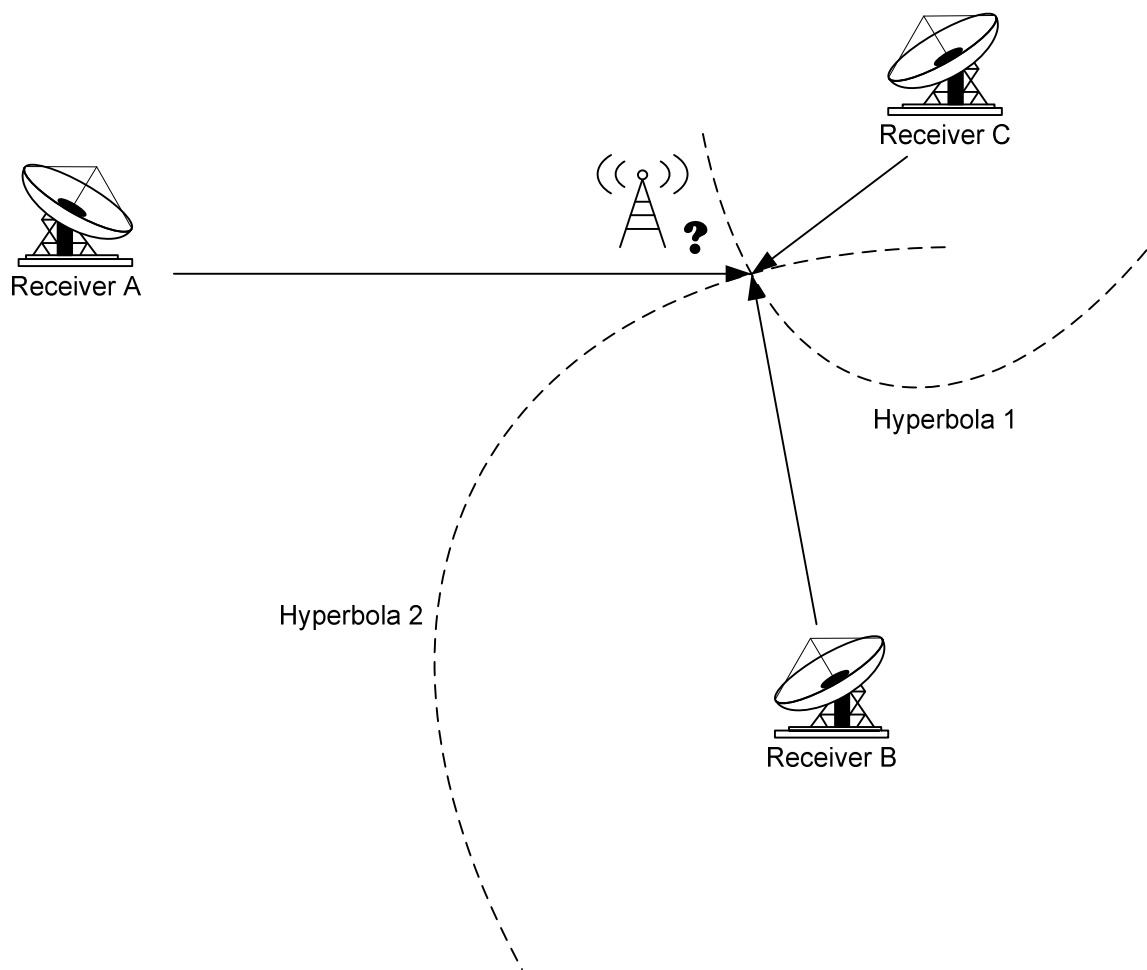


Figure 2.3

A basic diagram describing Multilateration

- **NAVSTAR GPS:** The Global Positioning System (GPS), also referred to as NAVSTAR GPS, is arguably the most well-known and comprehensive positioning and navigation system in the world today. A radiolocation system developed and maintained by the United States of America's Department of Defence, it employs a constellation of satellites to cover the entire globe [2] [4]. Although it was initially designed with military users in mind any person with an appropriate receiver can make use of this service, free of charge.
- **PN Codes:** Pseudo Noise Codes, Pseudo Random Codes and Pseudo Random Noise (PN, PR and PRN) refer to signals that have random noise-like properties, but are defined by a small finite set of variables [5]. Ideally, Pseudo Noise should closely approximate Gaussian Noise for most applications. One of the simplest realisations of a PN signal is to modulate a suitably random sequence of ones and zeros using Binary Phase Shift Keying. Essentially the ones and zeros are mapped to +1 and -1 signal levels. These "suitably random" sequences of ones and zeros are called PN Codes. PN Codes will be explored in more detail in Chapter 4.
- **Spread Spectrum:** Spread Spectrum (SS) refers to a general group of modulation techniques where the bandwidth of the data signal is increased far beyond what is necessary to transmit the information by using PN Codes [5] [6]. This has a number of advantages which include resistance to intentional or unintentional jamming, low probability of intercept by unintended receivers and the possibility of multiple access for a number of users sharing a single spectral band [5] [7]. Spread Spectrum signals can also be used for position location and ranging purposes [5] [8] [4].
- **Direct Sequence Spread Spectrum:** Direct Sequence Spread Spectrum is the simplest form of Spread Spectrum modulation. A binary data stream is multiplied with a PN Code stream (also called a Spreading Code or Spreading Waveform); the result is used by a modulator (typically BPSK or QPSK) to produce a transmitter signal [9].
- **CDMA:** Code Division Multiple Access is a form of Direct Sequence Spread Spectrum (DSSS) where orthogonal codes are used to separate multiple users sharing the same spectral resources [6]. Typically these users employ Spread Spectrum techniques for data modulation where the data is simply multiplied with a Pseudo Noise signal, which results in any single user's signal occupying the entire frequency band. In a CDMA system each user will be assigned a unique code (usually special types of PN Codes) for use during modulation. By design all the codes used in a single CDMA system will be orthogonal, which means that they will have uniformly low cross-correlation functions and thus allow the receiver to suppress all other users' signals when demodulating the intended user's signal.
- **OFDM:** Orthogonal Frequency Division Multiplexing, also known as FDMA (Frequency Division Multiple Access), is a form of Frequency Hopping where, similar to CDMA, orthogonal codes are used to separate multiple users sharing common spectral resources [6] [7]. However, instead of multiplying these orthogonal codes directly with the data signal during modulation, the codes are used to hop the data signal between a number of carrier frequencies.

- **TOA & TDOA:** Time-of-Arrival and Time-Difference-of-Arrival are two types of time-based radiolocation techniques (other techniques include measuring signal strength and determining the angle of arrival) [3] [8] [2]. Both methods effectively measure a distance variable, which may then be used to calculate a position fix. TOA systems, such as GPS, typically measure the travel times of received signals and then employ Trilateration algorithms to calculate positional information [2] [4]. TDOA systems are useful when direct measurement of signal travel time is not possible or practical, but the difference in travel time between two known locations can be determined. Multilateration algorithms may then be used to calculate positional data [3] [8].

## 2.2 Possible solutions

The previous section covered various radiolocation and radionavigation concepts. Several of these concepts are in fact also methods of position location. This section will discuss briefly a number of solution possibilities, after which the most appropriate technique will be selected.

### 2.2.1 Measured Signal Strength as an Indication of Distance

This method simply measures signal strength and then use the Friis-equation to solve for distance. Trilateration can then be used after three such distances are measured. Measuring signal strength is, however, notoriously inaccurate. Consider the Friis-equation (as described by [10]):

$$P_r = \frac{G_t G_r \lambda^2}{(4\pi R)^2} P_t \quad [W] \quad (2.1)$$

$P_r$  is received power,  $P_t$  is transmitted power,  $G_t$  and  $G_r$  are the antenna gains,  $\lambda$  denotes wavelength and  $R$  represents the distance travelled. This can be rearranged as follows:

$$P_r = \left( \frac{G_t G_r \lambda^2 P_t}{(4\pi)^2} \right) \frac{1}{R^2} \quad [W] \quad (2.2)$$

The difference in measured power levels for  $R = 1$  and  $R = 11$  meters is 20.8dB. This is easily measurable, but for  $R = 100$  and  $R = 110$  meters the difference is 0.8dB. As  $R$  increases in value it becomes very difficult to measure the change in received power, making this method very inaccurate at longer distances. Measuring received signal strength will therefore not be considered any further.

### 2.2.2 Difference in Phase as an Indication of Distance

This method measures the difference in phase of a signal as it arrives at the various receivers. A difference in phase translates to a difference in distance travelled, which can be used by a multilateration algorithm to determine a position. This is an old and well-known method, employed by earlier systems such as the Omega radionavigation system [1].

Phase difference measurements as a position location method poses two major problems to this project. Firstly, and most importantly, it would be very impractical to use this method with multiple transmitters. Each transmitter would need its own frequency; multiple transmitters would quickly take up the limited space available in the radio spectrum.

The second problem concerns the ambiguity of phase measurements. A measurement of  $30^\circ$  could also be  $360^\circ + 30^\circ$ , or it could be  $720^\circ + 30^\circ$  or any integer number of wavelengths +  $30^\circ$ . To mitigate this problem one could use a wavelength which is comparable with the longest distance that might be measured. Consider the equation:

$$\lambda = \frac{c}{f} [m] \quad (2.3)$$

Where  $\lambda$  is wavelength in meters,  $c$  is the speed of light and  $f$  is the operating frequency. To obtain a wavelength of 100m in air, the operating frequency would have to be 3 MHz. Longer ranges would require even lower frequencies, which would make the design of small transmitters very difficult.

Besides the brute force solution of picking a very low frequency, one could also measure phase differences at additional frequencies for the same transmitter. Choosing these frequencies wisely would result in a longer unambiguous range. It would, however, compound the problem of multiple users. Phase Difference measurements will therefore also not receive any further consideration.

### 2.2.3 Using Spread Spectrum Signals to Determine Distance

After the simpler solutions discussed previously were evaluated and dismissed, more sophisticated methods were looked at. The first and most obvious system to investigate is GPS, since it is so widely used and well-known.

The Global Positioning System is very complex. It requires extremely precise timing on a global scale, with very sophisticated receivers decoding the navigational signals. Much research and development has gone into (and is still going into) squeezing every last drop of information from the signals that the GPS satellites transmit. At the heart of this system, however, lies a relatively uncomplicated signal structure that may provide the solution for this project.



The satellites from the first fully operational constellation each transmitted two distinct signals using two carriers [2] [4]. Both these signals are implementations of Direct Sequence Spread Spectrum (DSSS) modulation [2] [4]. Spread Spectrum signals are known for their suitability in ranging and positioning applications [5] [8], which is why it was decided to give this some serious consideration.

Let us consider the structure of a basic DSSS signal which is not modulating any data. Without the addition of data there is only the PN Code, a sequence of ones and zeros with specific pseudorandom qualities. One of these qualities is a very sharp auto-correlation function [5]. This means that the SS signal will be perfectly correlated with a copy of itself if that copy is aligned with the original. If, however, the copy is shifted away from this point of alignment it should be uncorrelated with the original, as shown in Figure 2.4. This point of highest correlation is called the correlation peak and can be used to determine the time of arrival for an SS signal.

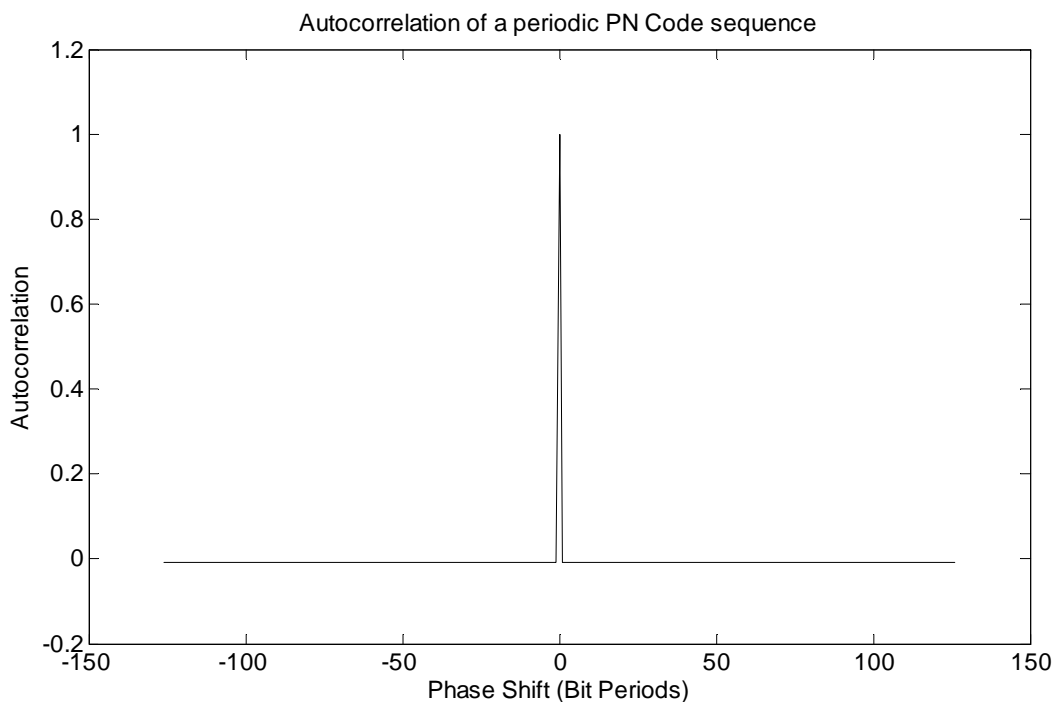


**Figure 2.4**

**Graph showing the autocorrelation function of a PN Code sequence.**

Correlators are one of the principal components of a DSSS receiver. They are used to align a locally generated PN Code with the PN Code of the incoming signal. When the correct amount of time delay has been determined the incoming signal can be demodulated or that delay can be used as a parameter in a position location algorithm. This is what a GPS receiver does with the satellite signals that it tracks.

After conditioning, an incoming signal is fed to a correlator (or several), along with a locally generated PN Code. This correlator then determines by how much the locally generated PN Code must be delayed to align it with the incoming signal. Since it is known when the signal left the satellite (all GPS satellites operate under strict precision timing) the delay measured by the correlator is equivalent to the time (and therefore distance) that the signal travelled<sup>1</sup>.

GPS clearly demonstrates that DSSS can be used for position location. There are a few more questions that need to be answered before going ahead, such as can this method be used to track several targets simultaneously? Can a cost effective and inconspicuous implementation be achieved?

The answer to the first question can be found in CDMA, a multiple access technique which employs Spread Spectrum (SS) modulation. In CDMA systems multiple users can transmit data at the same time, as long as they use orthogonal PN Codes during modulation.

To answer the second question one must consider the complexity of building a Spread Spectrum transmitter. The simplest case would consist of a PN Code generator and the minimum RF components necessary to transmit the signal. No data needs to be transmitted. The RF components are needed regardless of which type of signal will be transmitted, thus the complexity is determined by the PN Code generator. There are a number of simple Linear Shift Register Feedback Configurations that can do the job [4] [5] [11]. Gold Codes are a popular choice since they combine two simple PN sequences in a particular way to produce a large number of PN Codes [5] [11].

To summarise: DSSS can be used effectively for position location purposes. Multiple targets can easily be incorporated by using orthogonal PN Codes to separate them. Generation of PN Codes is quite simple if using Linear Shift Register Feedback methods. RF tags would only require a small number of logic and RF components to transmit the basic DSSS signal needed for location measurements. Spread Spectrum signals could definitely provide the basis for the design of a radiolocation system.

#### **2.2.4 Other techniques**

Other techniques that could also be used in a radiolocation system include Angle of Arrival (AOA) methods and pulse radar methods. Angle of Arrival techniques use specially designed antenna arrays to estimate the direction from which a received signal is coming. Angle estimations can be used in conjunction with Triangulation algorithms to find the location of a signal source.

There are many pulse radar systems and technologies that provide tracking and identification functionality. One such system is the Ultra-Wideband Precision Asset Location (UWB PAL) system

---

<sup>1</sup>This is not strictly true. There are various errors which must be taken into account. Since it would be too expensive to keep all GPS receivers synchronised with the satellite constellation, a major error source is the unknown difference between the receiver's clock and GPS system time. This error is mitigated by tracking at least four satellites, from which three spatial dimensions and one time dimension is extracted [2] [4].

developed by Multispectral Solutions. It uses UWB pulses instead of DSSS signals to locate a target. UWB radar pulses can be generated that are very short, which gives it the ability to operate in severe multipath environments [12].

Although Angle-of-Arrival (AOA) methods can be used, especially in conjunction with other ranging techniques, it will not be looked at any further. One of the constraints of this project is to refrain from using AOA methods.

## **2.3 Conclusion**

The use of Spread Spectrum signals looks to be a promising candidate. It is a proven technology which can accommodate multiple users and should be cost effective to implement. It fits all the constraints placed upon the project in Chapter 1 and is therefore the method selected for further study in the next chapter.

# Chapter 3

---

## Strategy Development

The previous chapter decided to investigate Spread Spectrum techniques as a means of position location. This chapter will look at the proposed ranging signal in more detail and then develop a strategy for extracting the required information from it. This will allow for a basic layout to be made for both the transmitter and the receiver. First, however, the basic system configuration will be considered.

### 3.1 System Configuration

Figure 3.1 shows a diagram depicting the basic configuration that will be used for the rest of this project. A single transmitter, broadcasting a Spread Spectrum signal, will be placed on the target. Several receivers will be placed around it to take TOA (Time-of-Arrival) measurements, which are sent to a central processing unit (for instance a PC or laptop computer). All the receivers are synchronised by means of a shared Local Oscillator (LO) source. The receivers compare the incoming signal with a locally generated PN Code (identical to the transmitter PN Code) and then determine how far they have been shifted apart by using a correlator. This delay between the transmitter and the receiver is passed on to the processing unit as the TOA measurement.

The TOA measurements made by the receivers will, of course, be completely incorrect, since there is no synchronisation mechanism between the transmitter and the various receivers. This is no problem at all. To overcome this hurdle multilateration algorithms will be employed. The receivers are not synchronised with the transmitter, but they are synchronised with each other. This means that although the absolute TOA measurement is quite wrong for any given receiver, the TDOA (Time-Difference-of-Arrival) measurement between any two receivers can be accurately calculated.

Each receiver is synchronised with every other receiver by means of a shared clock (LO) source. This means that the PN Code generated by each receiver will have a fixed relationship in time to every other receiver's PN Code. At start-up a calibration measurement can determine the relationship between the various generated PN Codes, after which it is very easy to convert the TOA measurements into TDOA measurements.

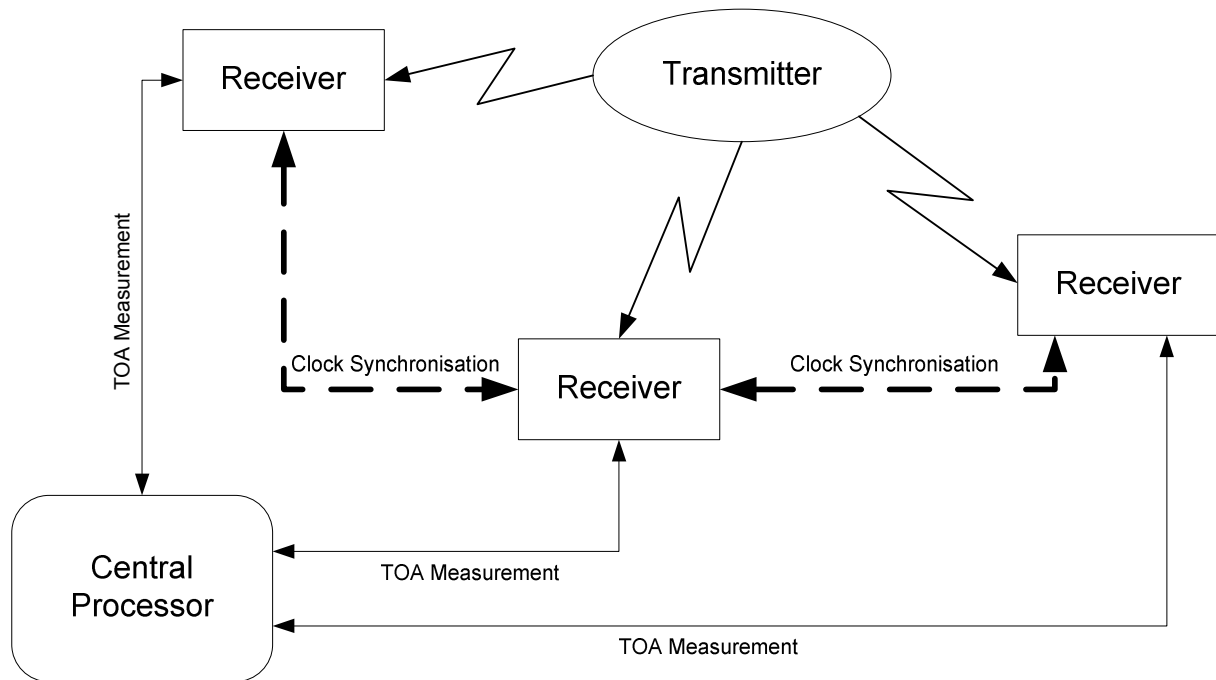


**Figure 3.1**

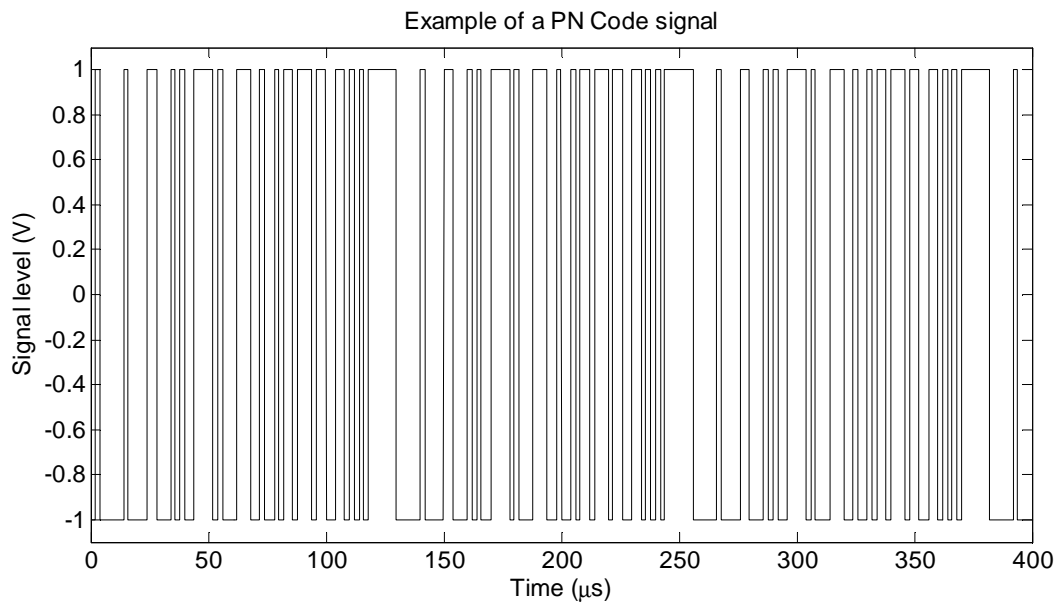
**A diagram illustrating system configuration.**

The following section will take a more detailed look at the PN Code ranging signal in terms of characteristics and interaction with other PN Code signals. This will provide a possible means for extracting ranging data, which will be expanded into a solution proposal in section 3.3.

### **3.2 Ranging Signal Characteristics**

In the previous section, a broad outline is given of how the entire system will be configured. The purpose of this chapter is to take that basic configuration and develop a strategy by which positional information can be obtained from the ranging signal. Before that can be done, the ranging signal must be studied in more detail.

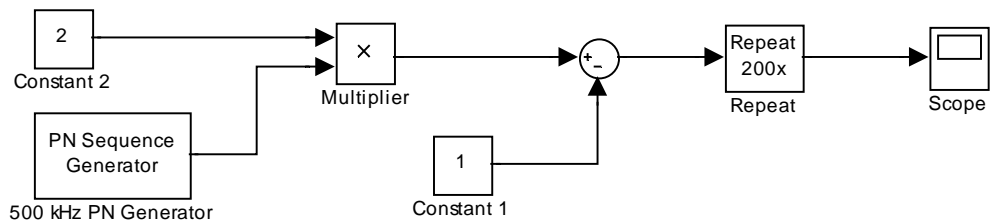
There are several signal properties that will be important at some point in the design of any piece of receiver hardware. Some of these can include signal strength, bandwidth, signal-to-noise ratio, operating frequency and modulation scheme. In Chapter 2 it was decided to use Spread Spectrum (SS) techniques for position location. This section will now take a closer look at what an SS signal looks like and how it interacts with other SS signals.



**Figure 3.2**

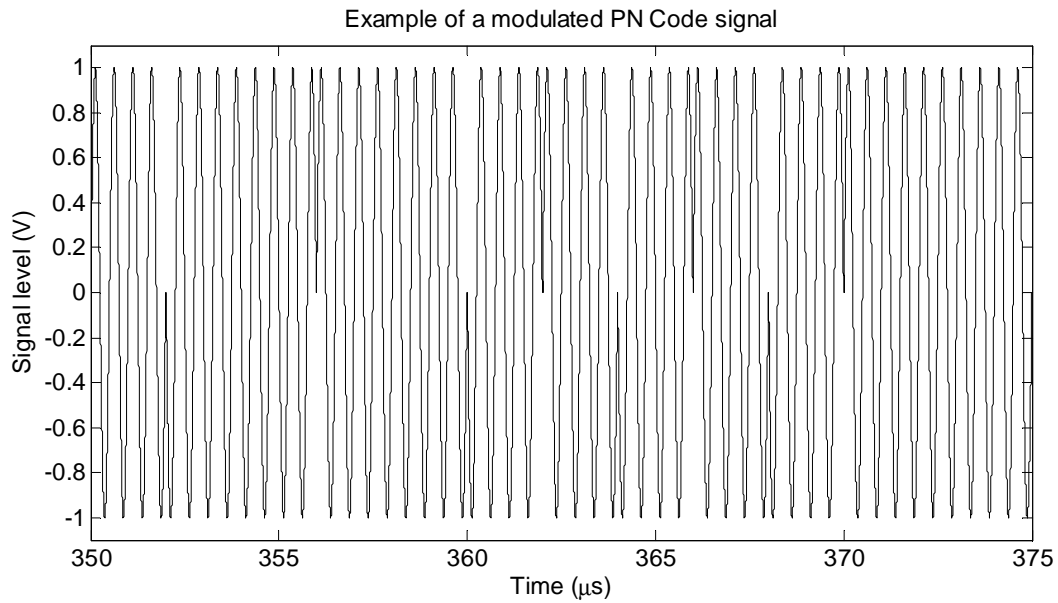
**A graph showing an example of a PN Code signal's structure.**

Figure 3.2 shows an example of the baseband PN Code signal. It is essentially a binary code containing pseudo-random data. In this particular example the code is short enough to repeat itself three times in the measured period. This signal can be created by the Simulink model shown in Figure 3.3.



**Figure 3.3**

**The Simulink model used to generate the signal shown in Figure 3.2.**



**Figure 3.4**

**An example of a PN Code signal modulated by a sinusoid carrier.**

Figure 3.4 shows the simplest example of Spread Spectrum modulation. A PN Code (with values +1 and -1) is multiplied with a sine wave. This effectively changes the phase of the sine wave by  $180^\circ$  whenever the PN Code flips between +1 and -1. It looks no different from Binary Phase Shift Keying, except that the data has been replaced by a PN Code. This basic SS signal can be produced with the Simulink model shown in Figure 3.5.

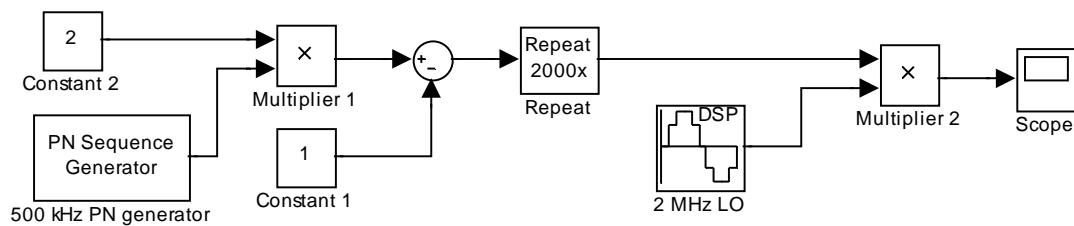


**Figure 3.5**

**The Simulink model used to generate the signal in Figure 3.4.**

Figure 3.6 gives an indication of the shape of the power spectrum that can be expected from PN Code modulation. A  $\text{Sin}(x)/x$  envelope can be seen, similar to BPSK. The carrier signal is suppressed, with the energy spread around it. If some way can be found to measure how densely signal power is concentrated around the carrier, that measurement can be used to determine the alignment of two PN Codes.

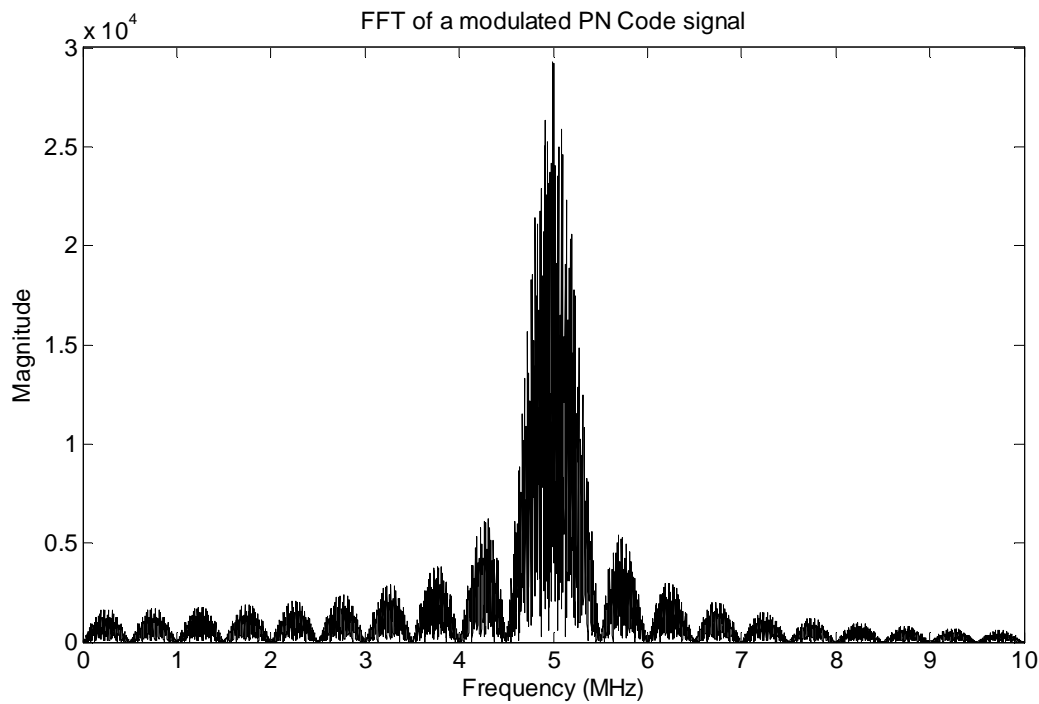


**Figure 3.6**

A graph showing the FFT of a modulated PN Code signal. The magnitude is not to scale.

This signal has inherited a number of properties from the PN Sequences that were investigated earlier. Multiplying the signal with the same PN Code, without shifting that PN Code out of alignment, should recover the carrier signal. This can be seen in Figure 3.7, where a modulated PN signal with added noise (to simulate a noisy channel) has been multiplied with the same PN Code. Since the two PN Codes are aligned the carrier is recovered.



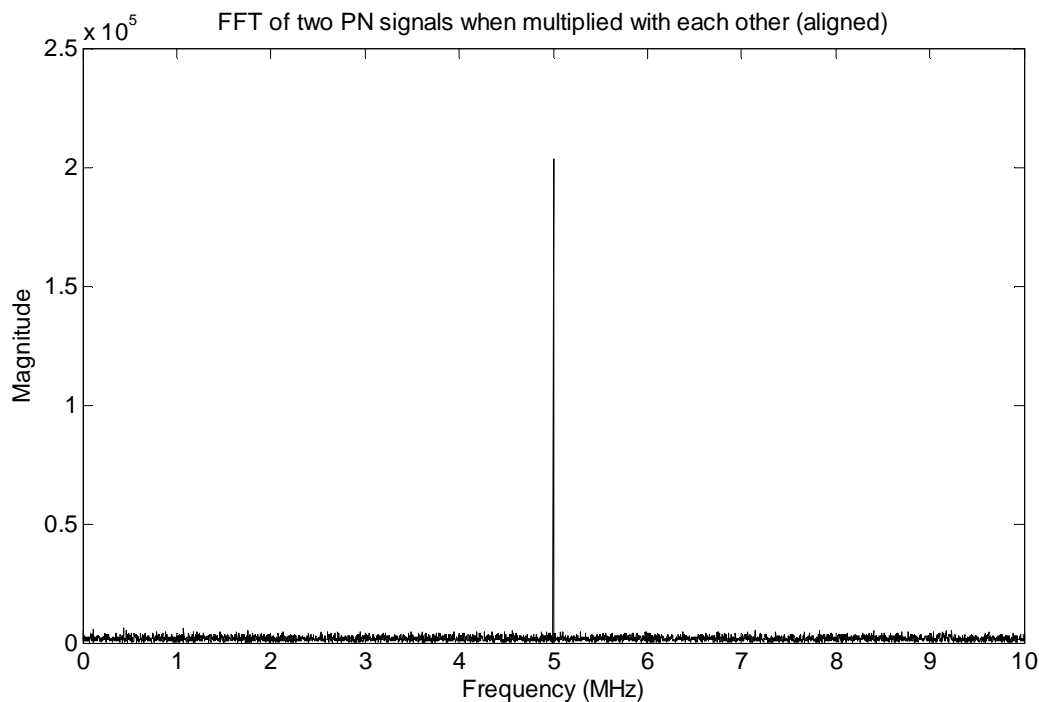


**Figure 3.7**

A graph showing the FFT of a signal produced by multiplying two PN Code signals (not to scale). The PN Codes are aligned in this example.

Multiplying the signal with another PN Code will result in another modulated signal, if the two PN Codes are uncorrelated [5] [13]. Multiplying with the same PN Code that has been sufficiently shifted in time will result in yet another modulated signal, if the PN Code has the correct auto-correlation properties [5] [13]. Multiplying with a PN Code other than the original or without correct alignment will simply generate another Spread Spectrum modulated signal. This can be seen in Figure 3.8, which is produced by the same Simulink model as Figure 3.7, except that the two PN Codes are out of alignment.

These two figures (Figures 3.7 and 3.8) illustrate a big difference in the spectra of the two signals. When a modulated PN Code signal is multiplied with the same PN Code one of two things can happen: If the two PN Codes are aligned they will reverse each other's effects, thereby recovering the carrier signal. If they are not aligned the result is simply another modulated PN Code signal. It is this property that the next section will utilise when it proposes a solution. By measuring the spectral energy in the vicinity of the carrier, it is possible to determine if the two PN Code signals that are being multiplied are correctly aligned.

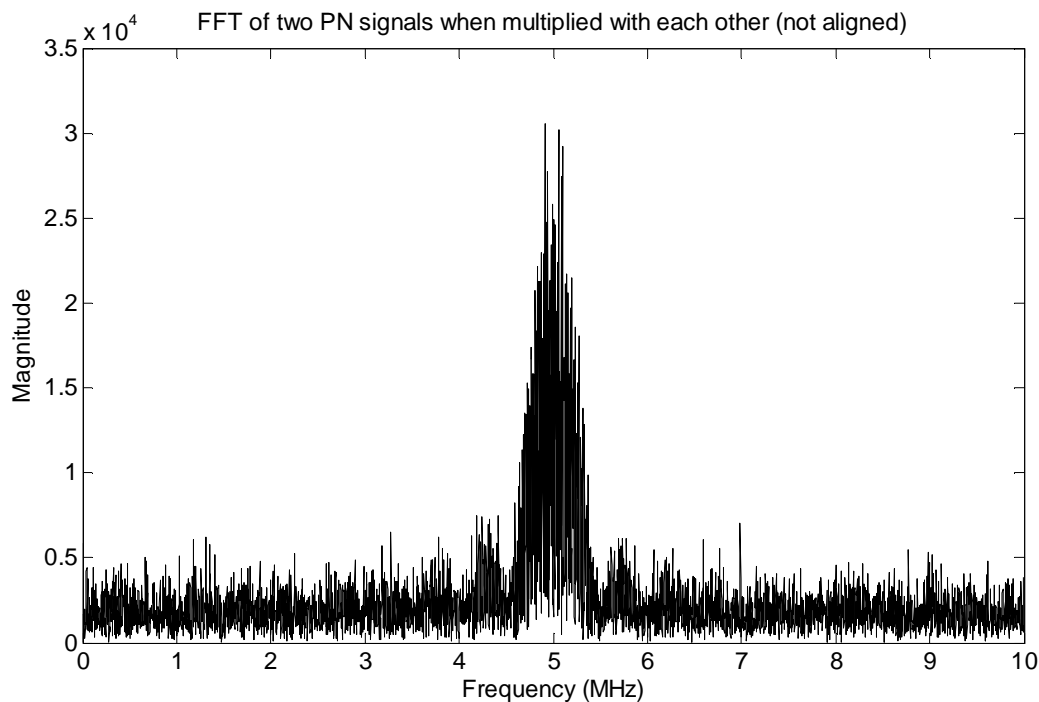


Figure 3.8

A graph showing the FFT of a signal produced by multiplying two PN Code signals (not to scale). The PN Codes are not aligned in this example.

### 3.3 Strategy Proposal

The previous section implied that ranging information could be extracted from the transmitter signal by measuring how much of the signal's energy is concentrated around the carrier. To be more specific: The measurement can be used to determine if two identical PN Codes are aligned in the time domain. If they are aligned, multiplying them will result in a signal whose energy will be concentrated near the carrier; if not, the signal's energy will remain spread out.

The following simulation was used to investigate the strategy mentioned above. A simple transmitter/receiver link was designed using Matlab's Simulink simulation environment. A PN Code is generated at a chipping rate of 500 kHz. This PN Code is then multiplied by a 5 MHz sinusoid to simulate a ranging signal, after which white Gaussian noise is added. This represents the transmitter and the noisy channel it would use for broadcasting the ranging signal. Figure 3.9 illustrates this model.

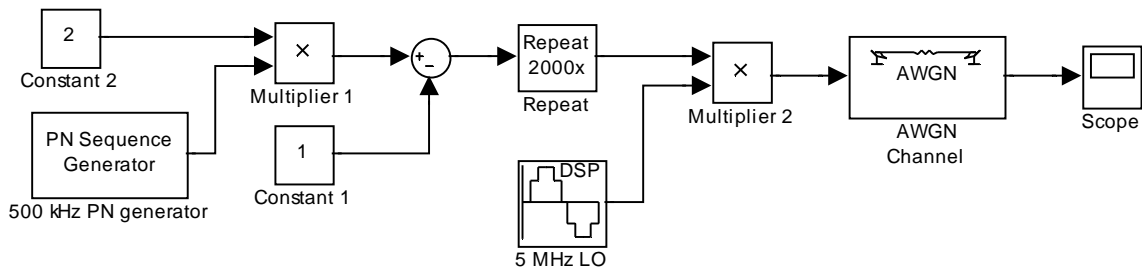


Figure 3.9

A Simulink model representing the proposed transmitter.

The receiver consists of a mixer and another PN Code generator. The transmitter signal is first multiplied by a 4.5 MHz sinusoid to simulate a down conversion of carrier frequency. The idea is not to recover the baseband signal, but to mix the ranging signal down to a lower Intermediary Frequency (IF) where it is more feasible to construct a filter that can monitor the energy around the carrier, after which the signal is multiplied by the second PN Code. This can be clarified by Figure 3.10.

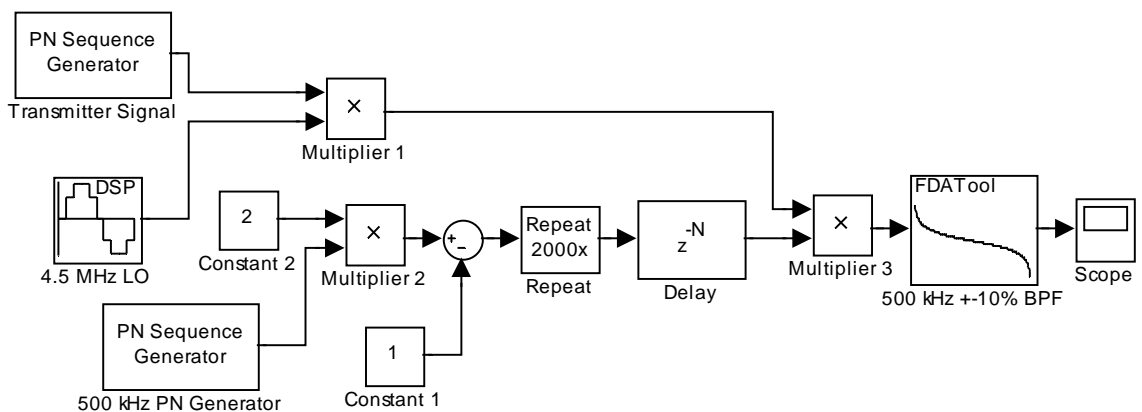


Figure 3.10

A Simulink model representing the proposed receiver.

The models shown previously (Figures 3.9 and 3.10) form the two basic subcomponents used to generate the signals for Figures 3.7 and 3.8. The last subcomponent, shown in Figure 3.11, models a diode power detector.

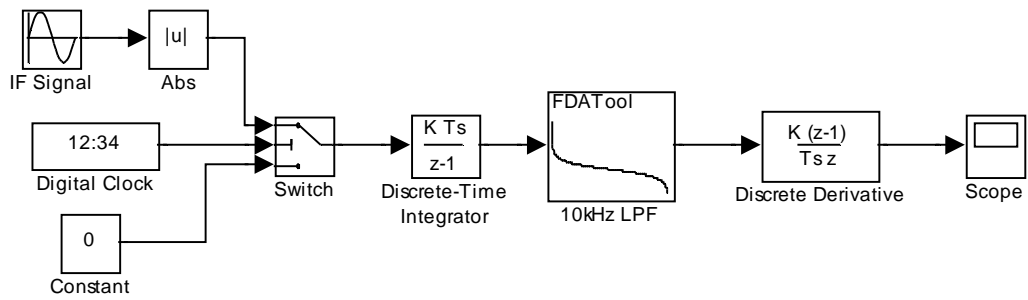


Figure 3.11

A Simulink model representing the proposed detector.

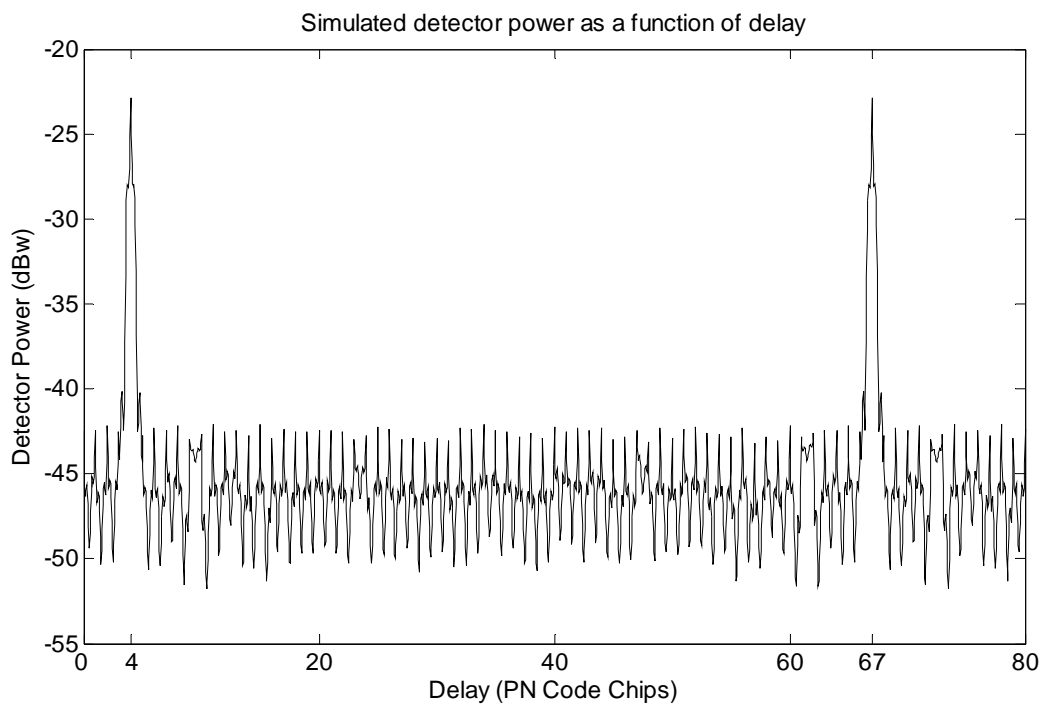


Figure 3.12

A graph showing the output power measured by combining the models proposed in Figures 3.9, 3.10 and 3.11.

By varying the amount of delay added between the transmitter and the receiver different distances can be simulated. The second delay component in the receiver must be equal to the first delay component

for the two PN Codes to be aligned. If the two PN Code Generators are synchronised (that is, they are working at the same clock frequencies) with each other and if the two signals are aligned the second delay component is equivalent to measured ranging data.

Consider the measurement in Figure 3.12: Output power is displayed (as measured by the diode detector section) for various amounts of delay added by the receiver. A maximum can be observed for a delay of four chips, which corresponds exactly with the delay of 800 samples that was added between the transmitter and the receiver (In this particular simulation 800 samples is equal in length to four PN Code chips).

This simulation shows that an uncomplicated configuration, using a bandpass filter and an RF power detector, can work. It also predicts the degree of accuracy that this strategy can achieve: resolution accuracy will be determined by the accuracy with which the correlation peak is detected. This will in turn be determined by the accuracy with which the receiver can delay its own PN Code. Chapter 5 will show that, for the implemented device, 83.3 ns is the smallest amount of delay that can be added. 83.3 ns translates to a TDOA resolution of  $\pm 12.5$  m in free space. Without any post-processing the system should, therefore, be able to achieve a resolution of at least 25 m.

## **3.4 Basic Layout**

The simulation models developed in the previous section provide enough detail to draw up basic layouts of the transmitter and the receiver. The next two subsections will define the basic building blocks for these components.

### **3.4.1 Transmitter**

The transmitter's design will be kept as simple and cost effective as possible. This is not too difficult, as the PN Code Generator can be implemented with a small number of inexpensive logic components or even a small FPGA. All it requires is a shift-register, a number of very basic logic components for feedback, a number of basic logic components to force the circuit into a consistent state during start-up and a clock. This is enough to generate the baseband ranging signal.

The RF Frontend is also relatively uncomplicated. All it needs to do is mix the baseband signal up to a suitable carrier frequency and feed this to an antenna. In order to do this a mixer, local oscillator (LO) and antenna is required, with the possible addition of some filtering. Figure 3.13 illustrates this basic layout.

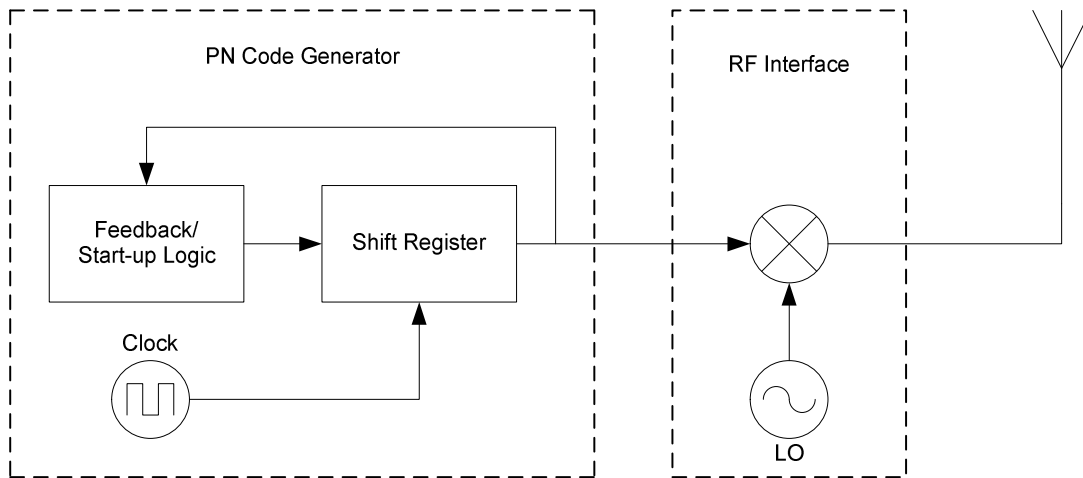


Figure 3.13

A diagram illustrating the proposed layout of the transmitter.

### 3.4.2 Receiver

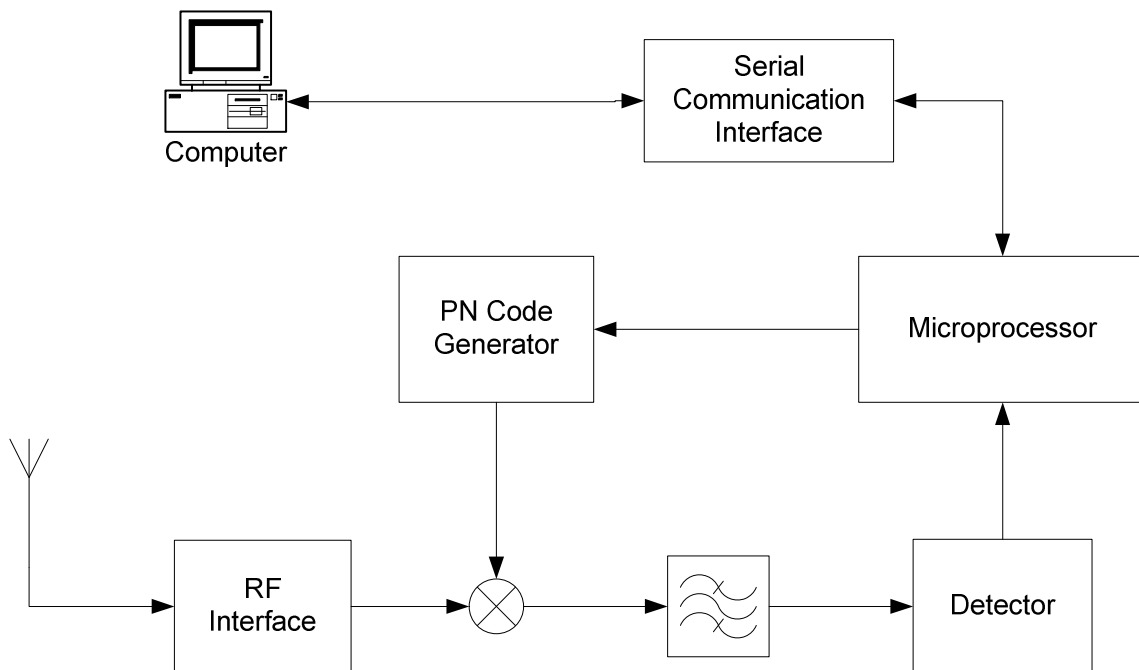


Figure 3.14

A diagram illustrating the proposed layout of the receiver.

The receiver is somewhat more complex than the transmitter. It is not enough to simply generate a PN Code; it must also be compared to an incoming signal to see if they are aligned. A correlator circuit must, therefore, be added. Further, it is also not sufficient for the generated PN Code to be compared to the incoming signal. The PN Code must also be delayed by carefully controlled amounts of time, for which a microcontroller is needed. The microcontroller is also needed to measure the output of the Correlator and relay this information to a Central Processor.

Last, but not least, an RF Frontend is needed. This subsection is also more complex than its transmitter equivalent. The incoming signal must now be received, filtered, amplified, mixed down to a suitable Intermediate Frequency and then amplified again.

After passing through the RF Frontend the incoming signal is fed to the Correlator. Here it is essentially multiplied with the locally generated PN Code, passed through a narrow bandpass filter and finally reaches an RF power detector. If the incoming signal and the PN Code are aligned, the result of their multiplication should concentrate most of the input power in a relatively narrow band. If they are not aligned, the power will remain spread out. Figure 3.14 illustrates this basic layout for the receiver.

# Chapter 4

---

## Transmitter Design

This chapter will explore all the details regarding the design of the transmitter. Before designing the transmitter, however, it is necessary to define the functionality that is expected from the transmitter:

- It must generate a periodic PN Code signal.
- It must transmit this signal in a suitable frequency band using simple Binary Phase Shift Keying.

There are also a number of additional requirements that, while not of a functional nature, are still just as important:

- The design must be cost-effective.
- It must be possible to shrink the design to fit onto a credit card sized PCB.
- It must be possible to easily extend or alter the design to incorporate multiple transmitters.

The functionality mentioned above divides the problem into two logical subcomponents. One part will be responsible for the generation of the PN Code; another part will be used to get the signal airborne. This chapter will therefore be split into two sections. One section will deal with PN Code generation, while the other will describe the RF Interface. These two sections will cover all the design aspects and parameters that still need to be fixed, such as what comprises a suitable band for transmission and what the PN Code structure should look like.

### 4.1 PN Code Generator

This section will describe the structure of the PN Code, as well as ways to implement it. Firstly, consider that any sufficiently random sequence of ones and zeros, with adequate cross-correlation properties could be used as a PN Code. Any device with enough memory, such as a microcontroller, could be used to store this sequence and then reproduce it. As long as the sequence is short enough to fit in the device's memory and the frequency is such that the device can keep up, this could be a viable solution.

Using a device with memory holds several advantages. It can be reprogrammed; a transmitter is not bound to any specific PN Code. Any random sequence can be programmed, not only a limited set of sequences (as is the case when using shift registers). There are also disadvantages, most notably higher costs.



There are also simple shift register configurations that can generate sequences with adequate randomness and correlation properties [2] [5] [13]. Shift registers are cheap and easy to use; a small number of components can go a long way. This makes them attractive from both a cost-effectiveness and PCB size perspective.

Both methods seem capable of doing the job. It was decided to start off with a shift register implementation, since it would be cheaper and easier to build. This does not mean that the idea of using programmable memory will be completely abandoned. For the moment shift registers are simpler and cheaper to use, especially at higher clock frequencies.

#### 4.1.1 Shift Register Sequences

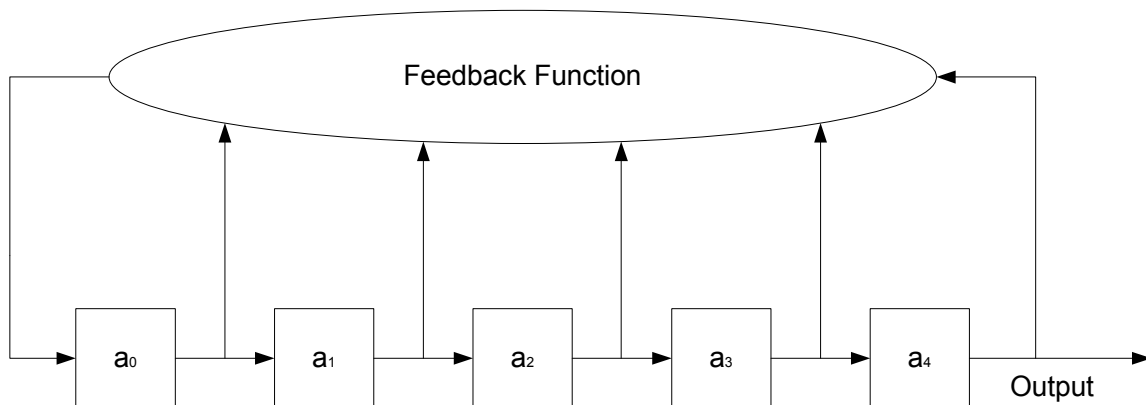


Figure 4.1

A diagram illustrating a general shift register feedback configuration.

Figure 4.1 illustrates a general shift register feedback configuration. Every memory element  $a_n$  stores one bit (a one or a zero). With every new time step all elements shift their contents to the right;  $a_n$  is set equal to  $a_{n-1}$ ,  $a_{n-1}$  is set equal to  $a_{n-2}$  and so forth. The last element,  $a_0$ , stores a new value given by the feedback function's output. The feedback function can be any linear or non-linear combination of the values stored in the register, as long as it produces a one or a zero. The shift register configuration output simply follows the element that is furthest to the right. This will produce a sequence of ones and zeros, another element being added with each time step. This sequence is dependent on the initial values of all the elements in the shift register, as well as the feedback function. By controlling these two aspects (especially the feedback function) bit sequences with specific properties may be produced [5] [11] [13].

The purpose of investigating shift register sequences is to find an inexpensive way of generating PN Codes with certain properties. Controlling the properties of the binary sequence can be accomplished by choosing an appropriate feedback function. Consider the following function (taken from [13]):

$$f(x_1, x_2, \dots, x_n) = c_1x_1 \oplus c_2x_2 \oplus \dots \oplus c_nx_n \quad (4.1)$$

where  $x_i$  denotes the various elements of the shift register, the constants  $c_i$  can be either 1 or 0 and the symbol  $\oplus$  denotes modulo 2 addition. When this function is used the configuration is known as a Linear Shift Register (LSR) [13]. Consider the following example of a three element LSR. The feedback function, the modulo 2 addition of  $x_1$  and  $x_3$ , is equivalent to the exclusive OR Boolean function, as shown in Figure 4.2.

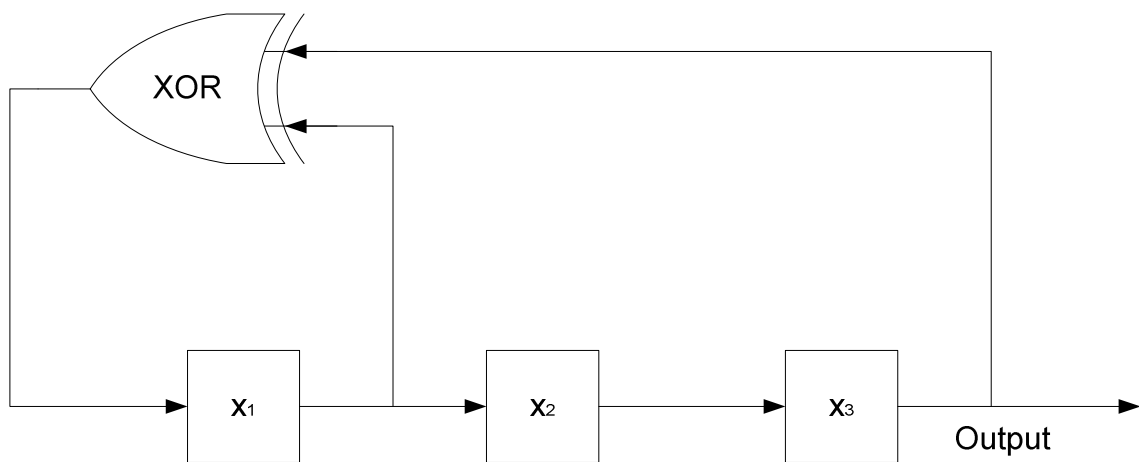


Figure 4.2

A diagram illustrating an example of a Linear Shift Register.

Let the initial states of  $x_1$ ,  $x_2$ , and  $x_3$  be 1. With each time step  $x_1$  and  $x_2$  will shift their contents to the right, while  $x_1$  will receive a new value from the feedback function. A sequence of ones and zeros will emerge at the output, as can be seen below:

$x_1$	$x_2$	$x_3$
1	1	1
0	1	1
1	0	1
0	1	0
0	0	1
1	0	0
1	1	0
1	1	1

Output = 1 1 1 0 1 0 0 1 1 1 0 1 0 0 1...

The question now is whether LSR sequences have all the properties that will be needed to produce a suitable ranging signal. Maximum Length (Linear) Shift Registers (MLSRs) can be used to generate binary sequences with all the properties required of suitable PN Codes, most notably adequate randomness and correlation properties. Proofs for these properties are given in [5] and [13]; the properties may be summarised as follows:

1. The number of ones and zeros in one period of the sequence is approximately equal.
2. Run lengths of ones and zeros will approximate a Bernoulli sequence (coin-flipping sequence), approximately one half of all runs will be one bit long, approximately one quarter of runs will be of length two, one eighth of runs length three and so forth. Runs cannot be longer than the length of the shift register.
3. The sequence will have a very sharp auto-correlation. If the sequence has a period of  $n$  bits, the auto-correlation will have  $n$  agreements for zero shift (or multiples of  $n$ ) and approximately equal numbers of agreements and disagreements for any other shift.

MLSRs are suitable as PN Code Generators for ranging purposes. It should be noted, however, that these sequences are not truly random. They are, in fact, determined by a small number of parameters; they cannot be used for secure applications [7]. This is not a problem yet, as secure transmissions are not required.

Another matter to be considered before moving on is extension to multiple transmitters. LSRs are suitable for this as well. A reasonably simple method exists to produce entire sets of PN Codes with good cross-correlation properties using two MLSRs [2] [11]. These sets of codes are called Gold Codes and can be used if multiple transmitters need to be accommodated.

#### **4.1.2 Design Parameters for MLSR Configurations**

The previous section explored a simple and inexpensive method of generating a suitable PN Code. It was found that Maximum Length Linear Shift Register (MLSR) feedback configurations can provide bit sequences with the correct randomness and correlation properties. MLSRs can further be used in a slightly more complex configuration to generate Gold Codes, should multiple transmitters be needed.

It is not necessary to accommodate multiple transmitters yet, as the goal is to design and implement a working example. An MLSR configuration was therefore chosen. The most important property regarding a MLSR configuration (from a design point of view) is the length of the shift register. Most commercially available shift registers are eight bits long, which would provide for a PN Code that is 127 bits long. The question is now whether 127 bits is long enough.

The length of the PN bit sequence determines several things. A longer sequence will require more time to acquire and track, since the receiver will have to measure the entire correlation function. Once the correlation function has been measured and the peak determined, it will require less time to track the peak; only the area around the peak needs to be measured. There are methods to reduce the amount of time necessary to lock onto the incoming signal. A preamble could be added to the sequence. Instead of measuring the entire correlation function, the receiver looks for the preamble; once found, the receiver can align its PN Code with the incoming signal.

Another aspect to take into consideration when looking at the bit sequence length is the correlation function itself. A longer bit sequence will produce a sharper correlation peak, consider the following equation for the auto-correlation of a periodic bit sequence (taken from [13]):

$$C(\tau) = \frac{1}{p} \sum_{n=1}^p a_n a_{n+\tau} \quad (4.2)$$

where  $p$  is the length and  $a_n$  is the  $n$ th bit of the sequence.  $\tau$  can be thought of as the phase shift. When working with binary numbers 1's and 0's are normally used. It is more convenient to use +1's and -1's when dealing with shift register sequences, in which case the following is true for MLSR sequences [5] [13] (equation taken from [13]):

$$C(\tau) = \begin{cases} 1, & \tau = 0 \\ -\frac{1}{p}, & 0 < \tau < p \end{cases} \quad (4.3)$$

Therefore, a larger  $p$  will result in a sharper auto-correlation function.

Thus far the periodicity of bit sequences has been slightly unclear. Sometimes they have been treated as a single set of bits with length  $p$ , sometimes (as in the auto-correlation function above) they are treated as an infinite repetition of bits with period  $p$ . It is useful to look at these bit sequences as a single set of  $p$  bits, but the physical implementation of the PN signal must also be considered. Shift register sequences generate periodic signals, which will continue to repeat for as long as the shift register is supplied with an appropriate clock signal. This periodicity restricts the maximum unambiguous range that can be measured. The maximum range that can be measured will also depend on the rate at which these bits are generated, which is in turn dependant on the frequency of the clock used to drive the shift register. Consider the equation for the distance that an electromagnetic wave travels given travel time:

$$l = ct_{travel} \quad (4.4)$$

Consider also that if the shift register is driven by a clock signal with a fixed frequency  $f_{clock}$  the period between consecutive bits (also called chips) will be the same as the period of the clock signal:

$$\begin{aligned} T_{chip} &= StartTime(a_{n+1}) - StartTime(a_n) \\ &= T_{clock} \\ &= \frac{1}{f_{clock}} \end{aligned} \quad (4.5)$$

The range is determined by the phase difference or displacement that is measured between the incoming and receiver PN Codes. The maximum phase difference that can be measured is  $p$ , the length of the bit sequence. The maximum travel time (and therefore range) that can be measured will be the period of the PN Code signal, which can be expressed as follows:

$$\begin{aligned} T_{PN\ Sequence} &= pT_{chip} \\ &= \frac{p}{f_{clock}} \end{aligned} \quad (4.6)$$

Substituting into Equation 4.4 gives:

$$Range_{max} = \frac{cp}{f_{clock}} \quad (4.7)$$

For  $f_{clock} = 1$  MHz (approximately the chipping rate of civilian GPS navigational signals) and propagation in free space the maximum unambiguous range that can be measured using a bit sequence of length 127 is 38 km.

Another aspect to consider is the influence of sequence length on the number of multiple users. For a given sequence length there is a maximum number of bit combinations that possess adequate randomness, auto-correlation and very importantly, cross-correlation properties. This must be taken into account when expanding to multiple transmitters.

Examining the effects of shift register size brings into question another design parameter, namely clock frequency. This parameter is more problematic than bit sequence length, as knowledge of the receiver is needed to make a proper decision. Shorter chip periods translate to higher range resolution. Receiver design will be constrained by cost and availability of components, which will in turn influence the most appropriate choice for clock frequency.

The example mentioned earlier of  $f_{clock} = 1$  MHz was not entirely happenstance. Not only is this frequency very close to that employed by GPS satellites, it also divides into 48 MHz. This is the maximum operating frequency of a commonly available microcontroller, the PIC18F2550. Instructions are executed at a fraction of the microcontroller's operating frequency, specifically 12 million instructions per second. Details of the receiver's design, including how control of the PN signal's timing is achieved, will be discussed in Chapter 5.

This section has so far described the two main design aspects of an MLSR configuration: Shift register length and clock frequency. It was decided to stick with one shift register, which can generate a sequence with a period of 127 bits. It should provide enough unambiguous range and a sufficiently sharp auto-correlation function whilst being short enough to track without difficulty. Clock frequency was also set to 1 MHz; this choice will be explained in the next chapter when receiver design is examined.

### 4.1.3 Implementation

The previous section of this chapter explored the two most important parameters of MLSR configurations, at least from a design perspective. The section concluded that, for the purposes of creating a functioning transmitter, a single eight bit shift register operating at a clock frequency of 1 MHz should be sufficient. More specifically, an eight bit serial-input parallel-output shift register should be used. This fixes the layout of the shift register feedback configuration, as depicted Figure 4.3.

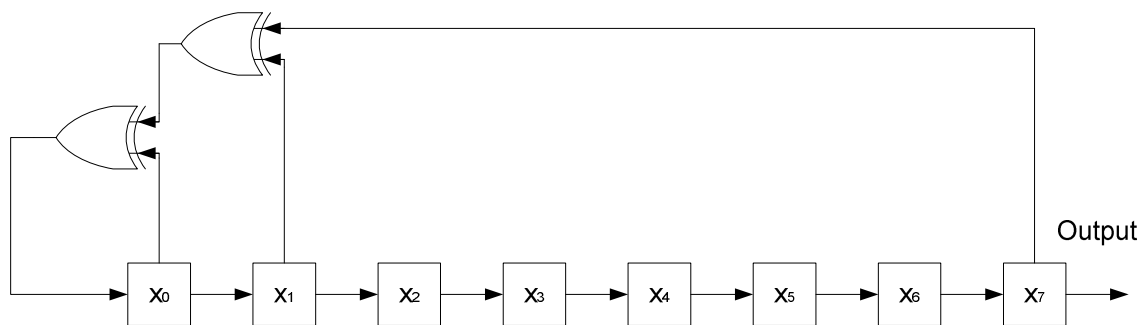


Figure 4.3

A diagram showing the layout of the shift register feedback configuration that will be used to generate the PN Code.

Logical Exclusive OR (XOR) gates are used to achieve modulo 2 addition. The output signal could be taken from any of the shift register's elements. The position of the elements that must be used to form an MLSR was taken from [13], which also provides a table of feedback configurations for various shift register lengths.

There are still a few components missing from the diagram above. A mechanism is required to force the circuit into a consistent initial state. The master reset function of the shift register could be used, which would force all the elements in the register to logical low. A small problem arises when this is done, as the all zero state is an invalid state for any MLSR configuration. The feedback circuit will produce another zero as next input, which would perpetuate the all zero state. To solve this a few extra components are needed to jump-start the sequence.

A very basic circuit using NOR-gates is added to monitor the contents of the shift register, shown in Figure 4.4. If there is at least one non-zero bit the circuit simply passes the result from the modulo 2 adder to the shift register's input. However, if all the bits are zero the circuit overrides the modulo 2 adder and feeds a logical one to the shift register's input, thus forcing the MLSR into a consistent state.

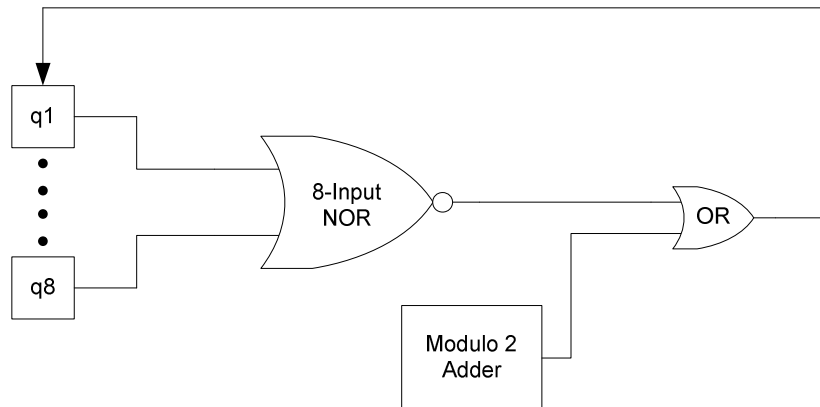


Figure 4.4

A diagram showing the circuit that will force the PN Code Generator into a consistent state at startup.

## 4.2 RF Interface and Peripheral Circuits

The transmitter had flexibility as its most important requirement for the RF Interface section, because the ranging signal it produces will be used for development and final testing. It is therefore essential that enough room be left to adjust parameters like the shift register's clock frequency and the carrier frequency.

### 4.2.1 Peripheral Circuits

The peripheral circuitry consists of the power supply and the clock signal source. Since adjustability is very important the clock signal must be inserted from an external source. This is very useful for studying the ranging signal.

The power supply is equally simple to design. All the active circuits require +5 V, for which a standard voltage regulator circuit is quite sufficient.

### 4.2.2 RF Interface

The RF Interface has to take the signal from the PN Code Generator and multiply it with an appropriate carrier signal. Flexibility is very important as design parameters for the receiver are not firmly fixed yet.

As with the clock signal the decision is to use an external source for the carrier signal. This means that a mixer is the only component still needed to produce the final ranging signal.

The SA602 mixer IC manufactured by NXP is the selected component for this application. It is a low cost, versatile product with a number of additional features. Implementing the SA602 is quite simple. The mixer requires two signals, a local oscillator and a data signal. Conventionally, the local oscillator is used as the carrier signal while the data signal is fed to the mixer input. However, for this application it is easier to use the PN Code signal as a local oscillator and feed the carrier to the mixer input. The diagram in Figure 4.5 shows how the mixer and the PN Code Generator are connected.

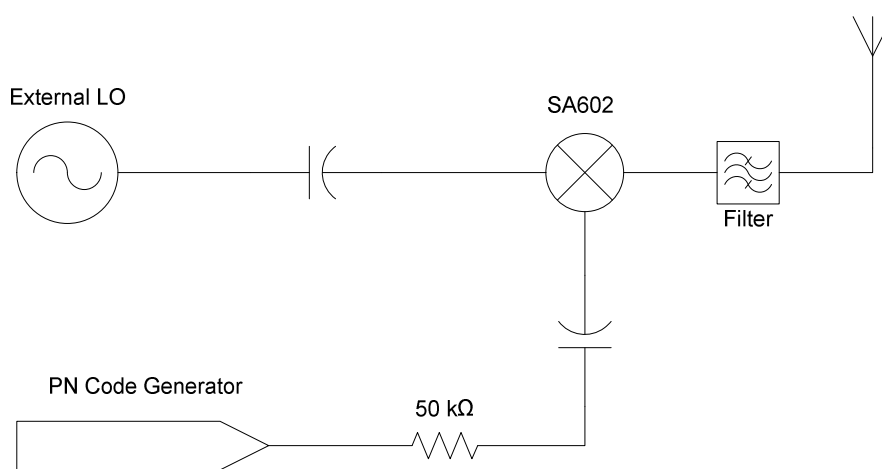


Figure 4.5

A diagram illustrating the layout for the RF Interface.

## 4.3 Experimental Measurements

A working transmitter has now been designed and implemented. The following two sections will present a number of physical measurements. The first section will mainly be dealing with the PN Code signal itself, showing what the signal looks like and highlighting any important properties. The second section will use the transmitter and a Spectrum Analyser to corroborate the simulation results from Chapter 3.

### 4.3.1 PN Code Signal Characteristics

The following figures show various measurements of the PN Code Generator's output signal. Figure 4.6 shows the PN Code signal as measured by an oscilloscope.



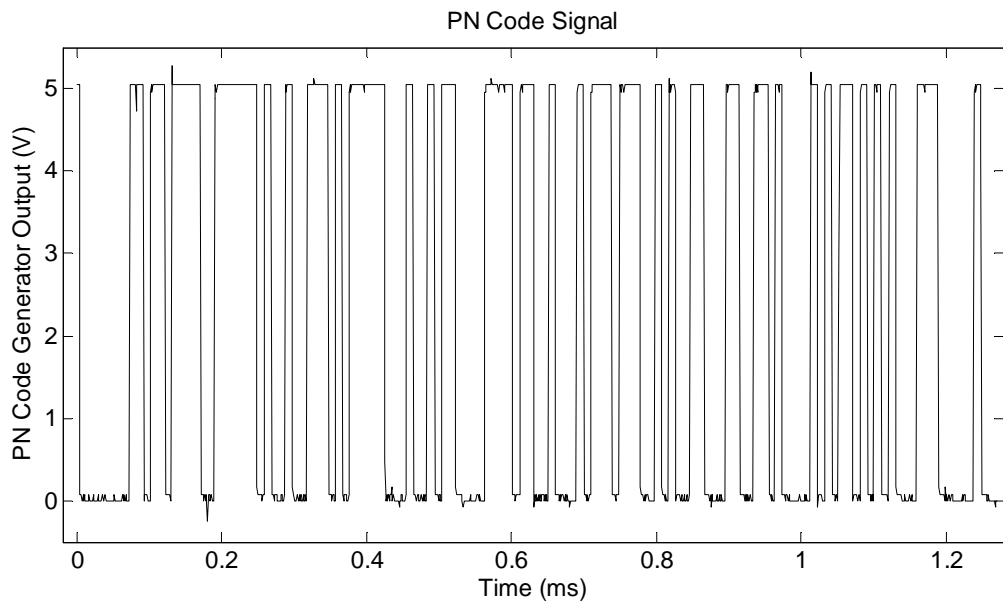


Figure 4.6

A graph showing the measured output for the PN Code Generator.

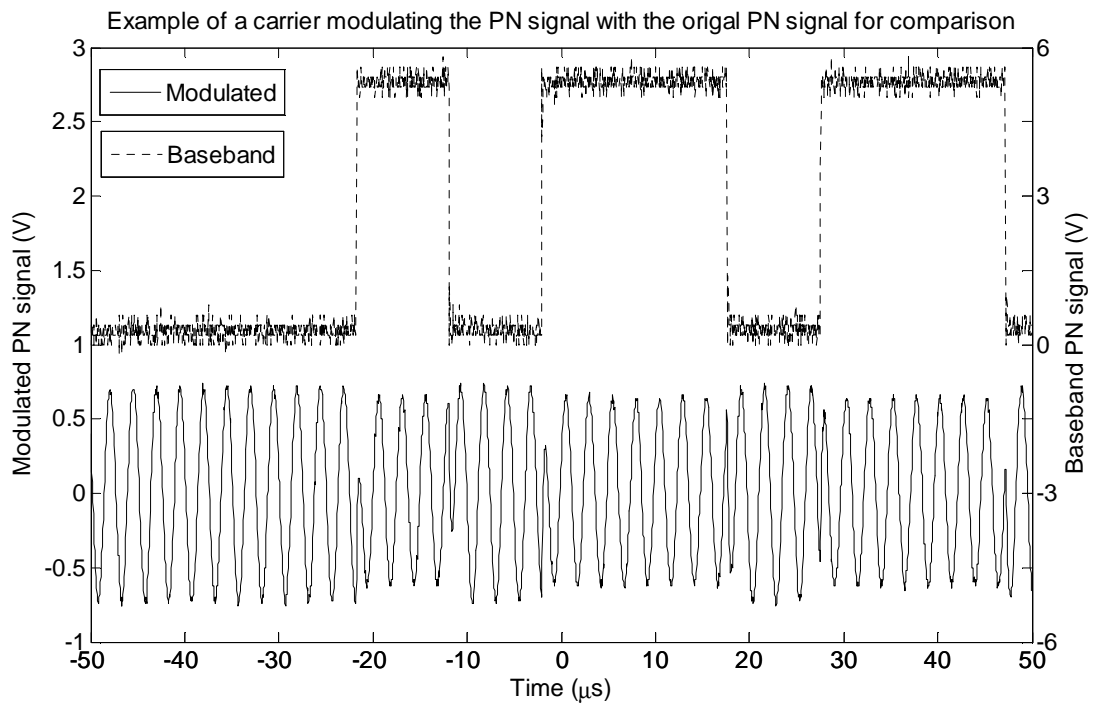


Figure 4.7

A graph showing the modulated output signal produced by the transmitter. The baseband PN Code signal is also shown for comparison.

Figure 4.6 shows the unmodulated version of the PN signal. The pseudo-randomness of the code can be seen here; it looks like a baseband binary data signal that is transmitting a jumbled sequence of bits. Figure 4.7 shows a similar measurement of the PN signal, this time after modulation.

The carrier frequency in Figure 4.7 was chosen in such a way as to show clearly the transitions in phase as the PN Code flips from a low to a high and vice versa.

The next two figures show the transmitter's output signal as measured by a Spectrum Analyser. Figure 4.8 shows the  $\text{Sin}(x)/x$  envelope:

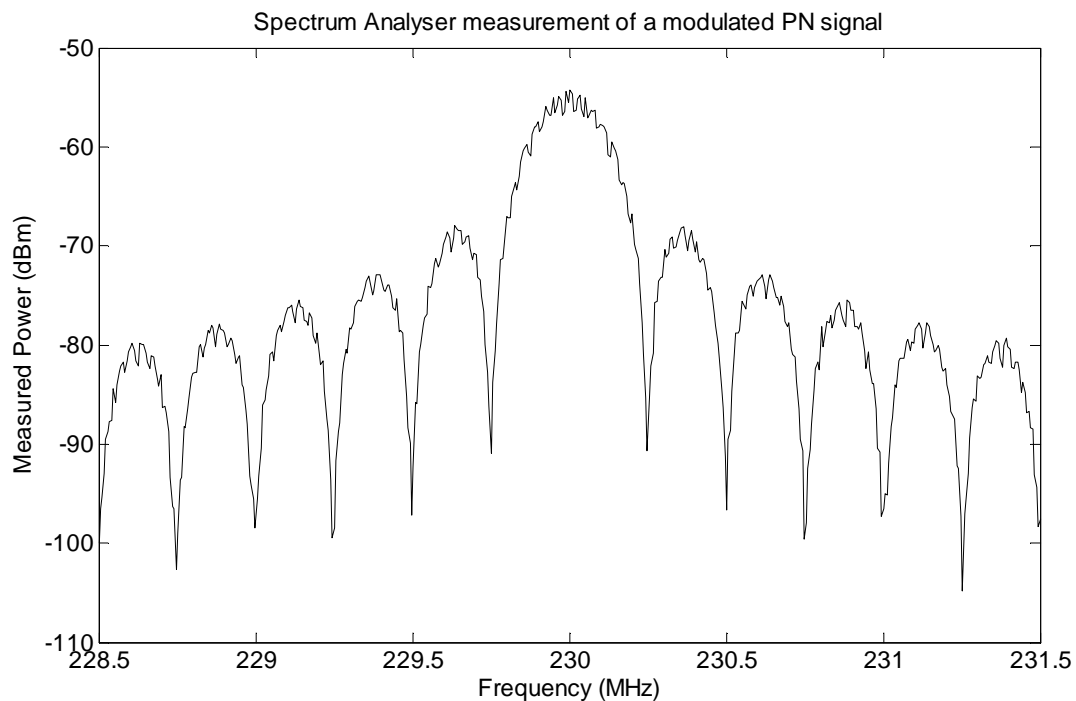


**Figure 4.8**

**A graph showing the measured spectrum of a modulated PN Code signal.**

To show the  $\text{Sin}(x)/x$  envelope the resolution and video bandwidths of the spectrum analyser were both set to wider values. While this measurement is useful to look at, it does not give a true account of the PN signal. The second measurement taken with the spectrum analyser, shown in Figures 4.9 (a) and (b), gives a more accurate depiction of the ranging signal's spectrum.

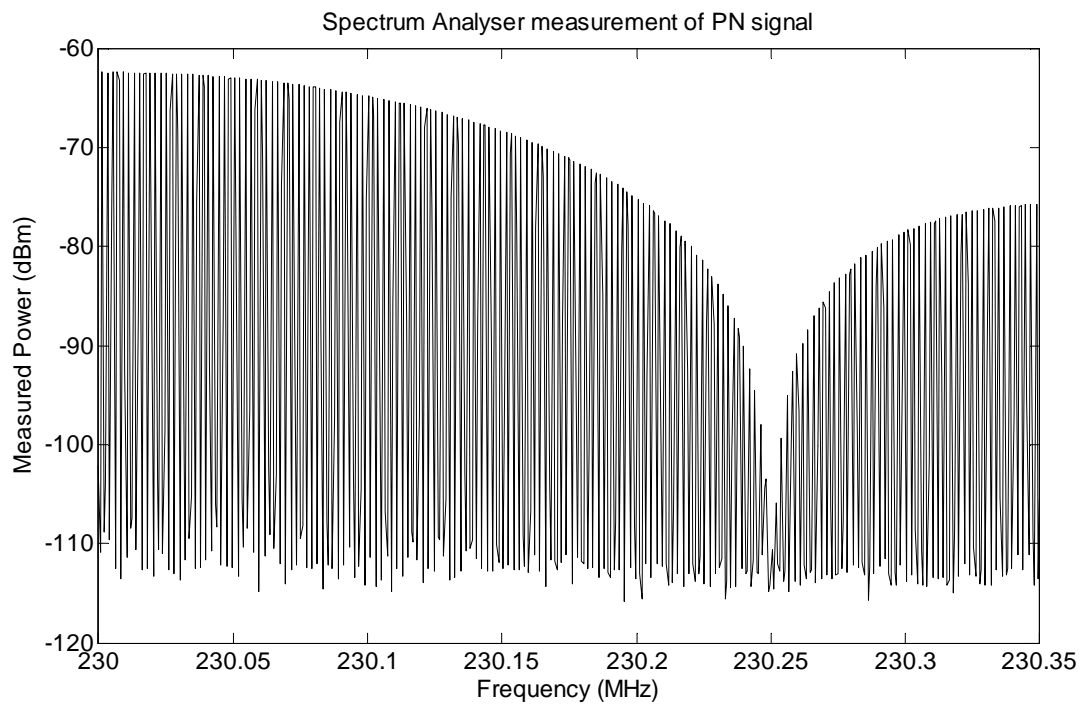


Figure 4.9 (a)

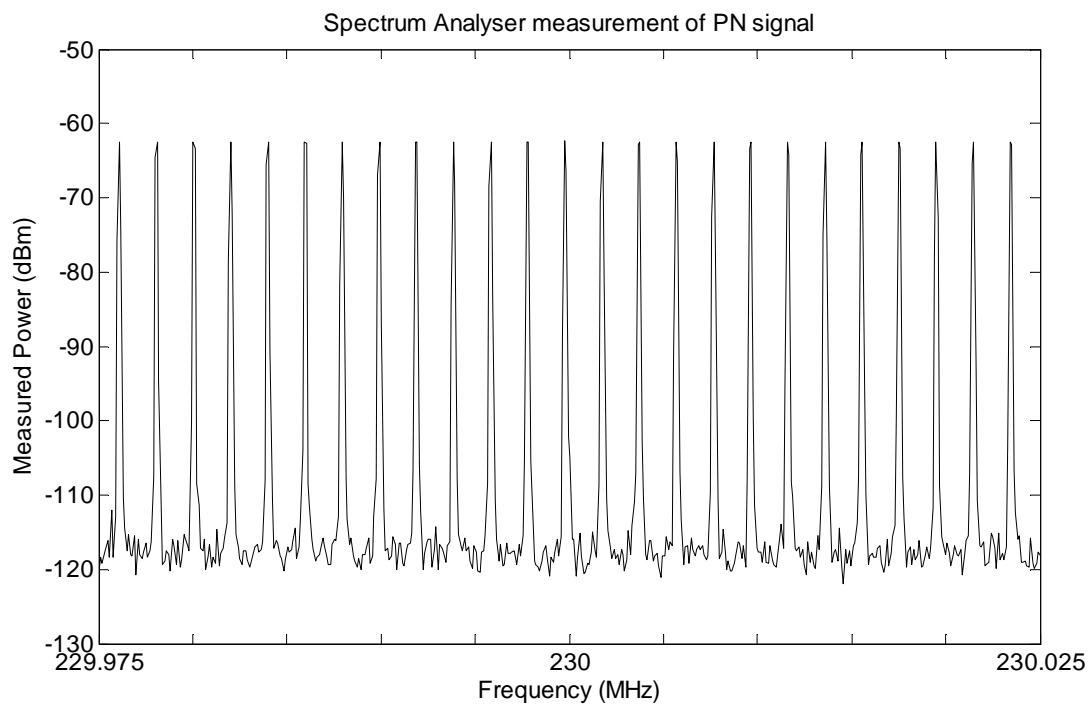


Figure 4.9 (b)

Figures 4.9 (a) and (b) illustrate the sampled nature of the frequency-domain PN Code signal.

The resolution and video bandwidths are reduced to narrower values for this measurement to show that the PN signal's spectrum consists of a series of impulses. This sampled appearance is of course due to the periodic nature of the time-domain signal.

### 4.3.2 Corroborating Measurements

Consider the following practical measurements:

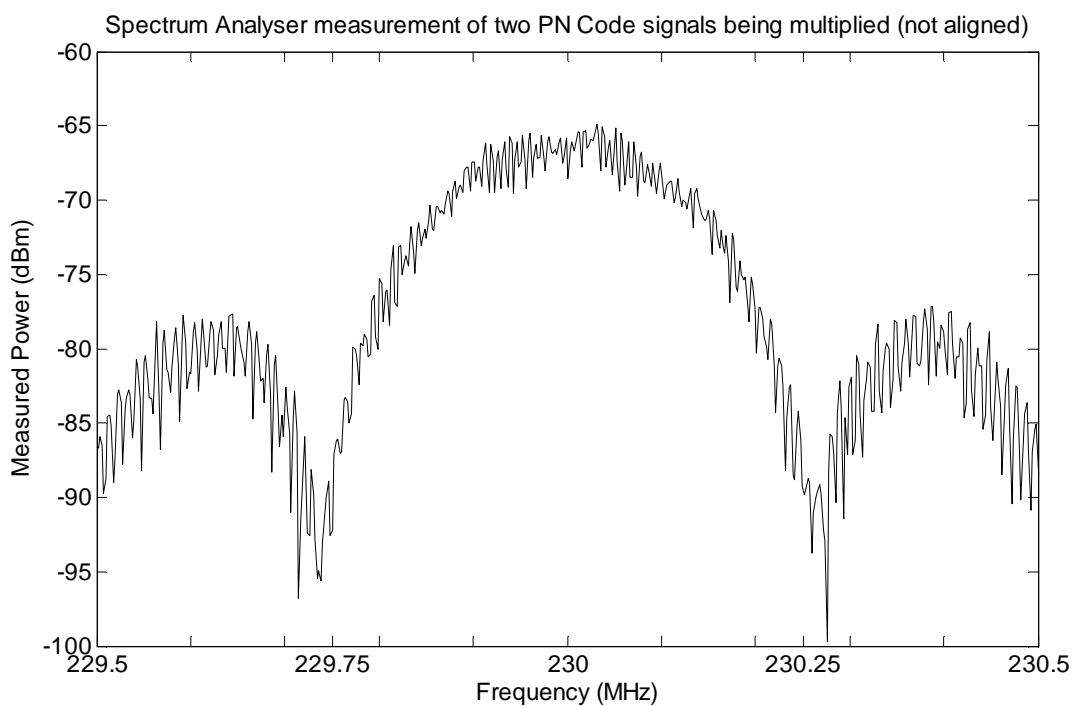


Figure 4.10

**A graph showing a practical measurement of two PN Codes after multiplication. The PN Codes are not aligned.**

Figure 4.10 is a measurement of two PN Code signals after multiplication with each other. The same  $\text{Sin}(x)/x$  envelope that was shown in the previous section (see Figure 4.8) can be seen here. These two PN Code signals are not aligned and the result is another PN Code signal.

Figure 4.11 is a measurement of the same two PN Code signals, only this time they are properly aligned. Multiplication has, in this case, stripped the PN Code away, thereby recovering the original carrier signal. The two figures show a difference of approximately 15dB (near the carrier) in power levels between a

regular PN Code modulating a carrier and that same signal after multiplication with a properly aligned PN Code. This is an important property of Spread Spectrum signals, both for this project and most other Spread Spectrum applications.

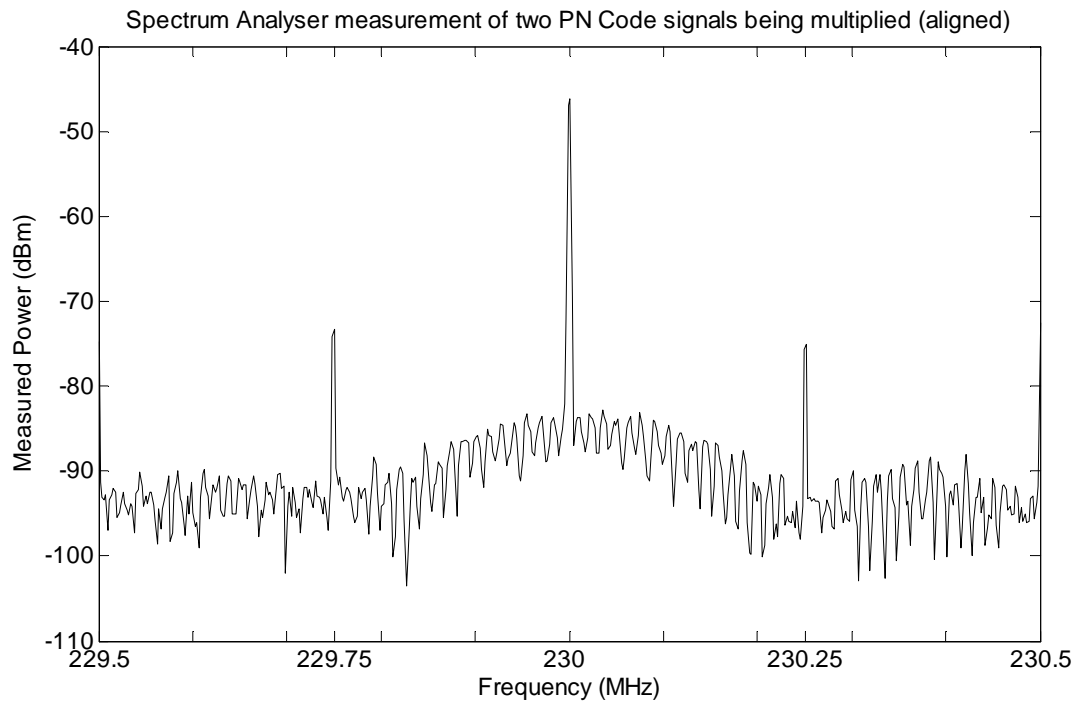


**Figure 4.11**

**A graph showing a practical measurement of two PN Code signals after multiplication. In this example the two PN Codes are aligned.**

The next step is to confirm, with physical measurements, the results from Chapter 3. A Spectrum Analyser was used to measure the maximum output power for the configuration in Figure 4.12. Two PN Codes are generated, of which the first one is multiplied by a carrier signal. That signal is then multiplied with the second PN Code, which is equivalent to the configuration of the receiver proposed in the Simulink model in Figure 3.10 (from Chapter 3). A Spectrum Analyser is utilised as a bandpass filter and power detector, measuring the power in the vicinity of the carrier. The two PN Codes are operated at slightly different chipping rates.

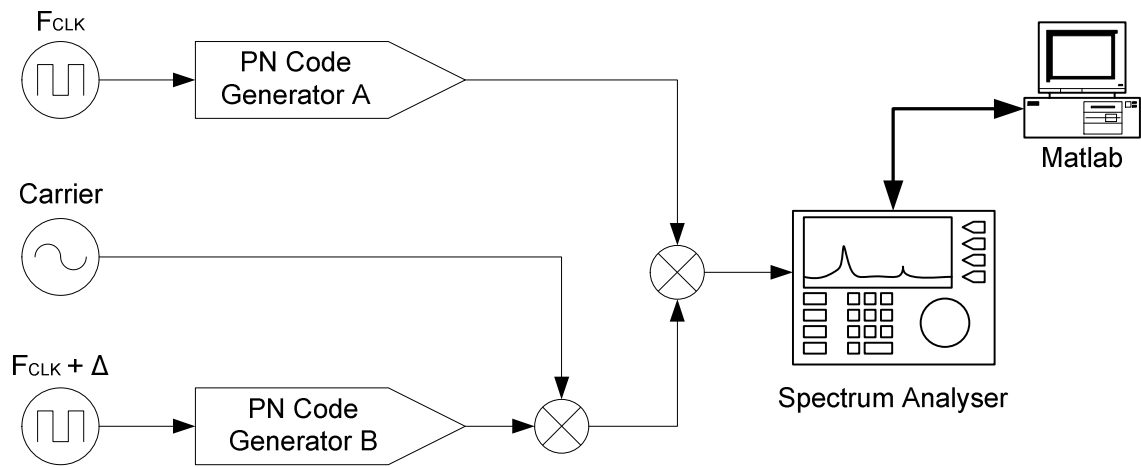


Figure 4.12

A diagram illustrating the setup for the measurement that will confirm the simulated results from Chapter 3.

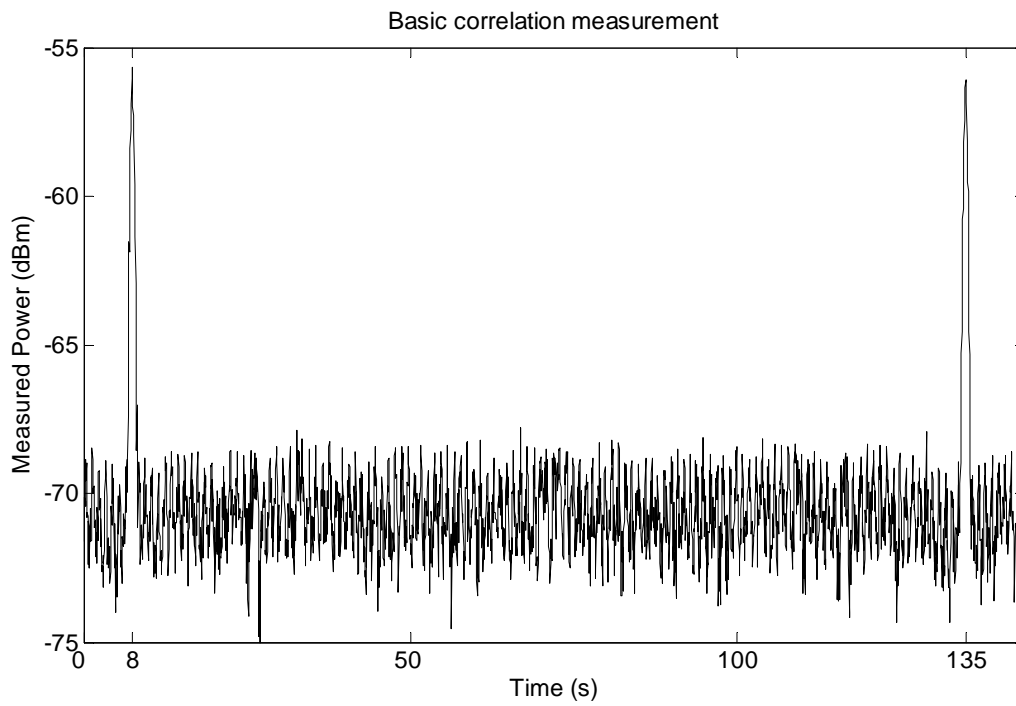


Figure 4.13

A graph of the output power measured by the configuration in Figure 4.12.

Operating the two PN Codes at slightly different chipping rates can be considered equivalent to a receiver sweeping the amount of delay between them. The difference in chipping rates is kept small enough that the Spectrum Analyser can keep up with each measurement. The graph in Figure 4.13 clearly shows a maximum where the two PN Codes are aligned. This practical measurement confirms what the simulations suggest: a simple configuration consisting of a multiplier, filter and power detector is capable of determining the alignment of two PN Codes. Combining it with a delay control mechanism makes it possible to measure the amount of delay that is needed to align the two PN Codes, which can in turn be converted to a range measurement.

# Chapter 5

---

## Receiver Design

Chapter 3 developed a strategy for extracting ranging information from the transmitter signal. It proposed a simple configuration using a multiplier, filter and power detector. Simulations and a preliminary measurement (using two PN Code Generators and a Spectrum Analyser) showed that the strategy can be effective. This chapter will now convert that basic layout into a detailed technical design.

### 5.1 Basic Layout

The diagram in Figure 5.1 illustrates all the modules that will be used to create the receiver. Most of these modules have been mentioned in Chapter 3, including the PN Code Generator and Power Detector. Other modules that will be needed include an RF Frontend and a Digital Processor.

The diagram does not only show the basic building blocks of the receiver, but also the path that the incoming signal would follow. The first block it has to pass through is the RF Frontend. This module is responsible for signal conditioning: Receiving, filtering, amplifying and mixing it down to an appropriate carrier frequency.

After signal conditioning two more blocks are incorporated, the PN Code Generator and another mixer. A reference signal is created by the PN Code Generator which is then fed, along with the conditioned transmitter signal, to the mixer.

The mixer forms the first part of a module that can be thought of as the Detector or Correlator. This module is responsible for comparing the conditioned transmitter signal with the reference PN Code signal. After the two signals are mixed, the resulting signal is passed through a narrow bandpass filter and fed to the Power Detector.

The reading from the Power Detector passes to the Digital Processor, which is the next module. The Digital Processor module has several functions, such as converting the voltage level from the previous section (Detector) into a digital power measurement. Other functions include control of the PN Code Generator and serial communications. Figure 5.2 shows a photograph of the receiver.



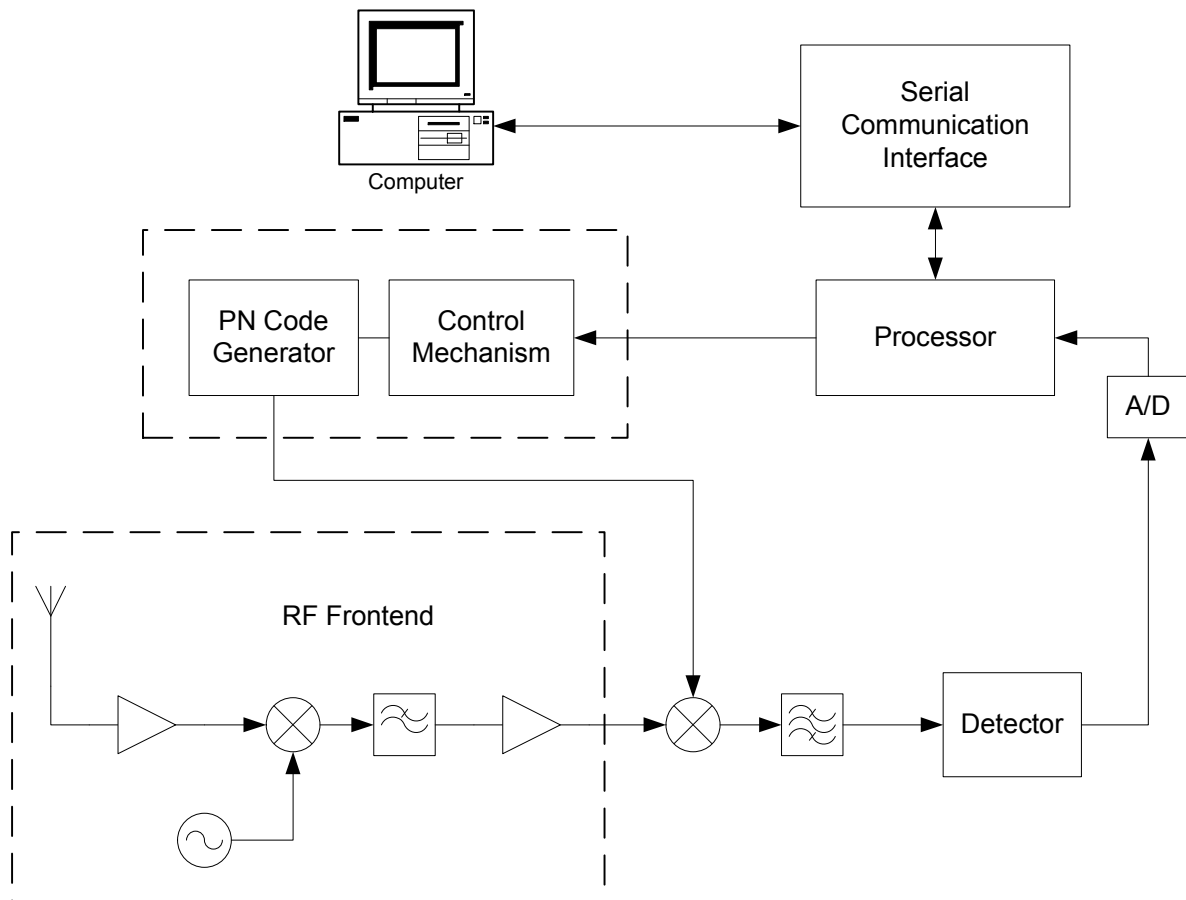


Figure 5.1

A diagram illustrating the basic layout for the receiver.

## 5.2 RF Frontend

This is a crucial point of entry for the transmitter signal. All the major signal conditioning will be done by this module, producing something that can be compared directly with the reference PN Code. Fortunately there is a standard pattern to work from when designing any RF receiver. The following components will be required:

- Antenna
- Low Noise Amplifier (LNA)
- At least one mixer
- A Local Oscillator (LO) to drive the mixer
- More amplifiers
- Filters

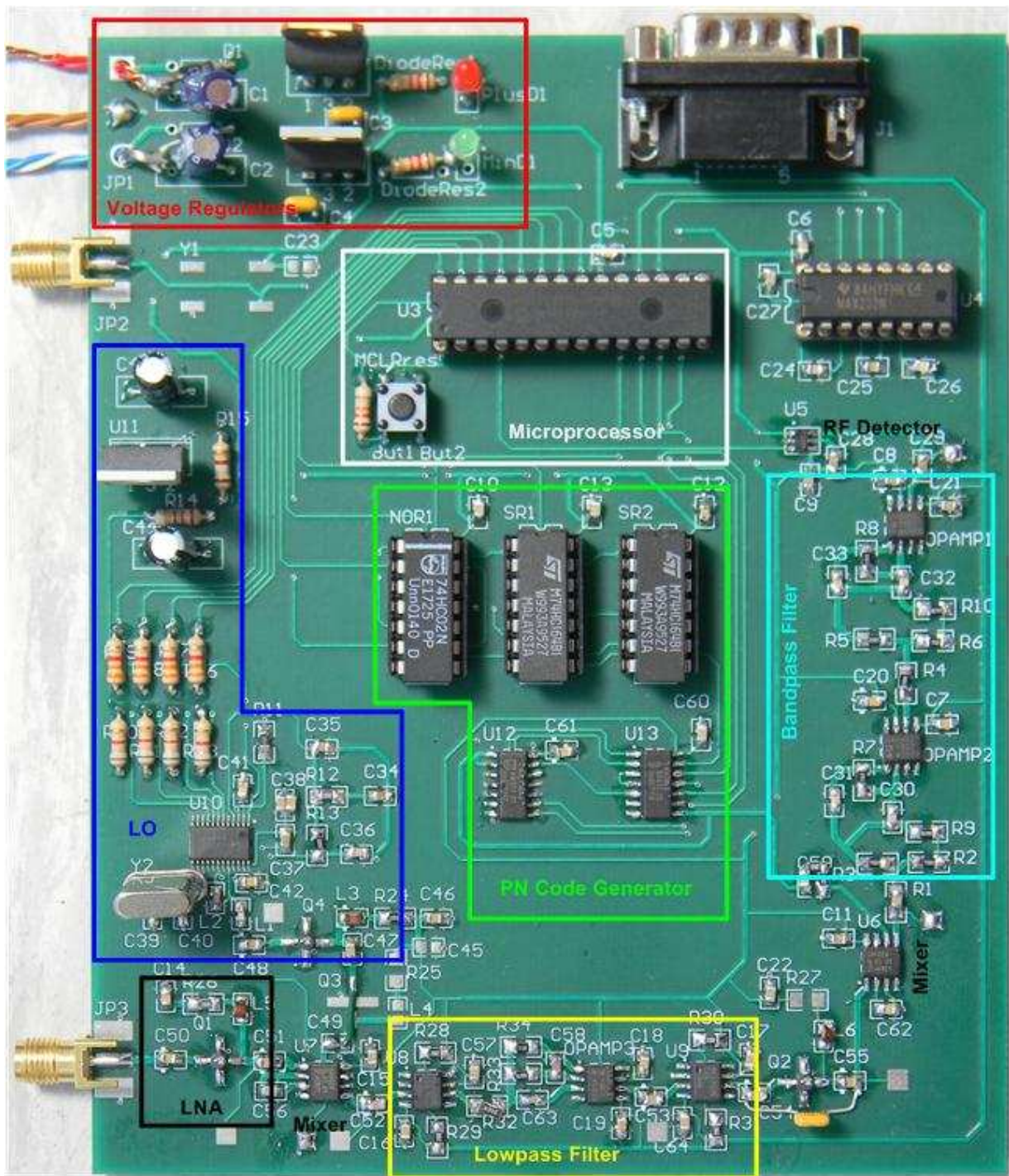


Figure 5.2

A photograph of the completed receiver board.

There are several important aspects to consider during the design/selection of each of these components, such as operating frequency and bandwidth. Bandwidth should be enough to allow the main signal lobe from the transmitter to pass without any attenuation. Since the PN Code Generator will be operated at 1 MHz a bandwidth of 2 MHz should be sufficient.

The next decision is carrier frequency, which is more difficult. Several factors must be kept in mind, but the most restrictive one is availability of spectral real estate. Transmission of radio signals is strictly regulated by Government, with only a few bands available to the general public. This, along with other factors, led to the 434 MHz ISM band being chosen. It is high enough in frequency to allow for a reasonably sized antenna, whilst being low enough in frequency to allow for an easier design. There is also the added bonus of it being a popular design frequency for various applications, such as remote controls for motor vehicle alarms, which should provide a number of off-the-shelf components. Figure 5.3 shows the basic layout for the RF Frontend.

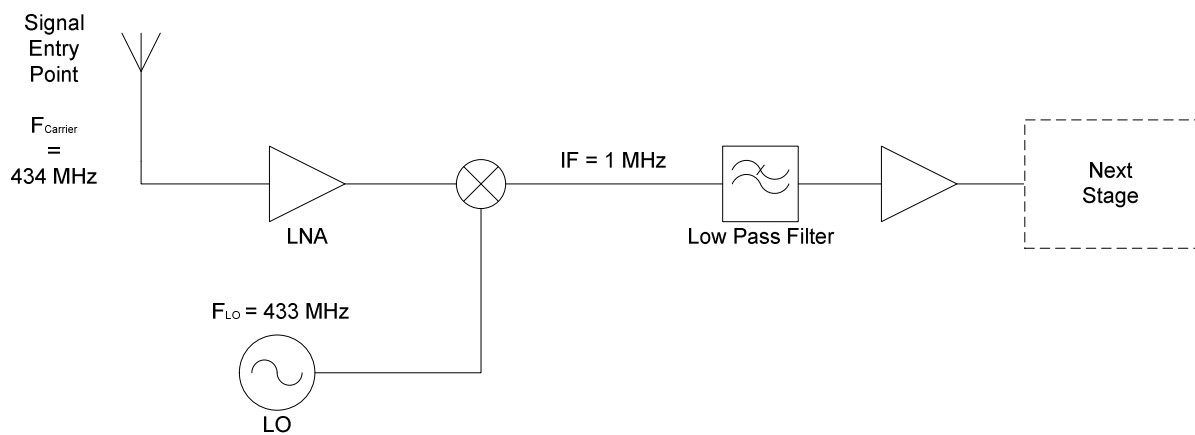
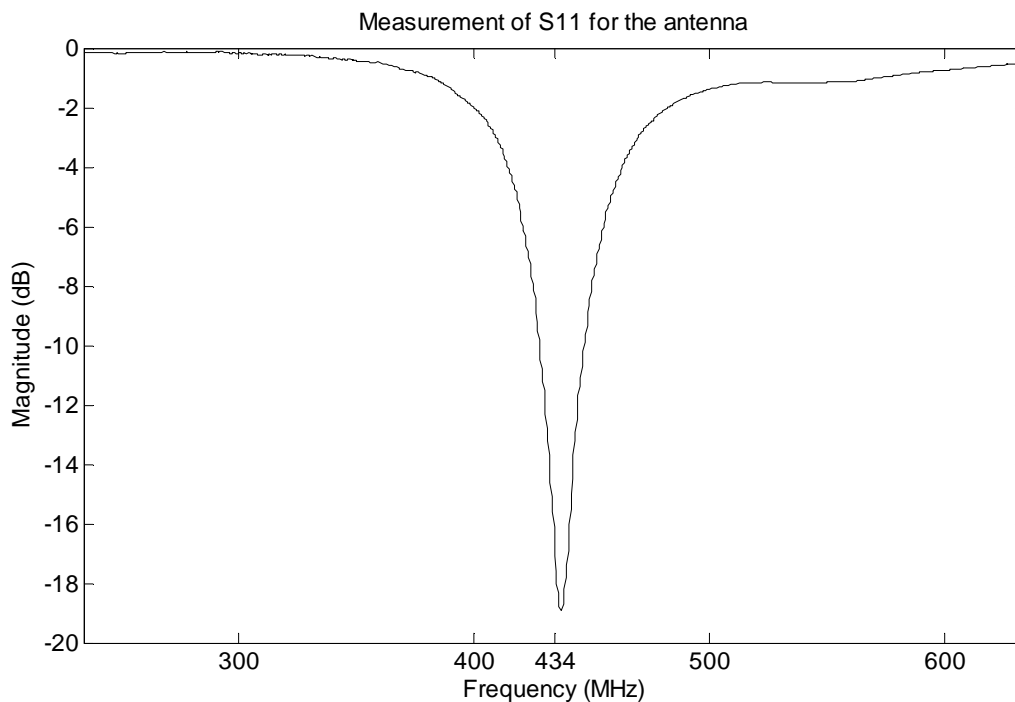


Figure 5.3

A diagram of the RF Frontend's layout.

### 5.2.1 Antenna

This is one of the easier components to place, as there are off-the-shelf options to choose from. The selected product for the receiver (and transmitter) is the T1.10 Helical Antenna manufactured by Taoglas. It operates across the desired frequency band (433 - 435 MHz), it has an impedance of  $50 \Omega$  and it is omnidirectional. This satisfies all the requirements for the antenna. Figure 5.4 shows the return loss of the antenna.



**Figure 5.4**

**A graph illustrating the return loss of the antenna.**

Other options include the design of a patch antenna or a small loop antenna [14].

### 5.2.2 LNA

Low Noise Amplifiers can be critically important components in receiver systems, since they largely determine the Noise Figure for the entire chain of components. In systems with very stringent Signal-to-Noise Ratio requirements this can be very problematic.

The requirements for this receiver's LNA are mostly determined by economic, rather than technical, considerations. A cost effective solution, that is capable of doing the job, is therefore needed. Monolithic amplifiers such as the ERA and MAR ranges manufactured by Mini-Circuits are quite sufficient.

Investigation of the various monolithic amplifiers led to the selection of the MAR-6+ amplifier. It has sufficient bandwidth (DC – 2 GHz), good gain (up to 22 dB) and a Noise Figure (3.0 dB) that is low enough to deliver adequate performance, but is also an economical choice.

Implementation of the MAR-6+ amplifier is quite easy, as long as basic high frequency layout principles are kept in mind. The recommended application circuit, shown in Figure 5.5, is used; with care taken to ensure that the amplifier is well grounded and that the biasing circuit is tightly packed. This should keep parasitic capacitances and inductances to a minimum.

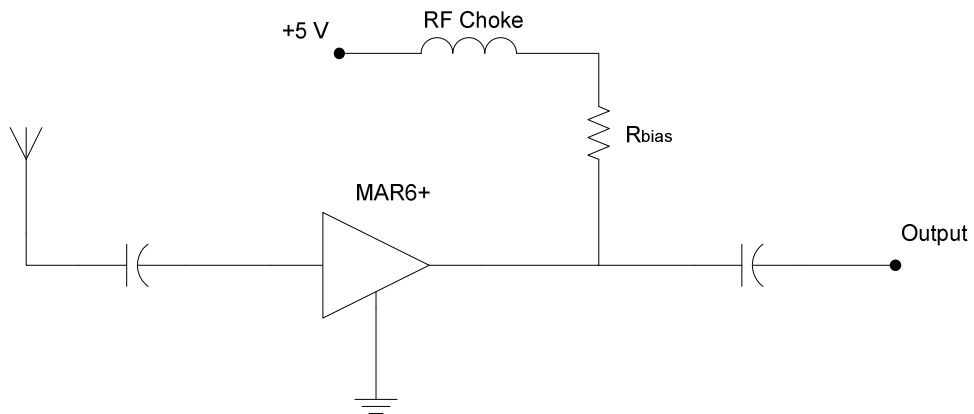


Figure 5.5

Application circuit for the MAR6+ amplifier.

<u>Parameter</u>	<u>Value</u>	<u>Remarks</u>
Gain	19 dB	Measured at 434 MHz
Noise Figure	3.8 dB	Measured at 434 MHz
Output Power at 1 dB Compression	1 dBm	Measured at 434 MHz
Minimum Gain	10 dB	Measured at 2 GHz, maximum rated operating frequency
Maximum Gain	21 dB	Measured at DC

Table 5.1

Table 5.1 shows a number of measured parameters for the amplifier. These parameters show that the MAR-6+ is an acceptable choice.

### 5.2.3 Mixer

The mixer is an important part of any transceiver system, as it allows the designer to move the data signal's carrier frequency up or down. It is an inherently non-linear component and as such there is a price to pay. Besides the desired action of multiplying the data signal with a new carrier signal, all manner of unwanted signals are also present in the output spectrum. Fortunately, most of the unwanted signals can be mitigated by controlling the spectrum at the input and by filtering the output. This will be handled by another subsection of the RF Frontend.

Selection of the appropriate component depends, as always, on the specific requirements of the application. The mixer is no exception. Component cost and availability is, again, the most important criteria, after which technical aspects like operating frequency range and insertion loss are considered. Since the carrier frequency of the incoming signal is 434 MHz the mixer must be able to handle frequencies up to about 450 MHz. Insertion loss, although not as important as operating frequency, should be kept as low as possible.

With these requirements in mind the SA602A, which was used to construct the transmitter, looks like a good choice. It is a double-balance mixer designed to operate in the VHF range (although it can be used as high as 500 MHz), with added functionality like an integrated oscillator and amplifier. It is also one of the most cost-effective products available.

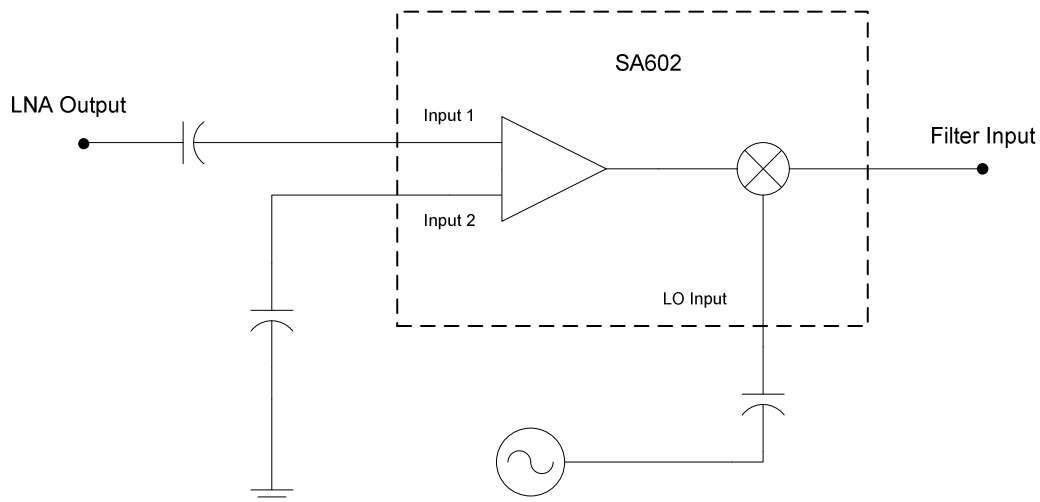


Figure 5.6

A diagram illustrating the application circuit for the SA602 mixer.

There are several suggested configurations for the input, output and oscillator subsections. The intended application of the SA602A will determine which configuration is best suited to the design. Since the incoming signal has a carrier frequency of 434 MHz, it will not be possible to use the built-in oscillator. It will therefore be necessary to use an external LO. Both the input and output used the Single-Ended configurations, as these are the simplest. More complex configurations can be used to filter the output, but since there is a separate section to deal with filtering the mixer's output it was decided to use the simpler option. Figure 5.6 shows the layout for the mixer.

Parameter	Value	Remarks
Gain	16.5 dB	Measure at 434 MHz
Frequency Range	>600 MHz	Measured up to 800 MHz
Output Power at 1 dB Compression	-1 dBm	Measured at 434 MHz
LO Input Power	0 dBm	
Port Isolation LO – Output	27 dB	LO power measured at output port
Port Isolation Input - Output	20 dB	Input power measured at output port

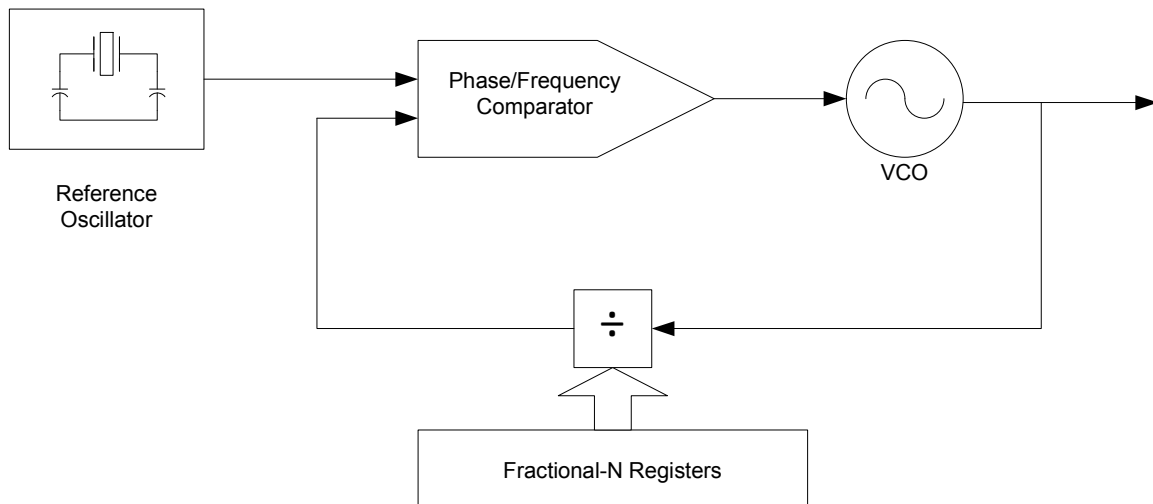
**Table 5.2**

Table 5.2 shows a number of measured parameters for the mixer. The SA602 performs quite well, adding gain of almost 17 dB.

#### **5.2.4 Local Oscillator**

The Local Oscillator (LO), like the mixer, is a well-known part of almost all transceiver systems. It must provide a stable frequency source with which to drive the mixer. Designing oscillators can be very difficult, depending on the requirements of the application [15]. For this project it was decided to use a Fractional-N Phase Locked Loop (PLL) technique, as this allows for more flexibility where frequency is concerned [16].

Figure 5.7 illustrates the basic layout of a Fractional-N PLL. Various subcomponents are required to build the PLL, but there are some commercial products available that combine all these into one integrated package.



**Figure 5.7**

**A diagram illustrating the basic layout for a Fractional-N PLL.**

A number of samples were obtained from Analog Devices for their ADF7011 product. The ADF7011 is actually an ASK/FSK/GFSK/OOK transmitter IC for use in the 433 MHz – 435 MHz and 868 MHz – 870 MHz ISM bands, but can be configured to function as a frequency source. It contains all the basic components needed to implement a PLL.

Figure 5.8 is a diagram of the ADF7011 that shows all the subcomponents implemented within the product and how they are connected. It also shows a number pins, some of which are used to input data, some of which are used to output data, as well as others that are used to connect additional circuits to the device.

Several additional components are needed to operate the ADF7011:

1. Power supply.
2. Microprocessor, for setting up the various registers and transmitting data.
3. Crystal resonator and capacitors to complete the reference clock module.
4. Loop Filter between the output of the Phase/Frequency Detector and the VCO input.
5. Matching Circuit between the RF output and the desired load impedance.
6. Capacitors, tied between GND (ground) and the  $C_{REG}$  pin as well as between  $C_{REG}$  and  $C_{VCO}$ .
7. One resistor tied between  $R_{SET}$  and GND.



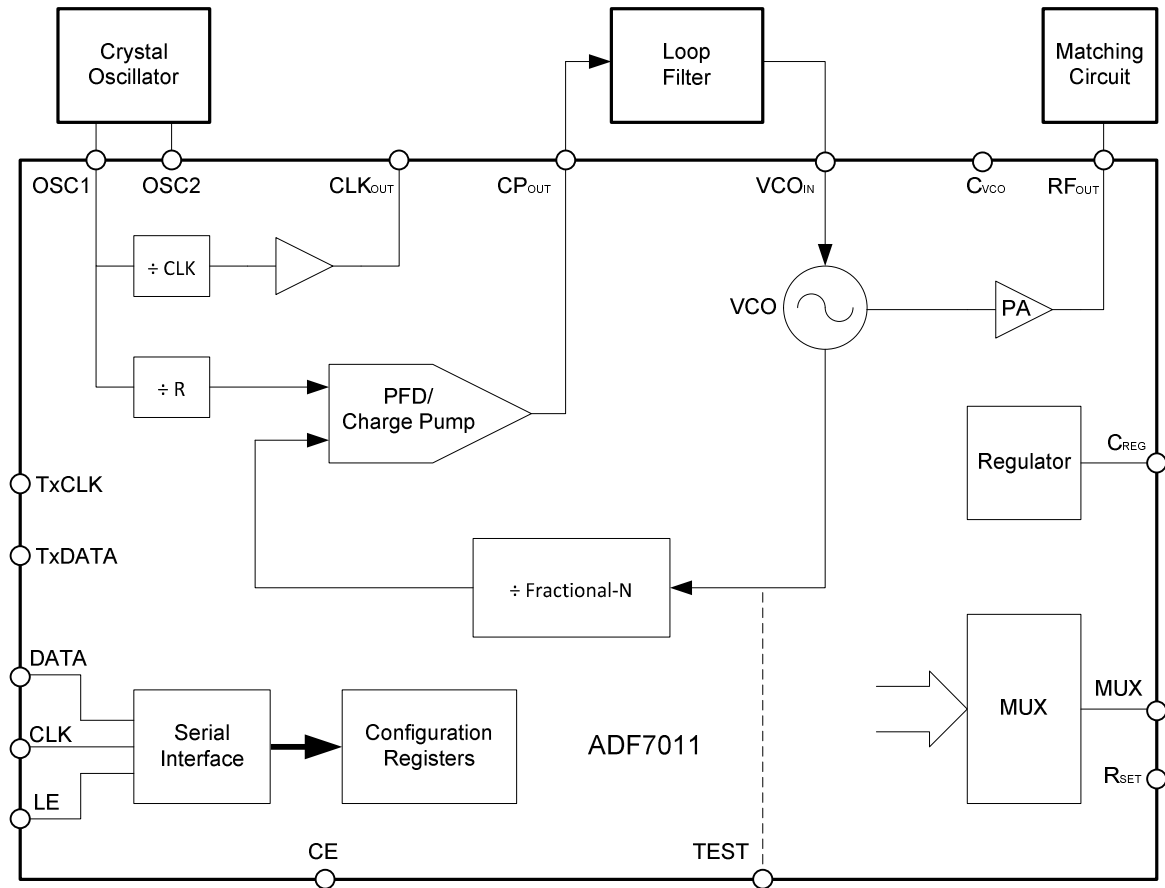


Figure 5.8

A diagram of the internal connections of the ADF7011 component.

These are all discussed in more detail in Appendix A.

Controlling the output frequency is accomplished by loading appropriate values into the various control registers. The following formulas are used to determine the PLL's output frequency:

$$F_{OUT} = F_{PFD} \times \left[ Int + \frac{(8 \times Frac) + Error}{2^{15}} \right] \quad (5.1)$$

and

$$F_{PFD} = \frac{F_{CRYSTAL}}{R} \quad (5.2)$$

Figure 5.9 shows the output spectrum of the LO as measured by a Spectrum Analyser:

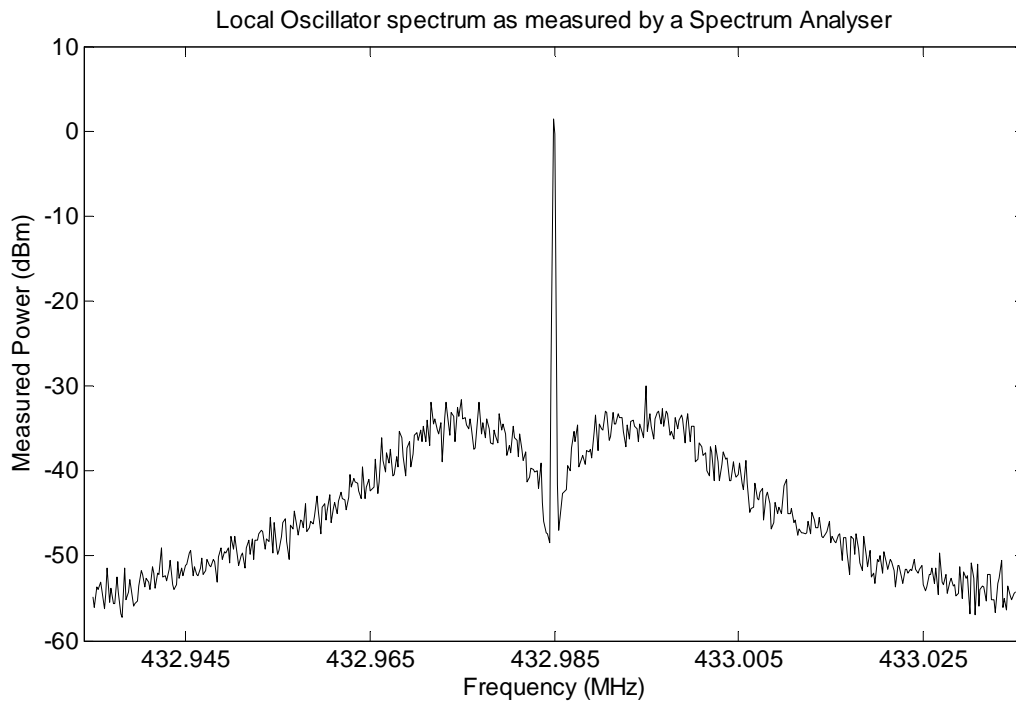


**Figure 5.9**

**A graph showing the measured spectrum of the LO.**

### **5.2.5 Amplifiers and Filters**

This is a less complicated section of the RF Frontend. The RF signal that was picked up by the antenna has already been amplified and mixed down to a suitable Intermediate Frequency. It is now the Amplifier/Filter Section's job to clean up the spectrum and add more gain.

In the case of the classical communication link, the filter section would now be dealing with a narrowband signal [9]. Subsequently, a narrow bandpass filter would be required, which could be designed using a number of methods and filter types, such as Butterworth, Chebychev and others. There are also various single components that could be used, such as a SAW filter. Another possibility to consider, if the operating frequency is low enough, is an active filter using an op-amp. An active filter does not require any inductors and it can also add a modest amount of gain.

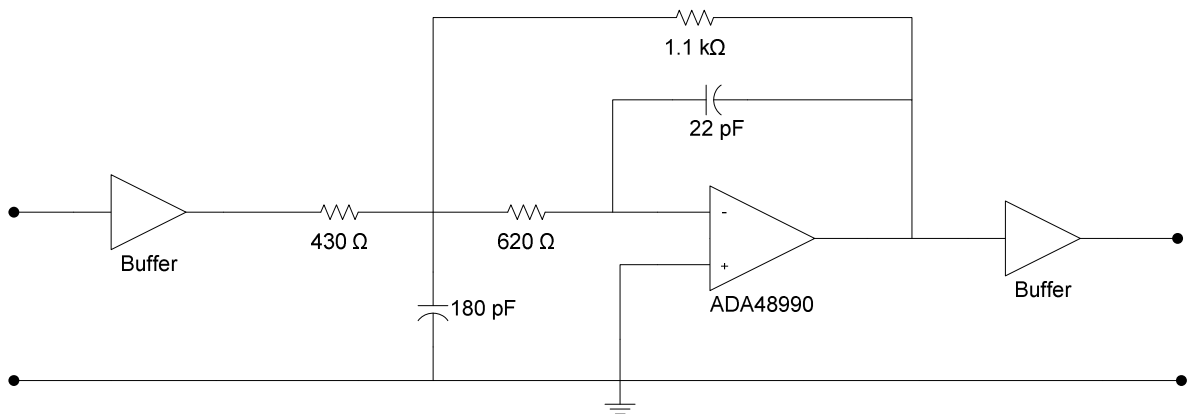


Figure 5.10

A circuit diagram of the lowpass filter.

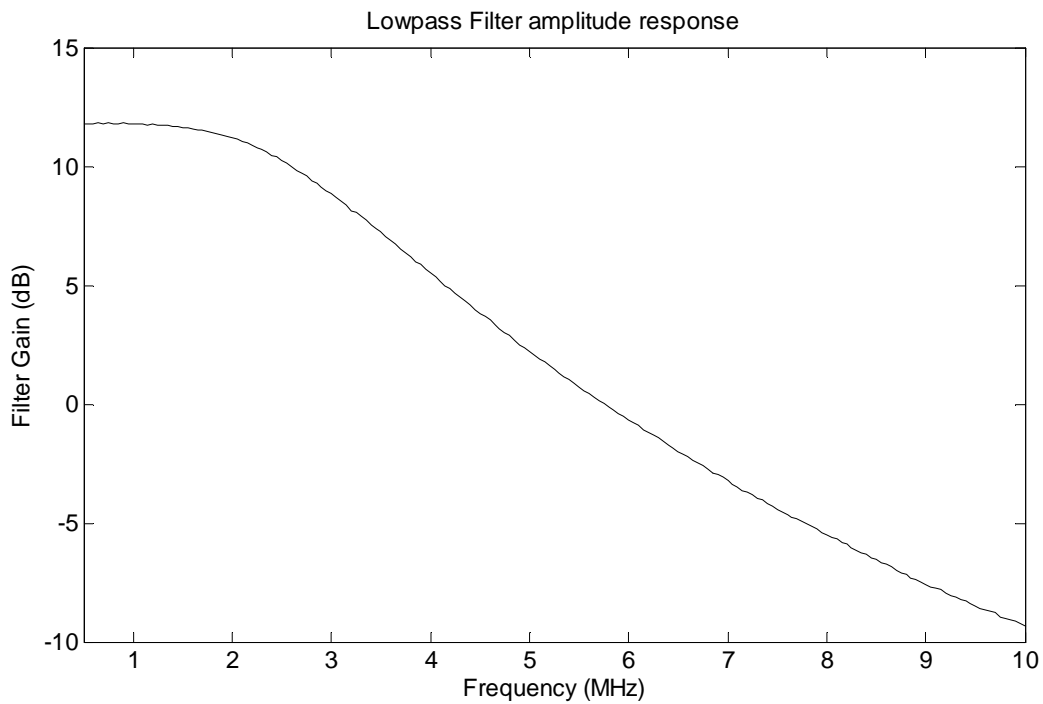


Figure 5.11

A graph showing the lowpass filter's frequency response.

The signal in this application has a relatively large bandwidth. After the mixer stage the signal is centred around 1.015 MHz, with the main signal lobe being 2 MHz wide. A low-pass filter is therefore needed. A

design using the FilterPro program by Texas Instruments showed that an op-amp with a unity-gain bandwidth of approximately 600 MHz is needed for an active filter design to be viable. As with the LO, samples could again be obtained from Analog Devices, this time for the ADA48990-1 component.

It was decided to build a Butterworth filter using a single op-amp, since a sharp cut-off is not needed (unwanted signals will be far enough from the desired frequency band for the filter to achieve sufficient suppression) and it is better to distort the ranging signal as little as possible. Another requirement for the filter is that it have as much gain as the op-amp's bandwidth allows. Keeping these properties in mind, the circuit in Figure 5.10 was designed using FilterPro.

The illustration in Figure 5.11 shows the filter's frequency response, which is more than adequate for this application. High speed buffers are added before and after the filter to prevent other components from influencing the frequency response.

### 5.3 PN Code Generator

The PN Code Generator is somewhat less complicated than the RF Frontend, yet still very important. It has to replicate the PN Code of the transmitter exactly, but allow the microcontroller to shift the Code's position in time. This is accomplished by adding a delay mechanism whereby the microcontroller can temporarily halt the PN Code Generator for short periods at any time. If this signal is compared to another PN Code it will create the effect of being shifted in time.

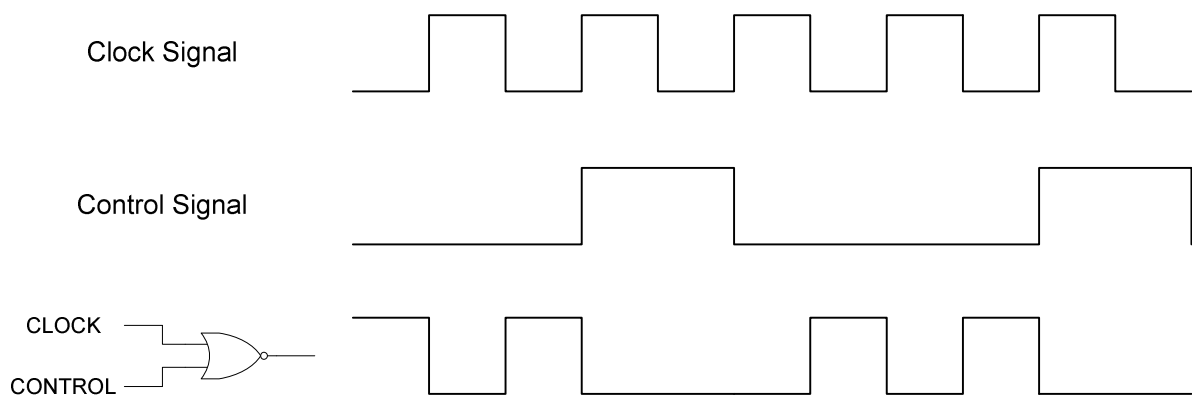


Figure 5.12

A diagram illustrating the Delay Control Mechanism.

Adding arbitrary periods of delay requires control of the clock signal that drives the Linear Feedback Register. Disabling the clock signal freezes the register, enabling it unfreezes the register which will then continue where it was halted. This can be achieved by feeding the clock signal to a logical NOR gate, along with a control signal. The control signal must be kept at a logical low level to allow the clock signal to pass unhindered. When it is time to suppress the clock a logical high must be applied by the control signal for at least the length of one clock period, as shown in Figure 5.12.

Assuming a suitable control signal can be generated, it is now possible to delay the PN Code by a minimum of one clock period. This is not nearly good enough. The ranging signal runs at a clock frequency of 1 MHz. The smallest amount of delay determines the accuracy of the receiver; in this case it would be 1  $\mu$ s or a resolution of 300 metres. To increase the accuracy it is necessary to place a frequency divider of some sort between the PN Code Generator and the clock source that allows the clock to run at much higher frequencies than the ranging signal. The frequency divider must then divide the clock signal down to 1 MHz.

### 5.3.1 Frequency Divider

Building this intermediary circuit is not very difficult. A circular shift register with an appropriate number of bits can be used to generate a clock waveform. If, for example, the register is eight bits long, with four consecutive bits set to logic 0 and the next four set to logic 1, a square waveform running at 1 MHz can be generated by driving the shift register with an 8 MHz clock signal, as shown in Figure 5.13.

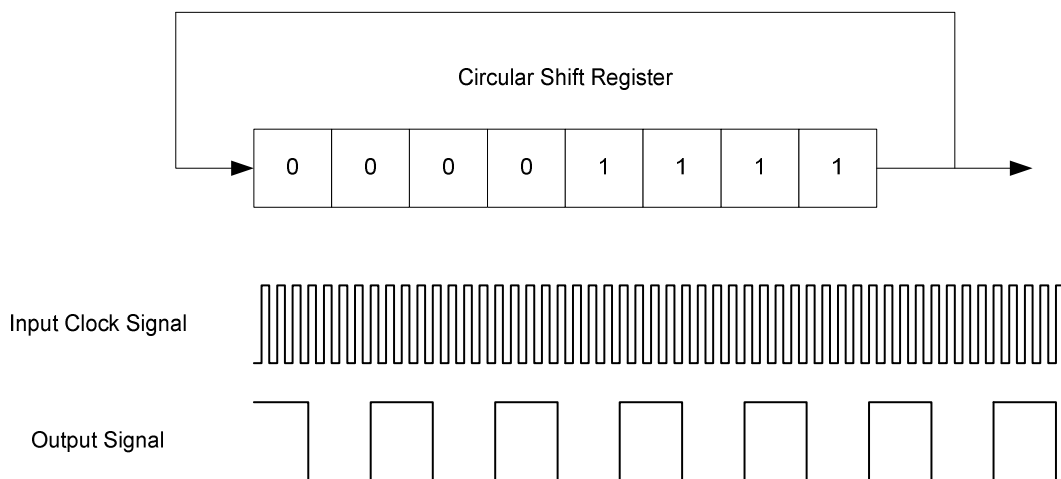


Figure 5.13

A diagram illustrating the Frequency Divider.

Halting the circular shift register would also halt any devices it was driving, for example a PN Code Generator. The difference is that the PN Code can now be delayed in much smaller increments. If, in the example above, it is possible to suppress the 8 MHz clock signal for one period, that would translate to a delay of 125 ns or a resolution of 37.5 metres (instead of 300 metres). With this mechanism the resolution is no longer determined by the clock frequency of the ranging signal, it is determined by the highest clock frequency at which the Frequency Divider can be operated and controlled. Delaying the Frequency Divider is done by suppressing the clock signal for one period at a time.

The highest resolution is determined by the shortest period of time that the Microprocessor can suppress the shift register's clock signal. This is equivalent to the shortest period it would take to execute one instruction. In the case of the PIC18F2550, which is the processor used in this application, the shortest period is 83.3 ns (if the processor is run at its maximum rated operating frequency of 48 MHz), which corresponds to a maximum resolution of 25 m.

Combining the elements above, with a few extra NOR gates to load the shift registers, produces the circuit shown in Figure 5.14.

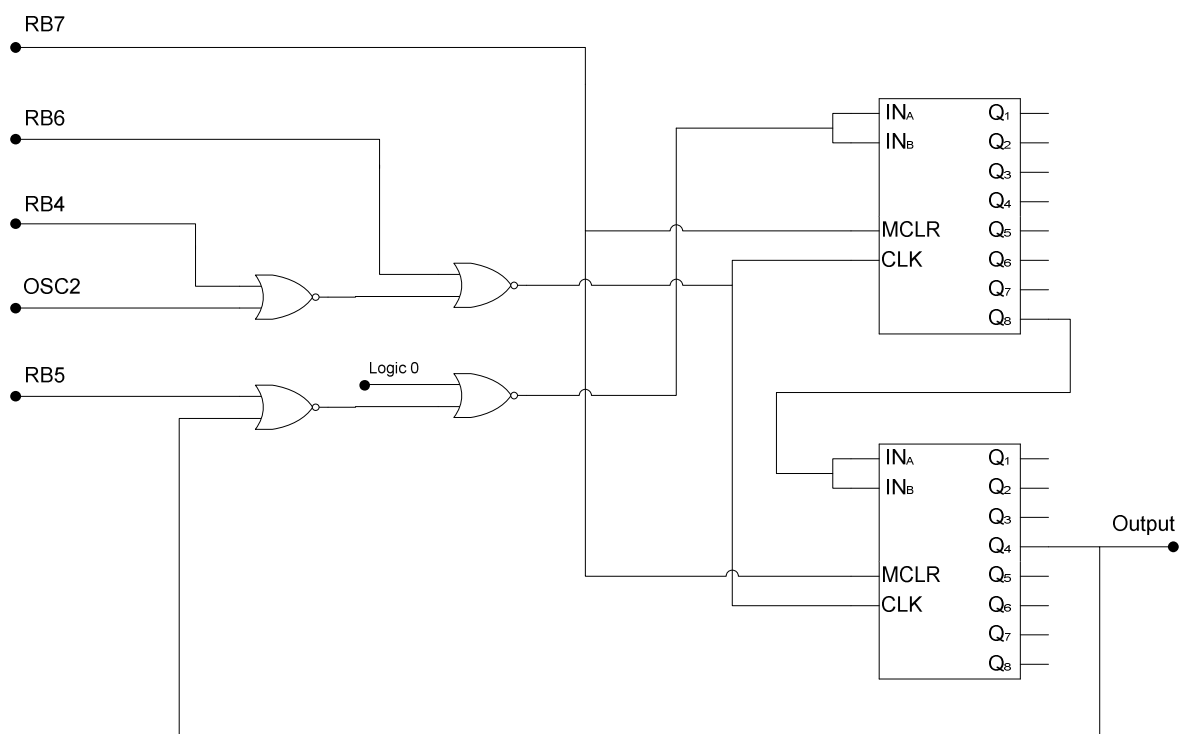


Figure 5.14

A circuit diagram for the Frequency Divider.

Two regular shift registers in a feedback configuration are used to form the 12 bit circular shift register needed to divide the input clock frequency of 12 MHz down to 1 MHz. Pin RB5 is used to insert data into the feedback path and is used when loading the registers with their initial values. Pins RB4 and RB6 are used to disable/enable the clock signal and to clock in data on pin RB5 when setting up the shift registers. Pin RB7 is connected to the Master Clear inputs of both shift registers and is used to force the registers into a consistent state before loading initial values. The last pin, OSC2, provides the 12 MHz input clock signal. This clock signal is generated by the processor.

### 5.3.2 PN Code Generator

The second part is the actual PN Code Generator. Almost exactly the same circuit as for the transmitter is used here. An eight bit shift register is used in a feedback configuration where the first, second and last bits are fed to an XOR adder and the result forms the new input, as shown in Figure 5.15.

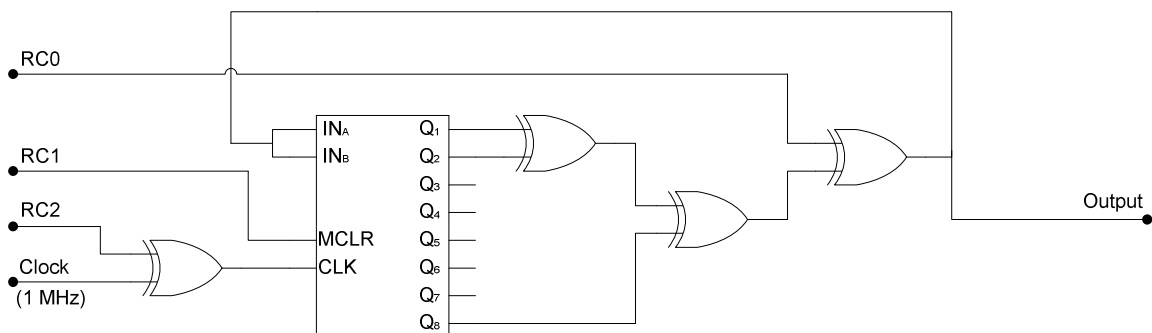


Figure 5.15

A circuit diagram for the PN Code Generator.

Two XOR gates are used to form the adder. A third XOR gate, along with pin RC0, allows the processor to insert a logical 1 into the feedback loop. Pin RC1 is the Master Clear line; pin RC2, along with the fourth XOR gate, allows the processor to clock the data that RC0 is inserting into the feedback loop. These three pins are needed at start-up to force the PN Code Generator into a consistent state, that is, all register elements are set to zero except for the first element.

The ranging signal from the transmitter can now be reproduced and shifted in time before being fed to the Correlator. This provides the mechanism whereby the microprocessor can align the incoming and reference PN Codes.

## **5.4 Mixer, Filter and Power Detector**

This section forms the Correlator and Detector. The ranging signal and the signal produced by the PN Code Generator are multiplied by a mixer, passed through a bandpass filter and fed to an RF Power Detector. If the correct amount of delay is added the Pseudo Noise part of the ranging signal will be removed and most of the power that was spread out over a wide band will be concentrated around the carrier.

An incorrect amount of delay will simply produce another Spread Spectrum signal. By monitoring the power around the carrier it is possible to see when the ranging signal and the local PN Code are aligned.

### **5.4.1 Mixer**

The same mixer that was used in the RF Frontend is used here. It is cost effective and simple to implement, but also adds some extra gain. The signal from the PN Code Generator is used like an oscillator signal, with the ranging signal forming the input. As with the transmitter, the signal from the PN Code Generator is too large. The same voltage divider is used to solve this problem.

### **5.4.2 Filter**

The filter is a bit more complicated than the mixer. A narrow bandpass filter centred on the intermediate carrier frequency is needed. The easiest option would be something like a single component SAW filter. Unfortunately these have to be custom made, unless a standard operating frequency is used.

Another option to consider is an active filter design. With an active filter inductors are not needed, which translates to an easier design. Quality factors of components are also not as important, which could otherwise restrict the minimum bandwidth of the filter. The only problem is finding an op-amp with sufficient bandwidth.

Enough samples of the ADA4899 that was used in the RF Frontend could be procured to build this filter as well. Using the FilterPro design tool provided by Texas Instruments produced the circuit shown in Figure 5.16.



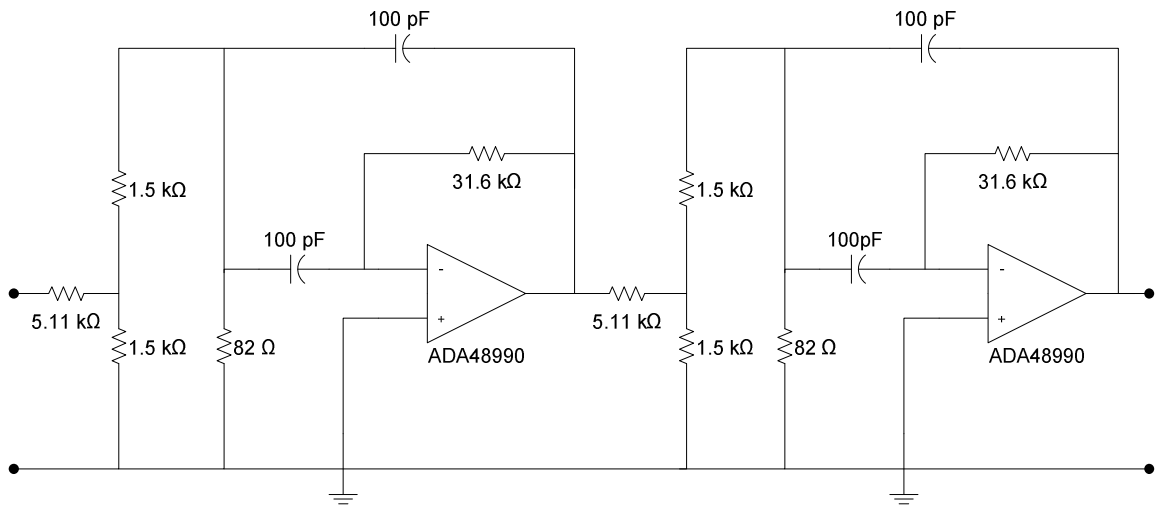


Figure 5.16

A circuit diagram for the bandpass filter.

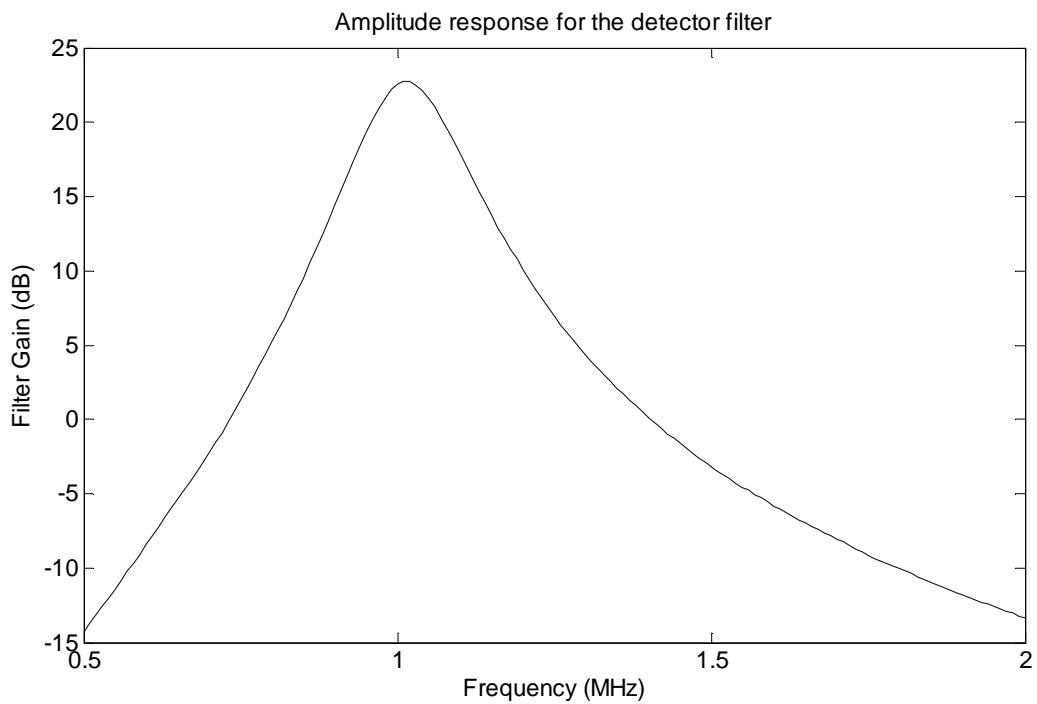


Figure 5.17

A graph of the bandpass filter's frequency response.

Two op-amps are employed to achieve a second order filter. The Quality Factor is kept as high as practical component values allow, which means the bandwidth of the filter will be as narrow as possible for this design. The filter response shown in Figure 5.17 was obtained.

### 5.4.3 RF Power Detector

As mentioned previously, the last component of this section is the RF Power Detector. This component is required to measure the power of the filtered signal and convert it to a DC voltage that the Microprocessor can sample with an Analogue-to-Digital Converter. The bandwidth of the device is not important as long as it covers an area around 1 MHz. Phase is also not important, only the magnitude is required.

The LTC5507 fits the description above very well, but is also a cost-effective solution. Basically it is a diode detector with an additional buffer circuit. The LTC5507 is very easy to implement as it only requires a small number of external components to function. The diagram in Figure 5.18 shows the pin layout and all the extra components needed to operate the LTC5507:

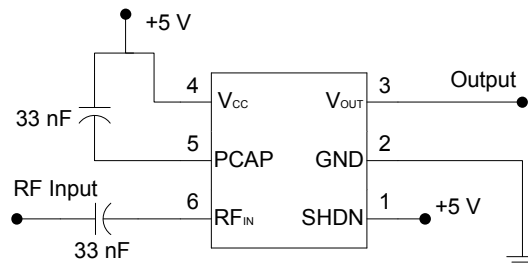


Figure 5.18

A circuit diagram for the RF Power Detector.

Component values were chosen according to the datasheet's instructions.

#### 5.4.4 Summary

Figure 5.19 reviews the total gain for the receiver:

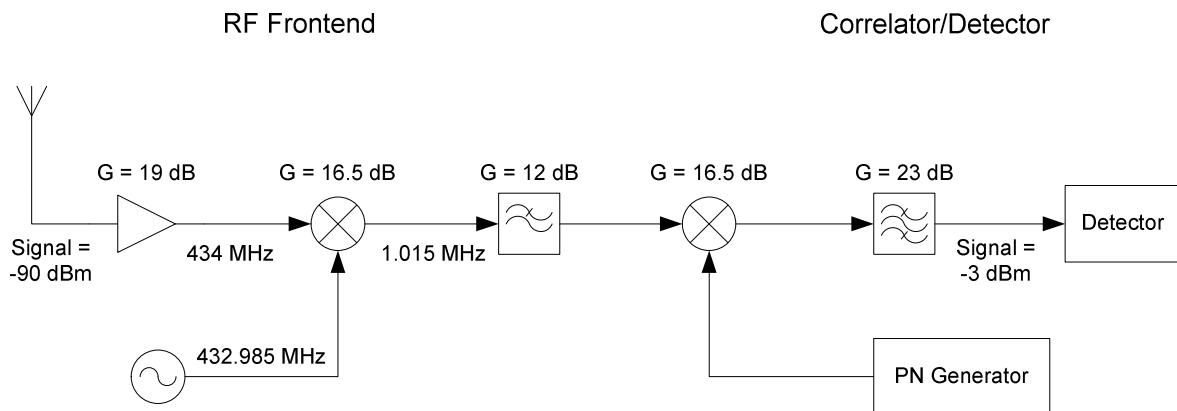


Figure 5.19

A diagram showing the gain for the different components of the receiver board.

### 5.5 Digital Processor and Peripheral Circuits

This is the last section of Chapter 5 and will cover the Microprocessor and peripheral components needed to control and support the other modules. The Microprocessor is the most important and will be covered last.

#### 5.5.1 Power Supply

This is a straightforward part of the receiver to build. Almost all the active components used in the receiver's design require a +5 V supply, except for the ADF7011, which has its own regulator circuit. The op-amps and the buffers also require a -5 V supply. Two linear regulators are used in a standard configuration to create the necessary voltage levels.

## 5.5.2 Oscillator

This oscillator is the 48 MHz clock signal that drives the Microprocessor. All receiver boards have to be synchronised, which requires a common clock signal. This is achieved by adding an additional SMA connection that allows for an external clock signal to be applied. This same connection can also be used as an output, thereby allowing one receiver board with a clock signal generator to drive any other boards in use. This is shown in Figure 5.20.

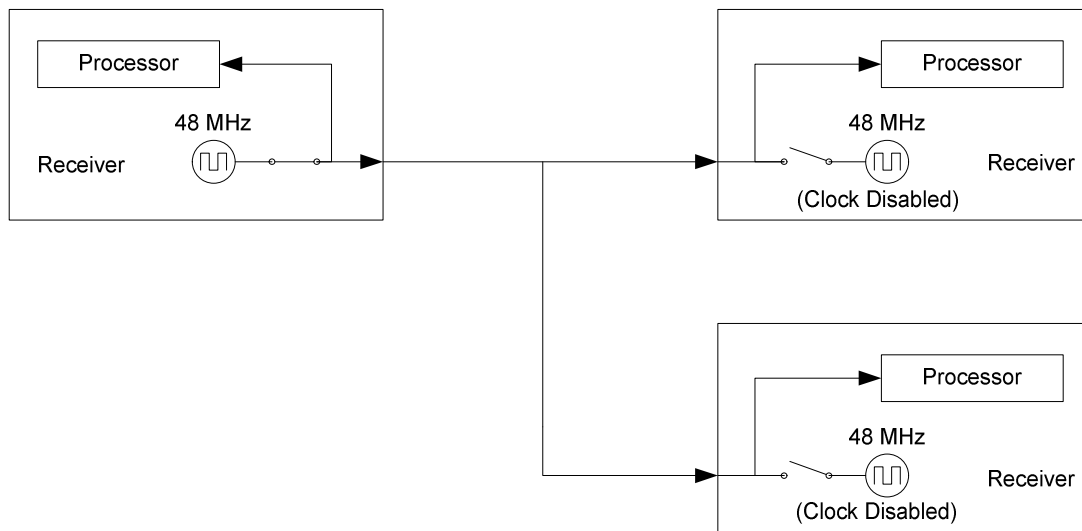


Figure 5.20

A diagram illustrating how multiple receiver boards will be synchronised.

Unlike the Local Oscillator frequency for the RF Frontend, 48 MHz is a popular standard frequency. As such a simple and relatively inexpensive component, manufactured by Epson, can be used.

## 5.5.3 Serial Communication

Communication between the receiver module and a Central Computer is needed to relay the measured data. This data can then be processed and used to create a graph showing the correlation between the two PN Code signals or to calculate a positional fix. Simple serial communication using RS232 methods is used, as this is very easy, quick and cost effective to implement.

### 5.5.4 Central Processor

The Central Processor links all the other sections of the receiver module together. It is used to control the Local Oscillator for the RF Frontend as well as the PN Code Generator. Most importantly, it is used to measure the output voltage level of the Power Detector and communicate the information to a computer. The diagram in Figure 5.21 shows how these sections are connected.

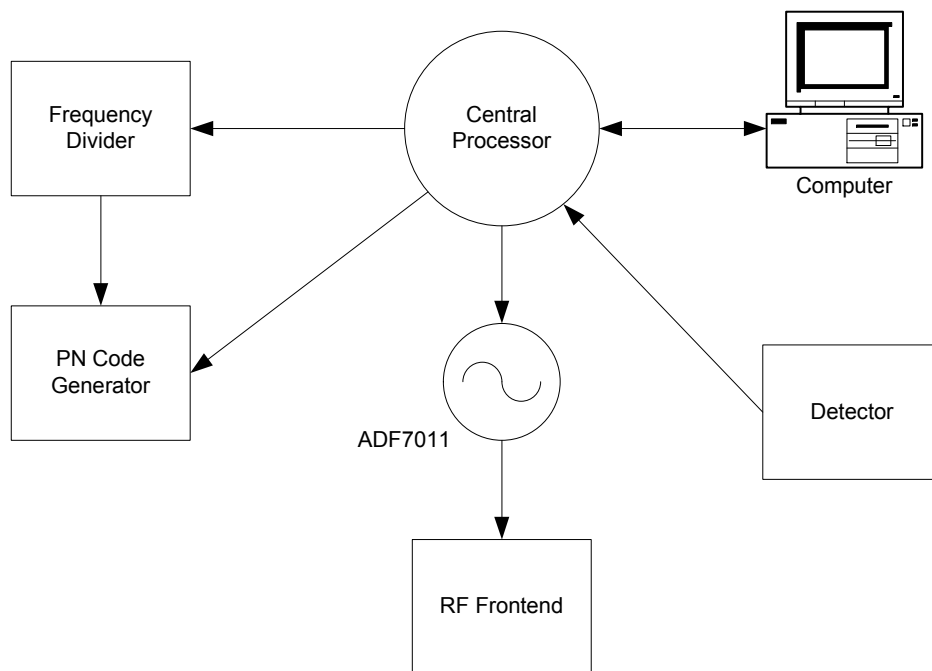


Figure 5.21

A diagram showing the connectivity of the various receiver modules.

The Central Processor is an important component and will be responsible for several tasks. Before specifying which properties it should have it would be pertinent to check for the minimum functionality needed to perform the various tasks required of it. One of the first tasks to be completed is setting up the various registers for both the PN Code Generator and the Local Oscillator. This requires a number of output pins that can be configured as logic pins. Controlling the PN Code Generator once all the necessary registers have been loaded, also requires more output pins. A clock signal, running at a lower frequency than the Processor's clock, is needed to drive the shift registers in the frequency division section of the PN Code Generator. Measuring the output voltage level of the Power Detector requires a basic Analogue-to-Digital Converter. The last item that must be available is support for serial communications.

These basic requirements can be summarised as follows:

1. Sufficient output pins.
2. Additional clock signals.
3. A/D Converter.
4. Support for serial communications.

A number of additional factors must also be considered, in addition to the basic features mentioned above. As always, cost is very important and a more cost-effective option is preferable. Available programming equipment will limit the number of options, as will available stock. It is also necessary that the Processor have a large enough set of instructions, enough memory and be fast enough to perform all its tasks. Since microprocessor technology has advanced quite far in the last few decades it is unlikely that speed will be a problem. This means that a faster microprocessor can be selected to increase accuracy or decrease measurement time. Another aspect to consider is that the chip will have to be reprogrammed many times. It would be prudent to select a packaging that easy is to remove, replace and reprogram.

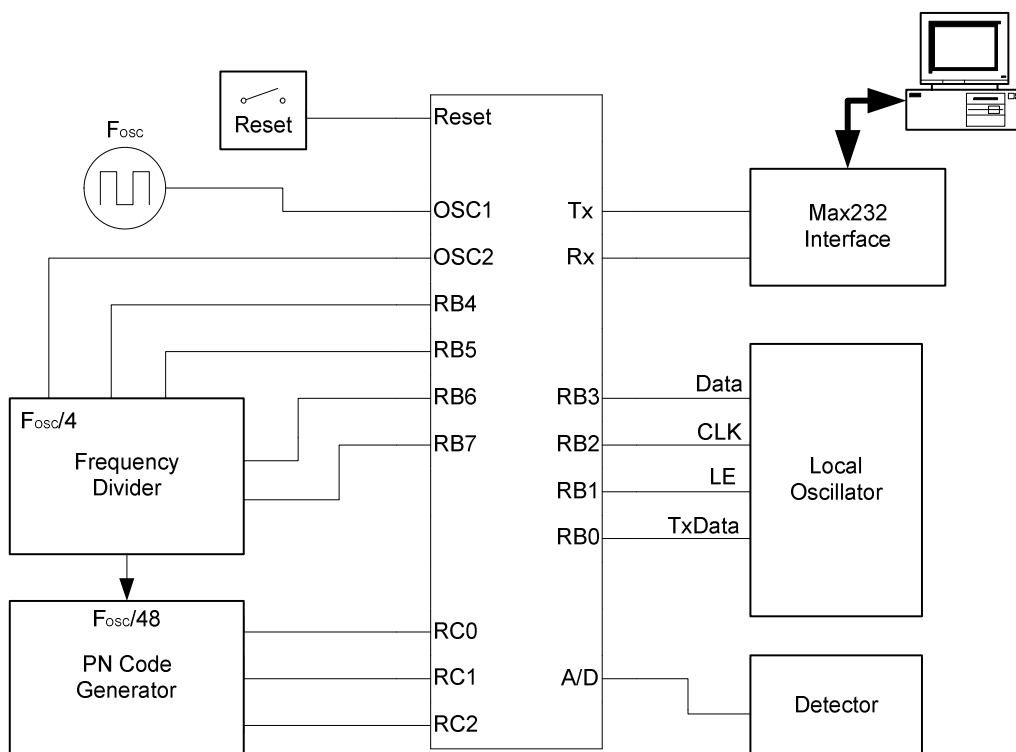


Figure 5.22

A diagram of the PIC's various pin connections.

All the factors mentioned led to the selection of the PIC18F2550 product. It can perform all the basic functions set out above. It is fast enough, has ample memory and is available in a DIP package for easy removal and reprogramming.

Operating the PIC is easy enough. It only needs three small peripheral circuits; a 5 V power supply, a reset button (optional) and a clock source. An oscillator circuit is provided on-chip for operation at lower frequencies, but in this case the clock signal must be supplied by an outside source. Power supply is already provided for by the regulators, as discussed in section 5.5.1. The diagram in Figure 5.22 shows the other pin connections for the PIC.

The functions of the various output pins (as connected in Figure 5.22) will not be discussed here, as they have already been covered in previous sections.

## 5.6 Embedded Software

This section will take a closer look at the procedures and algorithms needed for setting up and controlling all the modules connected to the Central Processor. Most of these will be straightforward loading of registers or assignment of variables and will be dealt with in section 5.6.1 (Setup Procedures). The second section, 5.6.2 (Measurement Algorithms), will deal with the actual measurement algorithms.

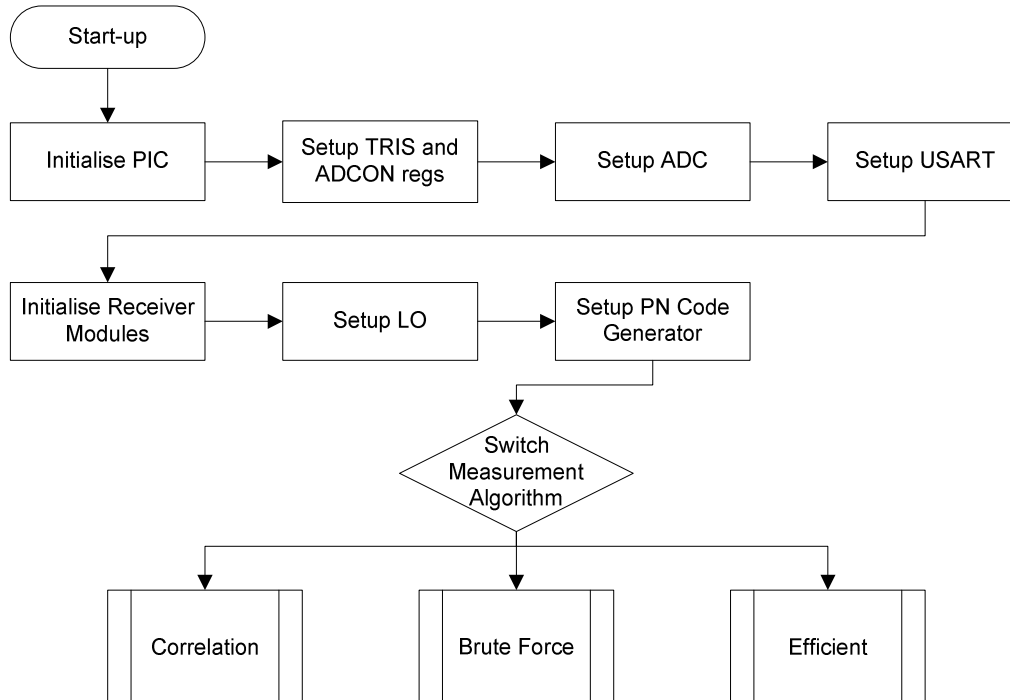


Figure 5.23

A flow-diagram showing the setup procedure for the microprocessor.

### 5.6.1 Setup Procedures

The first thing that must be done at start-up is to force the PIC into a consistent state. This mostly entails loading interrupt and tri-state registers. As soon as a consistent state has been reached the Processor can start to activate modules, beginning with its own features and then moving on to the other components on the receiver board. Once everything is up and running the PIC can start measuring data and relay it to a computer. The flow-diagram in Figure 5.23 will make this clear.

### 5.6.2 Measurement Algorithms

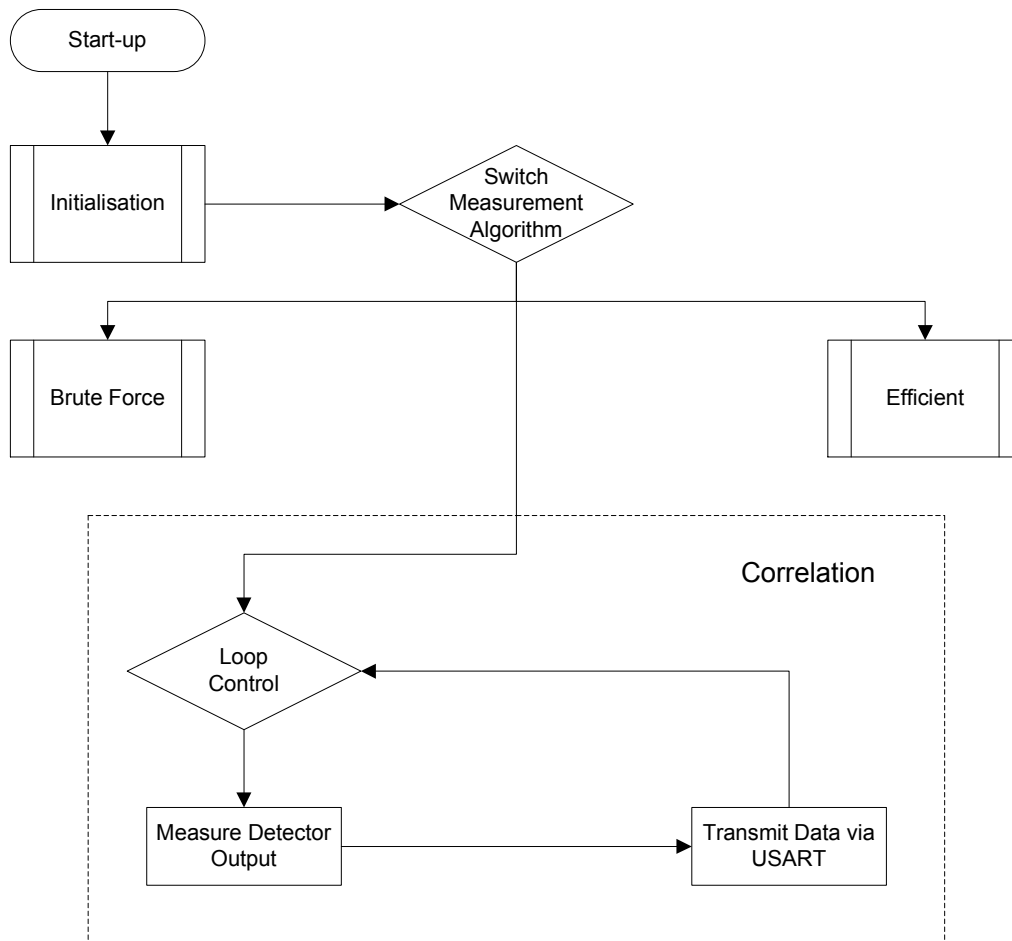


Figure 5.24

A flow-diagram showing the most basic measurement algorithm.



This section shows the three main algorithms that were used during the development and testing of the receiver. The first two are simpler intermediary algorithms, used mostly during the development stage. The third one is more complex, but also more efficient.

The flow-diagram in Figure 5.24 shows the first measurement method. It is little more than a direct measurement of the Power Detector's output and is used to measure the correlation between the incoming PN Code (from the transmitter) and the local PN Code.

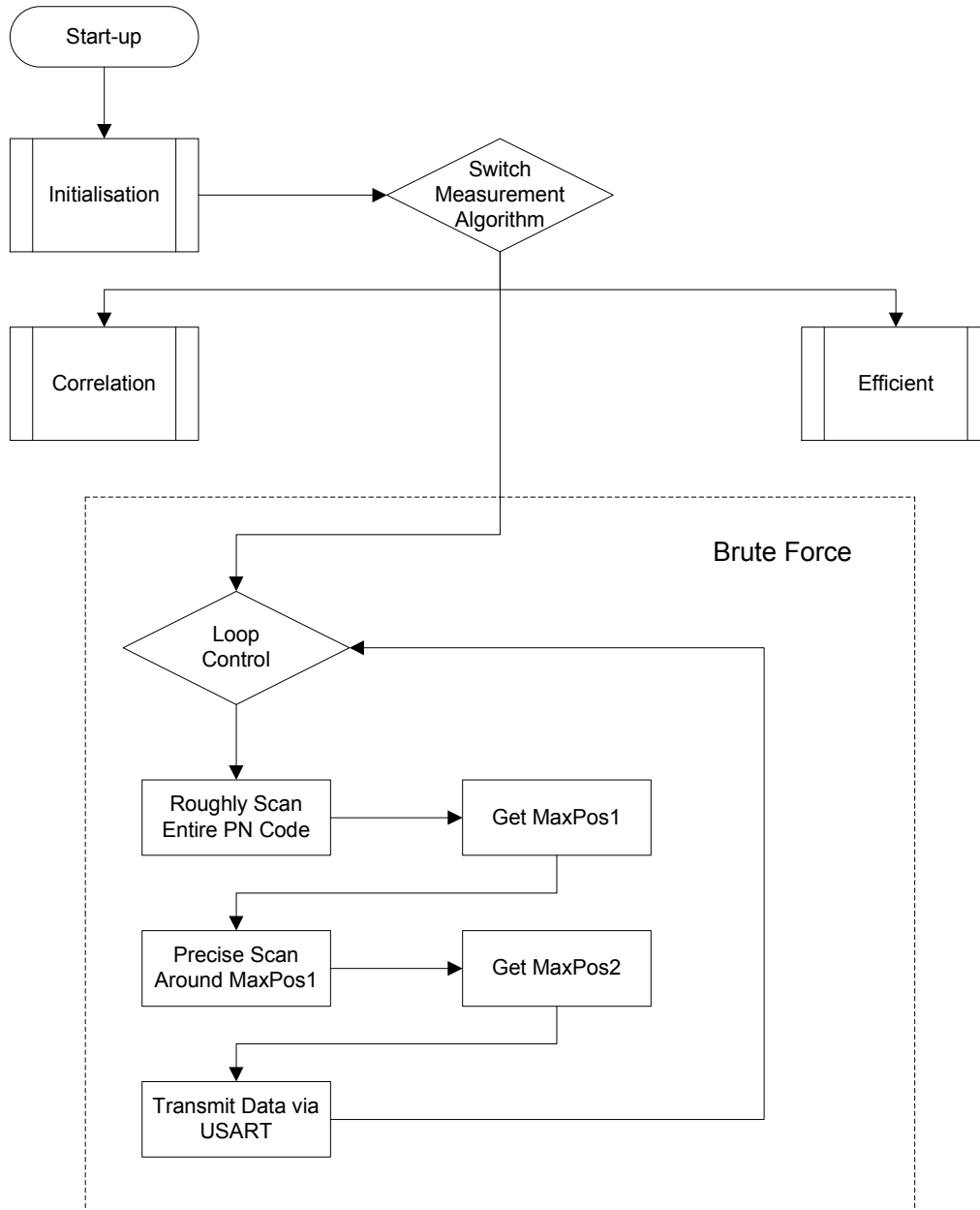


Figure 5.25

A flow-diagram of the brute force algorithm.

Next is the second algorithm, shown in Figure 5.25. It is a brute force measurement, meaning that it scans the entire length of the incoming PN Code, determines how far it has been shifted relative to the local PN Code and then repeats the process endlessly.

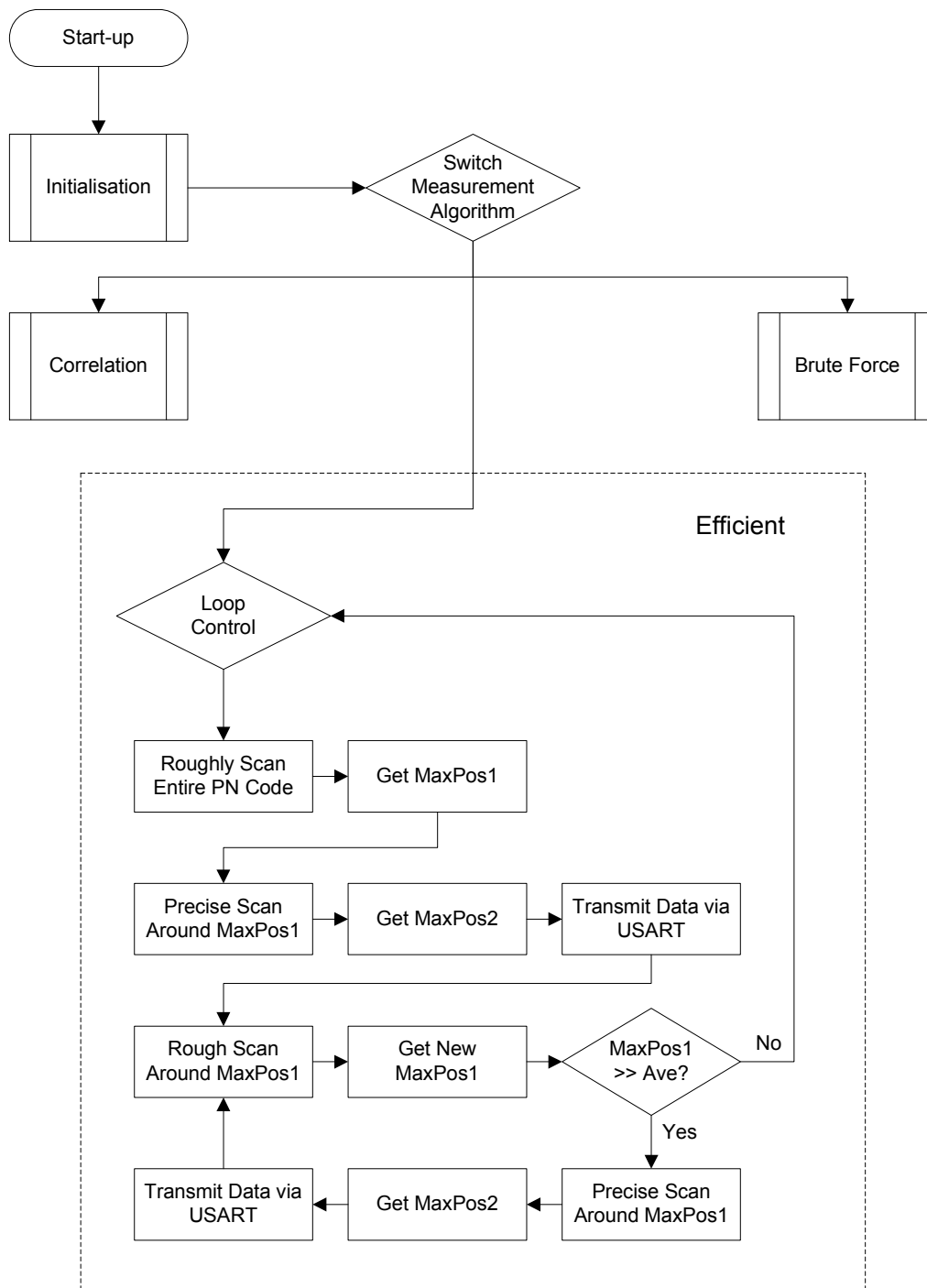


Figure 5.26

A flow-diagram of the efficient measurement algorithm.

While the second algorithm does measure the shift between the two PN Codes, it wastes a lot of time scanning unnecessary parts of the incoming PN Code. The third algorithm, shown in Figure 5.26, tries to mitigate this by guessing where the peak power should be and scanning there first.

# Chapter 6

---

## System Measurements

All the previous chapters have dealt with the development of a position location strategy and the implementation of a working example. It is now the task of the last chapter to take a number of physical measurements and compare the results with earlier theoretical predictions. Ultimately these measurements will lead to a conclusion: Was the proposed strategy successful and if so, to what degree?

### 6.1 Basic Correlation Measurement

This is the first and most basic of the measurements that will be taken in this chapter. Two PN Code signals will be created and multiplied with each other by using a transmitter and a receiver. The transmitter PN Code signal and receiver PN Code signal will run at slightly different clock frequencies. This is very similar to the experiment that was conducted at the end of Chapter 4 (see Figures 4.12 and 4.13), with the receiver taking the place of the Spectrum Analyser. The receiver will now simply measure the power levels at the detector and pass the data to a computer. The diagram in Figure 6.1 illustrates this configuration.

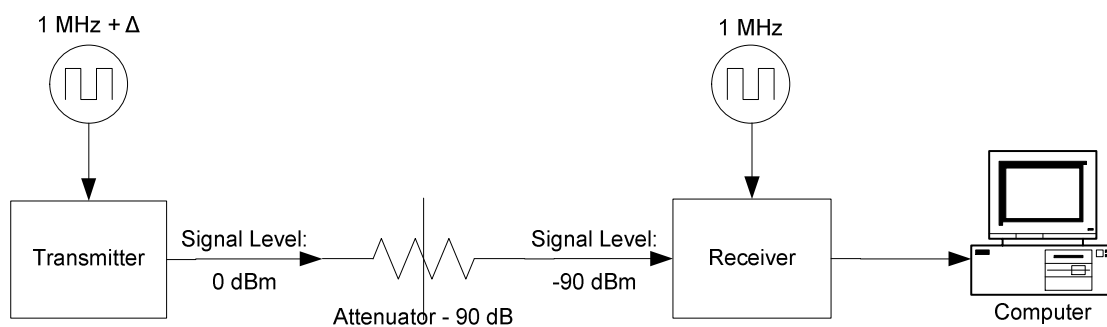


Figure 6.1

A diagram illustrating the basic correlation measurement setup.

Generating the two PN Code signals at slightly different frequencies is equivalent to adding incremental amounts of delay between them. This creates the effect of adding a delay element between the transmitter and the receiver that repeatedly sweeps from 0 to 127 chips.

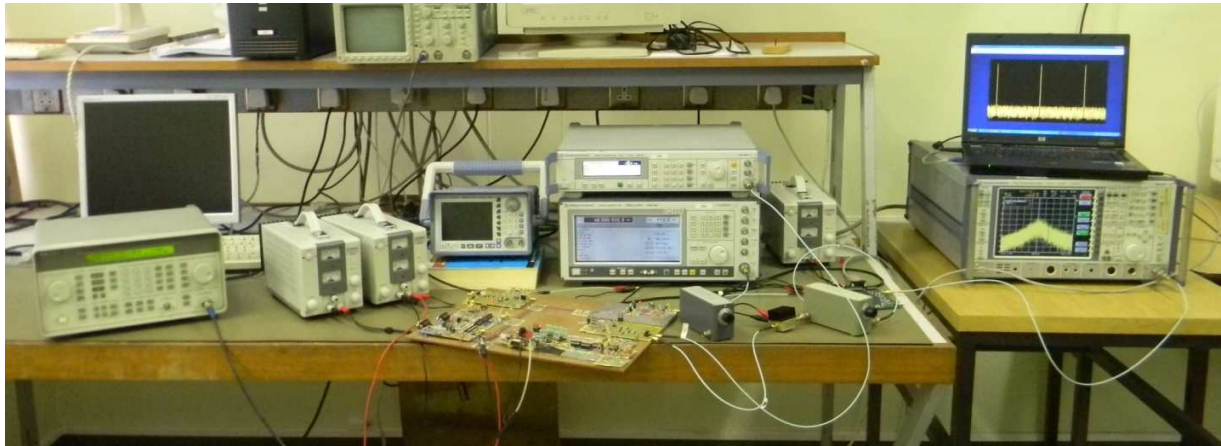


Figure 6.2

A photograph of the physical measurement setup in section 6.1.

Parameter	Value	Remarks
Transmitter Clock Frequency	1.000 001 MHz	A frequency difference of 1 Hz translates to a sweep rate of 1 chip/second.
Receiver Clock Frequency	48 MHz (1 MHz)	
Frequency Difference	1 Hz	
Transmitter Output Power	0 dBm	Receiver gain is 90 dB; detector input power should be about 0 dBm.
Attenuation	90 dB	

Table 6.1

The photograph in Figure 6.2 shows the setup of equipment and hardware; Table 6.1 is a summary of the parameters for this measurement. Two signal sources are used to drive the clock inputs for the hardware, an attenuator is inserted between the transmitter output and the receiver input (equivalent to signal attenuation when transmitting across a physical channel) and the measured data is passed to a computer via RS232 communications. The microprocessor on board the receiver has been programmed

to continuously convert the voltage level from the detector output into a digital power reading (see Figure 5.24 at the end of Chapter 5). The following graph, shown in Figure 6.3, was obtained.

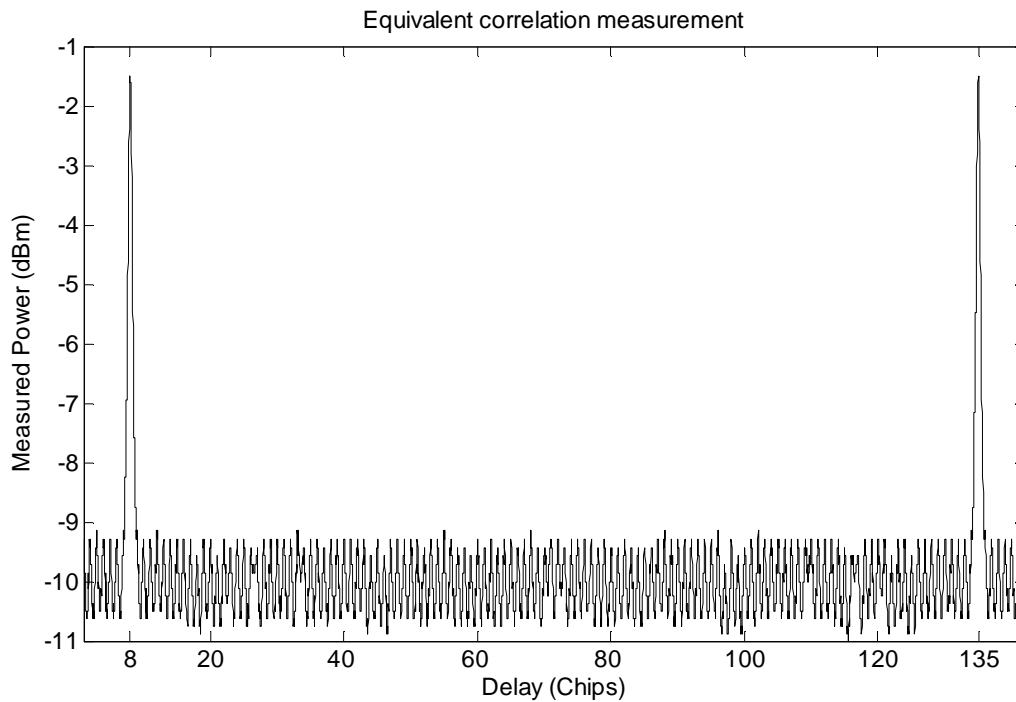


**Figure 6.3**

**A graph of the basic correlation measurement.**

The graph shows a very clear maximum where the two PN Codes are in alignment. This proves that the receiver is capable of distinguishing between aligned and non-aligned PN Codes, which is the first step towards a proper Time-Difference-of-Arrival measurement.

## **6.2 PN Code Tracking Measurement**

This measurement will use the difference between the maximum and average power from the previous measurement to determine the delay between an incoming PN Code and a local PN Code. A transmitter and receiver will again be used, but this time the receiver will employ the delay control mechanism to determine how far apart the two PN Codes are from alignment. The diagram in Figure 6.4 illustrates this configuration.

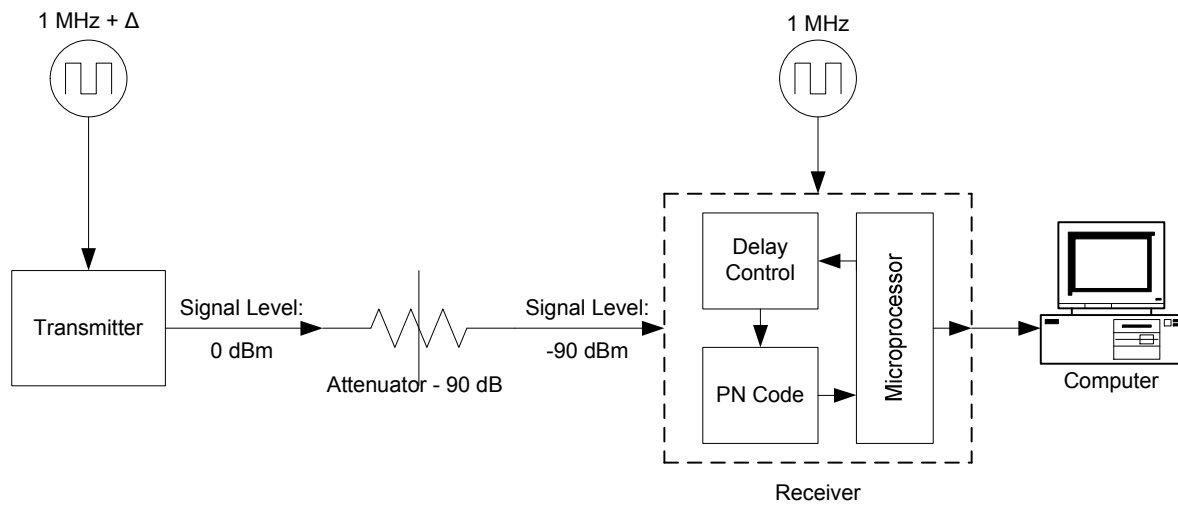


**Figure 6.4**

**A diagram of the setup for the PN Code tracking measurement.**

As with the previous measurement, the two PN Codes will be generated at slightly different clock frequencies. This is equivalent to changing the delay between the transmitter and receiver at a constant rate. The receiver will then attempt to keep track of this varying delay component. This measurement will confirm that the receiver can find and keep track of the delay between itself and the transmitter.

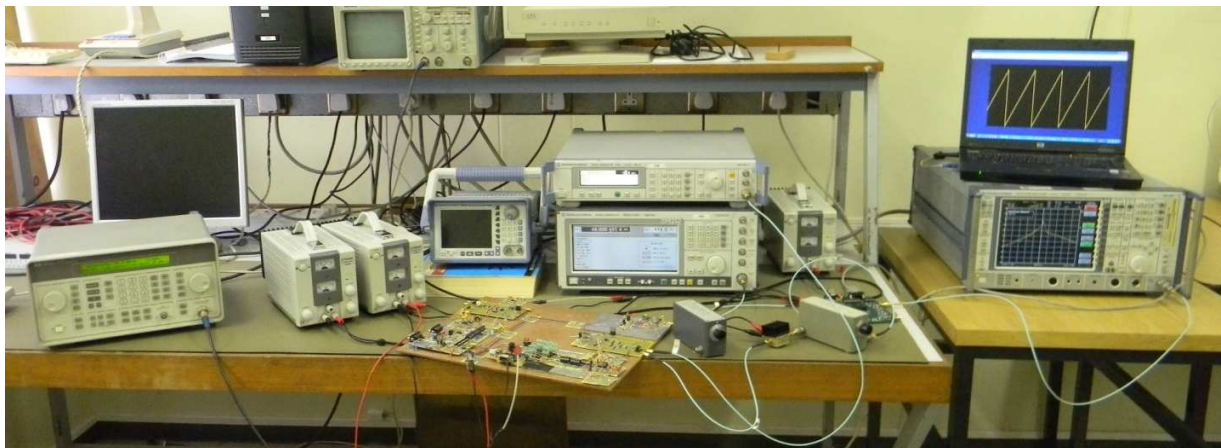


**Figure 6.5**

**A photograph of the physical measurement setup in section 6.2.**

Parameter	Value	Remarks
Transmitter Clock Frequency	1.000 009 5 MHz	A sweep rate of up to 20 chips/s could be measured before the receiver started to lag.
Receiver Clock Frequency	48 MHz (1 MHz)	
Frequency Difference	9.5 Hz	
Transmitter Output Power	0 dBm	Receiver gain is 90 dB; detector input power should be about 0 dBm.
Attenuation	90 dB	

Table 6.2

Figure 6.5 illustrates the physical setup of equipment and hardware; Table 6.2 summarises the parameters of the measurement. Two signal sources are used, along with an attenuator and a computer. In this experiment the microprocessor is programmed to insert incremental amounts of delay between the transmitter PN Code and the receiver PN Code and then measure the detector voltage for each increment. The maximum voltage corresponds to the correct amount of delay.

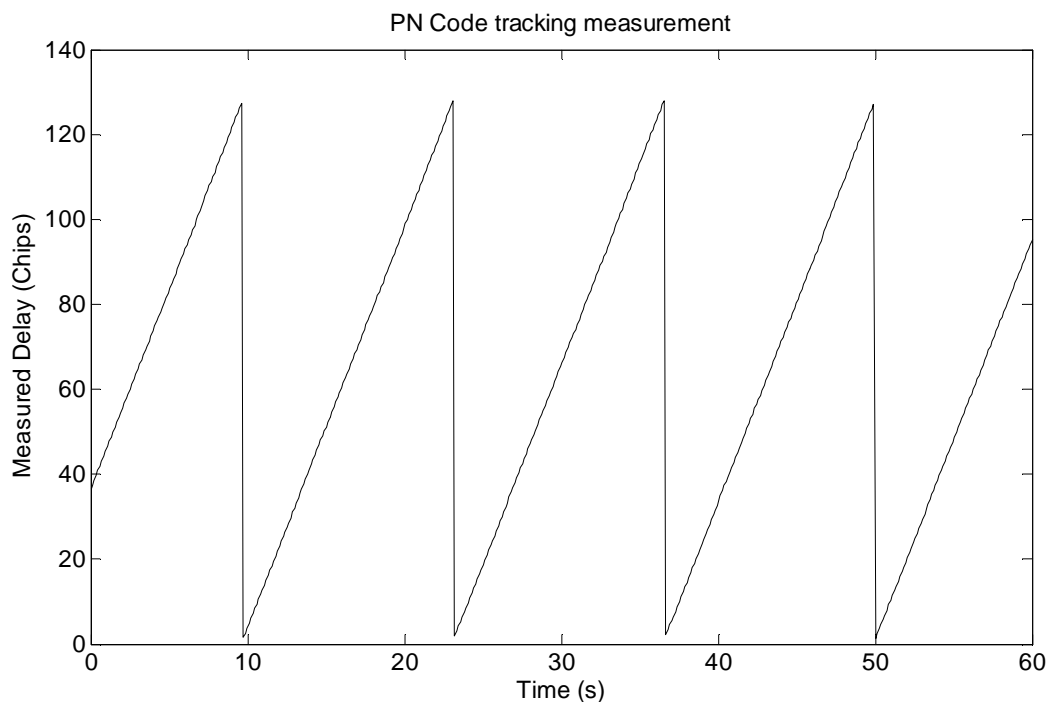


Figure 6.6

A graph showing the result of the PN Code tracking measurement.



The graph in Figure 6.6 has a distinctive saw-tooth shape. This is caused by the constant increase in delay between the transmitter and the receiver (as the difference in clock frequencies cause the PN Codes to slide past each other in the time-domain). The fact that the receiver can follow this curve is proof that it is capable of measuring the delay between itself and the transmitter's PN Code. This measurement can also be used to determine how much the transmitter and receiver clock frequencies can differ before the receiver is unable to measure the delay with accuracy. As Table 6.2 mentions, this difference in frequency can be pushed to 20 Hz before the receiver's measurement becomes unreliable.

### 6.3 Cable Length Measurement

This is the last measurement using only one receiver. Cables of varying length will be used to connect the transmitter output to the receiver input, thus adding a physical delay component. For this experiment the transmitter and receiver PN Codes will be generated using exactly the same clock frequency. This means that the cable forms the only delay element in the experiment. The diagram in Figure 6.7 illustrates this configuration.

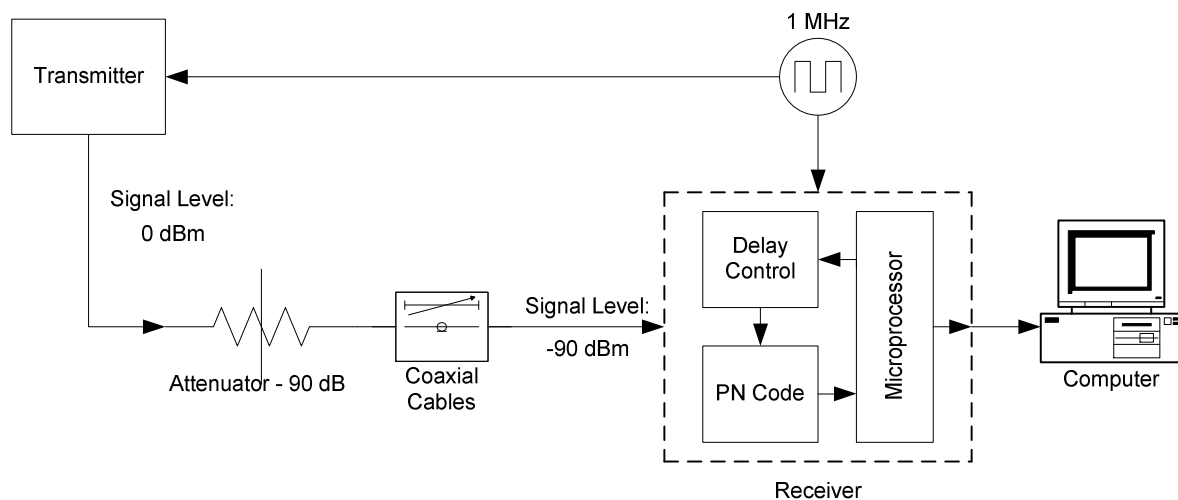


Figure 6.7

A diagram that illustrates the setup for the cable length measurement.

Recall that a microprocessor clock frequency of 48 MHz results in a resolution of 25 m (in free space). Regular coaxial cable, such as the type used in this experiment, has a dielectric material packed around the centre conductor. Since electromagnetic waves travel at lower velocities in dielectric materials than

they do in free space, the cables are divided into lengths of 17 m, which is equivalent to 25 m in free space.

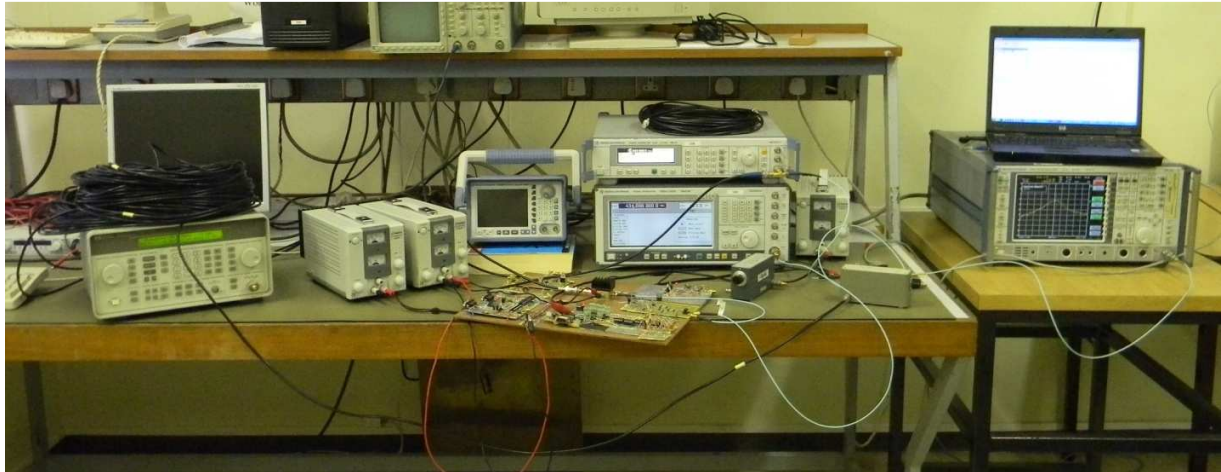


Figure 6.8

A photograph of the physical setup for the measurement in section 6.3.

Parameter	Value	Remarks
Transmitter Clock Frequency	1 MHz	The transmitter and receiver used the same clock.
Receiver Clock Frequency	48 MHz (1 MHz)	
Transmitter Output Power	0 dBm	Attenuation was varied as the cables added additional attenuation.
Attenuation	50 - 90 dB	

Table 6.3

Figure 6.8 shows the physical setup of equipment and hardware; Table 6.3 is a summary of the parameters of the measurement. The microprocessor in this experiment is programmed to measure detector voltage levels for various amounts of delay, looking for the maximum voltage level and the corresponding amount of delay. Since the incoming and local PN Codes are running at the same frequency, detection time is not important. This allows for a brute-force method to be used here.

Cable Length (in Metres)	Delay Measurement (in Fractional Chips)	Measured Cable Length (in Fractional Chips)	Measured Cable Length (in Metres)
0	1077	0 (Reference)	0
1 x 17 = 17	1078	1	17
2 x 17 = 34	1079	2	34
3 x 17 = 51	1080	3	51
4 x 17 = 68	1081	4	68
5 x 17 = 85	1082	5	85
100	1083	6	102

Table 6.4

Table 6.4 shows the measured data for this experiment. Every piece of cable that is a multiple of 17 m is measured quite accurately. This is not surprising, as 17 m corresponds with the smallest length of time that the receiver PN Code can be delayed. The receiver is therefore capable of aligning its own PN Code and the transmitter's PN Code exactly.

Adding lengths of cable that are not multiples of 17 m results in a different scenario. The receiver is unable to align the PN Codes exactly. The measurement jumps between the two nearest possibilities; with averaging this measurement can be refined. Table 6.5 shows the figures for a second measurement, where smaller lengths of cable are used.

Cable Length (in Metres)	Delay Measurement (in Fractional Chips)	Measured Cable Length (in Fractional Chips)	Measured Cable Length (in Metres)	Error (in Metres)
0	863	0 (Reference)	0	0
3.4	863.00	0.00	0	3.4
5.6	863.23	0.23	3.91	1.69
7.8	863.45	0.45	7.65	0.15
10	863.53	0.53	9.01	0.99
12.2	863.76	0.76	12.92	0.72
14.4	863.86	0.86	14.62	0.22
16.6	863.94	0.94	15.98	0.62

Table 6.5

These measurements are remarkably accurate. This is partly due to the transmitter and the receiver being synchronised for this experiment. As the measurement in section 6.4 will show, a more realistic setup will not achieve this degree of accuracy. This measurement is still noteworthy though, as it demonstrates the possible effectiveness of additional processing.

## 6.4 Time-Difference-of-Arrival Measurement

This is the last and most important measurement in this chapter. In this experiment two receivers will be used simultaneously to measure the delay between their own locally generated PN Codes and a transmitter PN Code. Varying amounts of delay will again be introduced by means of coaxial cables. Each delay measurement is equivalent to a Time-of-Arrival (TOA) measurement. Since there is no synchronisation between the receivers and the transmitter these TOA measurements cannot be used directly. It is, however, possible to derive Time-Difference-of-Arrival (TDOA) data from the TOA measurements by simply calculating the difference. Calculating TDOA data from inaccurate TOA measurements can be done in this case because the receivers are synchronised by means of a shared clock signal. The diagram in Figure 6.9 shows the configuration for this experiment.

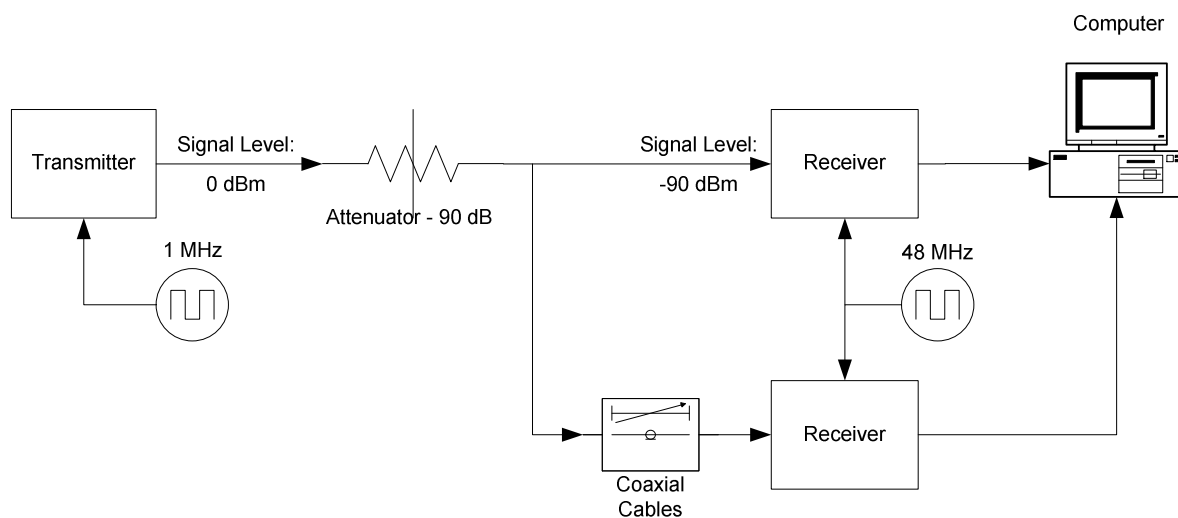


Figure 6.9

A diagram illustrating the setup for the TDOA measurement.

Figure 6.10 illustrates the physical setup of equipment and hardware; Table 6.6 is a summary of the experiment's parameters. The objective here is to simulate a field measurement indoors. This is done by

inserting an attenuator and varying lengths of cable between the transmitter and the two receivers. One receiver will be connected to the transmitter with no additional cables, while extra cable is inserted between the second receiver and the transmitter to simulate differences in travel time.



Figure 6.10

A photograph of the physical setup for the TDOA measurement.

Parameter	Value	Remarks
Transmitter Clock Frequency	1 MHz	The transmitter and receiver used separate clocks.
Receiver Clock Frequency	48 MHz (1 MHz)	
Transmitter Output Power	0 dBm	Attenuation was varied as the cables added additional attenuation.
Attenuation	50 - 90 dB	

Table 6.6

A calibration is done at the beginning by removing the extra coaxial cables and taking a reference measurement. In this case the TDOA should equal zero, but since the two receivers did not start running at exactly the same moment there is a constant error. The reference measurement is used to eliminate this constant error. Table 6.7 shows the measured values for the various lengths of cable.

Cable Length (in Metres)	Uncorrected TDOA Measurement (in Fractional Chips)	Corrected TDOA Measurement (in Fractional Chips)	Measured Cable Length (in Metres)	Error (in Metres)
0	933.99	0 (Reference)	0	0
17	934.955	0.965	16.41	0.59
34	935.955	1.965	33.41	0.59
51	936.97	2.98	50.66	0.34
68	937.965	3.975	67.58	0.42
85	939.025	5.035	85.60	0.60

Table 6.7

This experiment has managed to measure the cable lengths with very reasonable accuracy. The transmitter is not synchronised with the two receivers; consequently the measurement is not as accurate as the one from section 6.3. It is also necessary to employ some averaging. The measurements are still more accurate than expected. Previous predictions stated that the system should be able to resolve differences in arrival times to within  $\pm 12.5$  m in free space ( $\pm 8.5$  m when using coaxial cables), which this measurement has clearly achieved.

## 6.5 Discussion of Results

This chapter proposed four experiments to prove the feasibility of the position location strategy developed in Chapter 3. Each experiment added another level of complexity, building up to the TDOA measurement in section 6.4. The first measurement showed that the system can distinguish clearly between PN Codes that are aligned and PN Codes that are not aligned. A difference of almost 10 dB was measured. This property forms the basis on which the entire system was designed.

The next two measurements (sections 6.2 and 6.3) used the property from the first measurement to track an incoming PN Code signal. Section 6.2 showed that the receiver is capable of tracking a PN Code signal, despite the fact that the transmitter and the receiver are not synchronised. A difference in clock frequencies of up to  $\pm 20$  Hz could be tolerated.

Section 6.3 determined the maximum degree of accuracy that can be achieved by this system. Various lengths of coaxial cable were inserted between the transmitter and the receiver, after which the receiver was used to estimate the delay added by each cable. This delay was converted to a length parameter and compared to the appropriate cable length. The results showed remarkable accuracy. Predictions from Chapter 3 suggested that the system should be able to measure distance to within  $\pm 8.5$

m (for the dielectric material used in the coaxial cables,  $\pm 12.5$  m in free space<sup>2</sup>). This measurement was accurate to at least within  $\pm 3.4$  m, in most cases the error was less than  $\pm 1$  m. The increase in accuracy can be attributed to the synchronisation between the transmitter and the receiver, as well as the addition of post-processing done in Matlab.

The last experiment is the most complex and the most important measurement for this chapter and for this entire project. It aimed to replicate a real-life measurement by using two receivers simultaneously, thereby measuring the difference in arrival times (TDOA) of a transmitter signal that is being transmitted to both receivers. For this experiment the two receivers share a common clock signal, which synchronises them. The transmitter, however, is not synchronised with the two receivers, which is how the system would be configured in real-life.

The results from section 6.4 look good, though not as accurate as section 6.3. This is, of course, due to the transmitter not being synchronised with the receivers. Despite the decrease in accuracy the system was still able to measure the various cables more accurately than the minimum predicted in Chapter 3. This proves that the strategy developed in Chapter 3 is effective.

## 6.6 Evaluation of Project Success

There are a number of parameters that can be considered when evaluating the success of this project, most of them are summarised in Table 6.8. The most important measurable parameter is the degree of accuracy that was achieved. Chapter 3 predicted that the maximum error should be  $\pm 12.5$  m (in free space). This error was determined by the maximum frequency at which the microprocessor can execute single instructions (increasing this maximum frequency will reduce the predicted error). This level of accuracy was not only achieved by the measurements in Chapter 6, but remarkably improved in some cases. This proves that the radiolocation strategy developed during this project is effective.

The next two important factors that must also be evaluated are cost-effectiveness and device dimensions. Chapter 1 stated that any tags placed on targets must be cost-effective and inconspicuous. The transmitter circuit should be able to fit on a substrate the size of a credit card. These two goals were achieved by using an MLSR method to generate the PN Code. MLSR configurations use only a small number of low-cost components to produce a suitable PN Code, thus satisfying the need for small dimensions and a low-cost device.

---

<sup>2</sup> This is for the device that was implemented in this project. A chipping rate of 1 MHz for the PN Code signal and a clock frequency of 48 MHz for the microprocessor were used, which is equivalent to a resolution of 25 m ( $\pm 12.5$  m). Increasing the values of these parameters will increase the accuracy of the system.

<b>Goal</b>	<b>Successful</b>	<b>Remarks</b>
Effective Strategy Developed	Yes	All the measurements from Chapter 6 prove that the strategy developed in this project is effective.
Predicted Accuracy Achieved	Yes	Measurements from the third and fourth experiment in Chapter 6 exceeded predicted accuracy.
Inconspicuous Transmitter	Yes	Only a small number of components are needed.
Cost-Effective Transmitter	Yes	Components are low-cost.
Extendable to Multiple Users	Yes	Chapter 4 showed that Gold Codes can be used to extend the design to multiple users.

**Table 6.8**

Another requirement that had to be satisfied was extendibility to multiple users. CDMA provides a technique for accommodating multiple users sharing a single spectral band. Separation of individual tags is accomplished by assigning orthogonal PN Codes to all the users. These orthogonal codes can be generated by using Gold Code techniques, which are very similar to the MLSR methods used in this project.

All the major goals and requirements that were laid out in Chapter 1 have been achieved.



# Chapter 7

---

## Conclusion and Recommendations

### 7.1 Conclusion

This thesis identified a potential need for a localised position location system, expanded that idea into a formal problem statement and composed a list of goals, requirements and restrictions. A solution strategy was developed, implemented and measured. The measured results agree with the theoretical predictions; in some cases the physical measurements even outperformed simulated results. This confirms that the simulation models are valid. The Position Location Strategy that was developed during this project can be effective for localised position location purposes.

### 7.2 Recommendations and Further Study

There are few critical components that play a major role in the performance of the system as a whole. Improving these components can improve the performance of the entire system:

- **Microprocessor Clock Frequency:** This is the biggest factor limiting system accuracy for the current implementation. The shortest period of time that the receiver PN Code can be delayed by the Delay Control Mechanism determines the best resolution that can be achieved without employing additional post-processing of measured data. Replacing the current microprocessor with a faster equivalent should improve the accuracy of the system. However, processor clock frequency can only be increased up to a point before system noise will start to limit accuracy.
- **Detector Bandpass Filter:** The bandwidth of this filter determines how much energy is passed to the detector. As long as the bandwidth is large enough to pass the recovered carrier (after multiplication with a properly aligned PN Code) signal the filter should be kept as narrow as possible. By reducing the bandwidth of the filter, the amount of energy from noise and non-aligned PN Code signals that is presented to the Detector, is reduced. This increases the sharpness with which the Detector can distinguish between aligned and non-aligned PN Codes.
- **System Noise Figure:** Unnecessary System Noise reduces the clarity with which the Detector can distinguish between aligned and non-aligned PN Codes. The amount of noise that the Detector can handle will depend on the Bandpass Filter's bandwidth and signal strength.

- **Baseband PN Code Chipping Rate:** This parameter does not influence the accuracy of the system directly, but it does influence the maximum useful clock frequency that can be used to drive the microprocessor.

There are also a number of aspects that fell outside the scope of this project that merit further study:

- **Multipath:** Multipath can have a severely detrimental affect on radio transmission systems. Spread Spectrum Modulation exhibits some resistance to the effects of multipath, due to the increased bandwidth of SS signals. Investigation into the effects of multipath on this system, as well as the relationship between PN Code Chipping Rate (signal bandwidth) and resistance to multipath could be useful.
- **Multiple Simultaneous PN Code Transmissions:** This could provide additional improvements in terms of multipath resistance and system accuracy by transmitting several PN Code signals simultaneously (each PN Code with its own carrier signal).
- **Doppler Effects (for tracking of moving targets):** It was one of the assumptions made in Chapter 1 that the targets would be stationary or slow-moving, thus eliminating the need to take Doppler effects into consideration. The current system design could be extended to deal with Doppler effects, thus allowing for the location and tracking of moving targets as well.

# Appendix A

---

## Additional ADF7011 Information

The ADF7011 combines a lot of functionality into one package. Building the oscillator module required the VCO, Fractional-N PLL, reference clock and the feedback mechanism that controls the VCO and therefore the output signal. Other features that were useful included the adjustability of the output frequency (within limits) and the programmable amplifiers that control output power.

Reconfiguring the transmitter to function as a Local Oscillator is quite simple. All that is needed is to implement the device as directed and then use it to transmit only one bit continuously. Although Chapter 5 described the design of the LO, it omitted several details that were not important enough to mention in the main text. The following sections will discuss some of the smaller details regarding the implementation of the ADF7011 IC.

### A.1 Power Supply and Microprocessor

The ADF7011 requires a +3 V supply voltage (capable of delivering about 30 mA), whereas the rest of the receiver needs  $\pm 5$  V. It will therefore be necessary to add a separate regulator circuit to the Oscillator section of the receiver. This can easily be achieved by using the LM1086 voltage regulator.

The Microprocessor presents a similar problem, since it too operates at 5 V levels, whereas the ADF7011 requires 3 V levels. This can be solved by adding a voltage divider circuit between the output pins of the Microprocessor and the input pins of the ADF7011, thus allowing the use of the receiver's Microprocessor unit. Figure A.1 illustrates this:

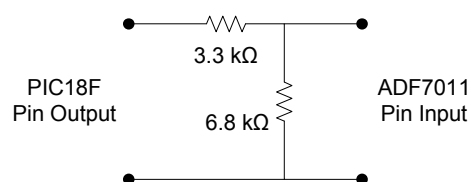


Figure A.1

## A.2 Crystal Resonator

All components necessary for the reference clock section of the ADF7011 are already included in the package, except for the resonator and the parallel capacitors. An inexpensive quartz crystal can be used to complete the oscillator. The values for the parallel resonant capacitors depend on the load capacitance of the quartz crystal.

Frequency tolerance and stability should be kept as tight as possible. An important property to consider is the range of acceptable frequencies. The ADF7011 requires a crystal with a fundamental oscillation frequency between 3.4 MHz and 22.1184 MHz. This led to the selection of the 11.0592 MHz XTAL003517 quartz crystal manufactured by IDQ. It has a frequency tolerance of  $\pm 20$  ppm, frequency stability of  $\pm 30$  ppm and a load capacitance of 30 pF. The crystal resonator circuit is shown in Figure A.2.

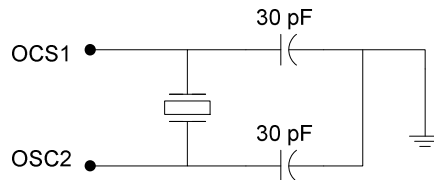


Figure A.2

## A.3 Loop Filter

A Loop Filter is needed to integrate the signal from the charge pump into a voltage that can be used to control the VCO. Two counters are used to keep track of the VCO output signal and the reference signal. An R Counter divides the reference signal by a ratio of R and forms one of the inputs to the Phase/Frequency Detector. The N Counter does the same for the VCO output signal and forms the second input to the Phase/Frequency Detector. The PFD then produces a signal, using the charge pump, which is proportional to the difference in phase and frequency between its two inputs. Figure A.3 illustrates this.

The circuit shown in Figure A.4 is recommended by the datasheet. This is a third order integrator. The most important property of the Loop Filter, from a general transmitter point of view, is its bandwidth. The Loop Filter bandwidth determines the amount of time needed for the VCO to attain lock, but the Loop Filter is also responsible for attenuating spurious levels generated by the PLL. This will have different impacts on the various modulation schemes.

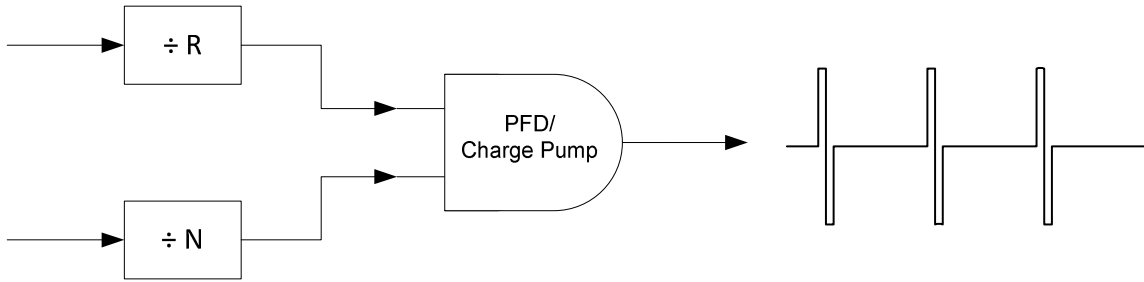


Figure A.3

Since this application was not concerned with any of the modulation schemes, a less careful design was sufficient. There is no need to jump quickly between power levels or different frequencies, which leaves spurious levels as the only concern. A narrower Loop Filter bandwidth was therefore selected. Specific component values were generated using the free design tool supplied by Analog Devices, ADIsimSRD Studio Ver 1.1.

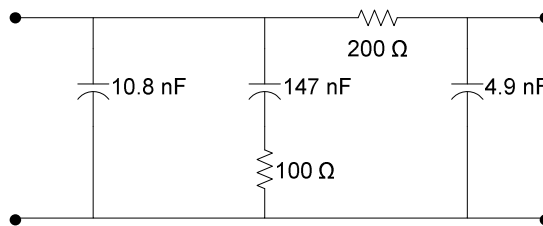


Figure A.4

#### A.4 Matching Circuit

This circuit is needed to improve the impedance characteristics of the RF output stage. The RF output must be tied to the voltage supply via an inductor, which influences the impedance as seen by the next stage. In some applications it might also be necessary to include a filter section to comply with government regulations regarding out-of-band power. The filter section and matching circuit can be designed separately, or they can be combined into one circuit.

For this particular application there were no government regulations to comply with at this point, since this IC will not be used to transmit anything. Only the minimum matching circuitry that was recommended by the datasheet was used, as shown in Figure A.5.

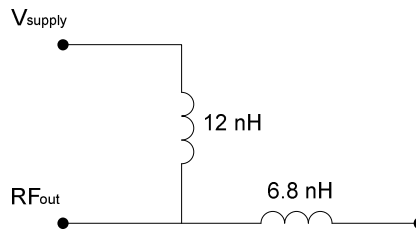


Figure A.5

## A.5 Additional Components

The last few components needed to complete all the extra circuitry for the ADF7011 is two capacitors and one resistor. All three components are prescribed by the datasheet. A  $0.22 \mu\text{F}$  capacitor should be tied between the pins  $C_{\text{VCO}}$  and  $C_{\text{REG}}$  to reduce noise on the VCO's bias lines. A  $2.2 \mu\text{F}$  capacitor should be tied between the  $C_{\text{REG}}$  pin and GND (ground). This capacitor reduces regulator noise and improves stability. Lastly a resistor must be tied between pin  $R_{\text{SET}}$  and GND to set the Charge Pump current and some of the internal bias currents. The default recommended value of  $4.7 \text{ k}\Omega$  was used.

## A.6 Register Setup

The next part that must be looked at is how to set up the various registers to produce the desired signal. There are four registers to consider:

1. The RF R Register, which controls the reference clock.
2. The RF N Register, which controls the Fractional-N PLL.
3. The Modulation Register, which selects the modulation scheme.
4. The Function Register, which enables various additional functions.

Access to these registers is via three pins on the ADF7011, the DATA (Serial Data Input) pin, the CLK (Serial Clock Input) pin and the LE (Load Enable) pin. These pins (along with the TxDATA or Transmit Data pin) are connected to the Microprocessor through voltage dividers described previously. Data is loaded into a shift register one bit at a time by presenting each bit to the DATA pin and then changing the CLK pin level from a logic low to a logic high. The most significant bit must be loaded first. Once all the bits have been loaded into the shift register a logic high is asserted on the LE pin to load all the bits into one of the registers. Two control bits are used to select the appropriate register.

Each of the four registers (and what their contents should be) will now be looked at in more detail.

Reserved		CLK <sub>OUT</sub>					XOD	4-Bit R-Value				11-Bit Frequency Error Correction										Control Bits	
DB23	DB22	DB21	DB20	DB19	DB18	DB17	DB16	DB15	DB14	DB13	DB12	DB11	DB10	DB9	DB8	DB7	DB6	DB5	DB4	DB3	DB2	DB1	DB0
0	0	0	0	0	0	0	0	0	1	1	0	0	0	0	0	0	0	0	0	0	0	0	0

**Table A.1**

Table A.1 shows the mapping of the R Register's bits. Most of these bits were left unchanged. Bits DB22 and DB23 are reserved and remained 00. The CLK<sub>OUT</sub> bits DB18 to DB21 were also left as 0000, since that output was not used. The XOD bit was set to 0, which enables the crystal oscillator. Bits DB13 to DB16 form the 4 bit R divide ratio, which was set to 0011, a ratio of 3. Next is the Frequency Error Correction Offset, bits DB2 to DB12, which was left as 00000000000. The Control Bits select the register to which this data is latched; in this case it was 00 which corresponds to the R Register.

LDP	VCO Band	8-Bit Integer-N								12-Bit Fractional-N										Control Bits			
DB23	DB22	DB21	DB20	DB19	DB18	DB17	DB16	DB15	DB14	DB13	DB12	DB11	DB10	DB9	DB8	DB7	DB6	DB5	DB4	DB3	DB2	DB1	DB0
1	1	0	1	1	1	0	1	0	1	0	1	1	1	0	0	0	0	1	1	1	0	0	1

**Table A.2**

Table A.2 shows the mapping of the N Register's bits. The first bit, DB23, remained 1. Bit DB22, which selects the frequency band for the VCO, was set to 1, which is the 433 MHz to 435 MHz band. All the rest of the bits, except for the last two (the Control Bits, 01 to select N Register), are used to control the output frequency. Bits DB14 to DB21 set the integer part and bits DB2 to DB13 set the fractional part of the N Counter. The following formulas are used to determine the PLL's output frequency:

$$F_{OUT} = F_{PFD} \times \left[ Int + \frac{(8 \times Frac) + Error}{2^{15}} \right] \quad (A.1)$$

and

$$F_{PFD} = \frac{F_{CRYSTAL}}{R} \quad (A.2)$$

Where Int and Frac are the integer and fractional values set in the N Register; Error is the Frequency Error Correction value set in the R Register;  $F_{CRYSTAL}$  is the resonant frequency of the quartz crystal and R is the divide ration set in the R Register. This gives an output frequency of 432.934 MHz.

Pre-scaler	Index Counter			GFSK Mod Control			Modulation Deviation						Power Amplifier						Mod Scheme		Control Bits			
	DB23	DB22	DB21	DB20	DB19	DB18	DB17	DB16	DB15	DB14	DB13	DB12	DB11	DB10	DB9	DB8	DB7	DB6	DB5	DB4	DB3	DB2	DB1	DB0
0	0	0	0	0	0	0	0	0	0	0	0	0	0	0	1	0	1	0	1	1	0	0	1	0

Table A.3

Table A.3 shows the mapping of the Modulation Register's bits. The first bit, DB23, selects the prescaler and was set to 0. The next two sections, Index Counter and GFSK Mod Control which comprise bits DB18 to DB22, remained 00 and 000 respectively. Modulation Deviation, bits DB11 to DB17, was set to 0000000. Bits DB4 to DB10 determine the output power and were set to 0101011. Bits DB2 and DB3 select the modulation scheme and were set to 00 for FSK. That leaves the Control Bits, which were set to 10 for loading to the Modulation Register.

Test Modes												MUXOUT				VCO Disable	Fast Lock		Charge Pump		Data Invert	CLK <sub>OUT</sub> Enable	PA Enable	PLL Enable	Control Bits	
DB23	DB22	DB21	DB20	DB19	DB18	DB17	DB16	DB15	DB14	DB13	DB12	DB11	DB10	DB9	DB8	DB7	DB6	DB5	DB4	DB3	DB2	DB1	DB0			
0	0	0	0	0	0	0	0	0	0	0	0	0	0	0	0	1	1	0	0	1	1	1	1			

Table A.4

Table A.4 shows the mapping of the Function Register's bits. The first two sections, Test Mode and Muxout (bits DB11 to DB23), remained unchanged as they were not used in this application. Next is VCO Disable, bit DB10, which was set to 0 for VCO ON. Bits DB8 and DB9 form the Fast Lock section and were left at default values. The Charge Pump section, along with the  $R_{SET}$  resistor that was chosen previously selects the maximum current of the Charge Pump. Bits DB6 and DB7 were set to 11 for a current of 2 mA. The next four bits DB2 to DB5 were set to 0011. That leaves the last two Control Bits, set to 11 for the Function Register.

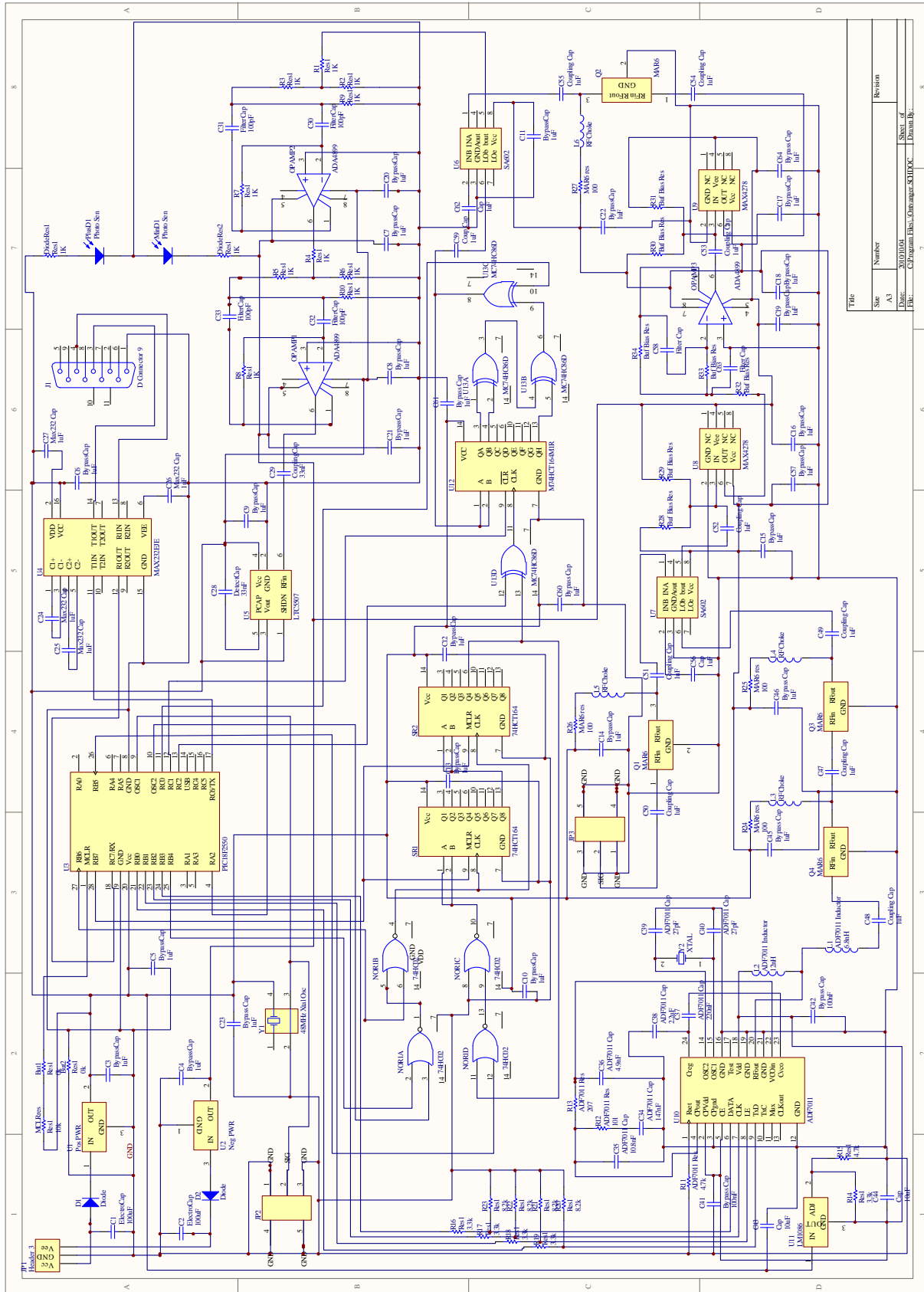


# Appendix B

---

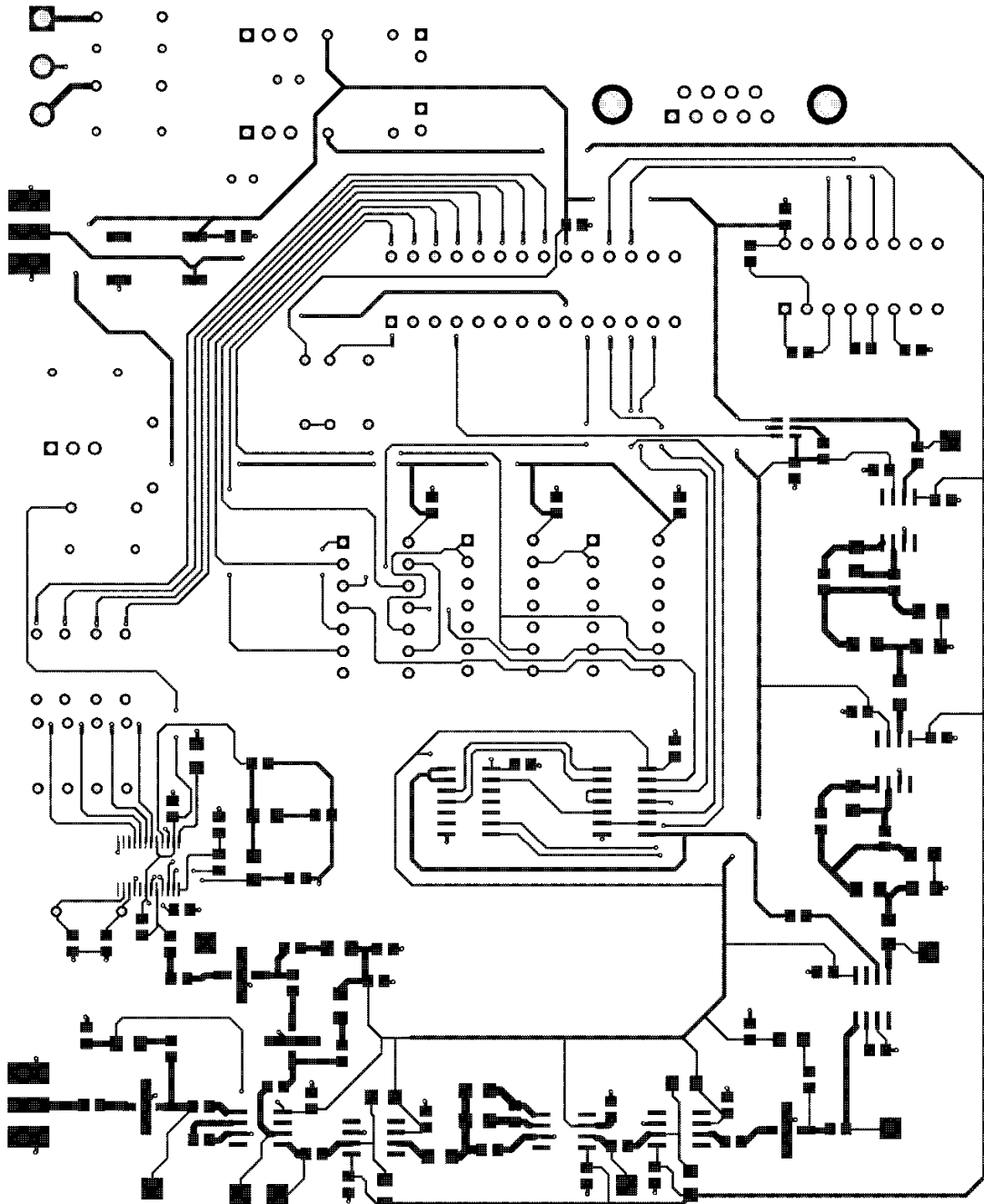
## Receiver Schematics and PCB Layout

### B.1 Receiver Schematics

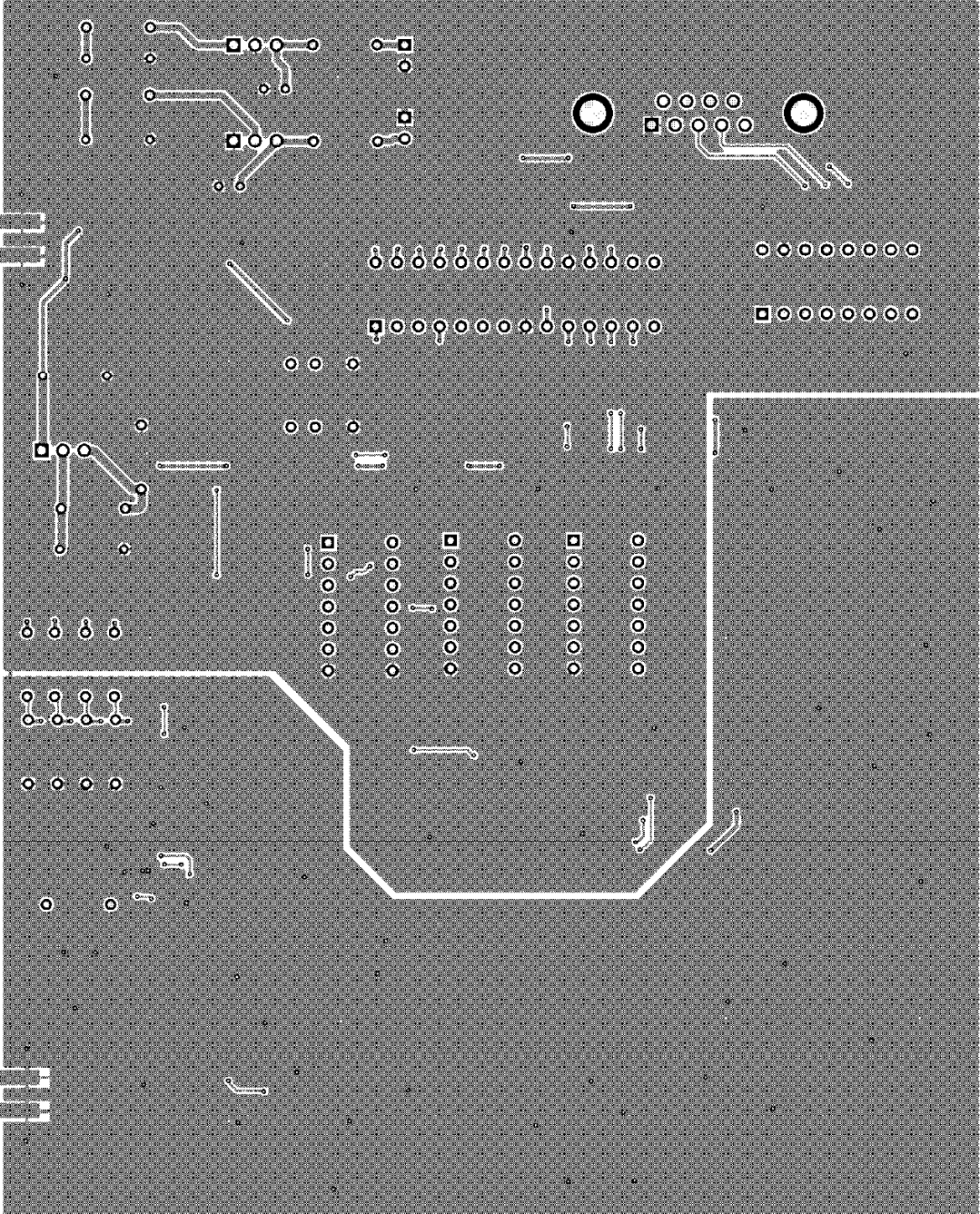


File	Size	Number	Revision
A3			
Date:	20201010		
File:	C:\Program Files\Autodesk\SolidWorks		
			Sheet of
			Drawn By:

## B.2 PCB Layout: Top Layer



**B.3 PCB Layout: Bottom Layer**



## Bibliography

- [1] Tom Logsdon, *Understanding the NAVSTAR GPS, GIS, and IVHS*, 2nd ed. New York, New York: Chapman & Hall, 1995.
- [2] Elliott D Kaplan and Christopher J Hegarty, Eds., *Understanding GPS: Principles and Applications*, 2nd ed. Boston: Artech House, 2006.
- [3] Creativerge, "Multilateration and ADS-B: Executive Reference Guide,".
- [4] Bradford W Parkinson and James J Spilker, Eds., *Global Positioning System: Theory and Applications*. Washington, DC: American Institute of Aeronautics and Astronautics, Inc., 1996, vol. I.
- [5] Andrew J Viterbi, *CDMA: Principles of Spread Spectrum Communication*. Reading, Massachusetts: Addison-Wesley Publishing Company, 1995.
- [6] Henrik Schulze and Christian Lüders, *Theory and Applications of OFDM and CDMA*. Chichester, West Sussex, England: John Wiley & Sons, Ltd, 2005.
- [7] David L Nicholson, *Spread Spectrum Signal Design: LPE & AJ Systems*. Rockville, Maryland: Computer Science Press, Inc., 1988.
- [8] Paul Andrew Goud, *A Spread Spectrum Radiolocation Technique and its application to Cellular Radio*. Calgary, Alberta: The University of Calgary, 1991.
- [9] Rodger E Ziemer and William H Tranter, *Principles of Communications: Systems, Modulation and Noise*, 5th ed. Hoboken, New Jersey, USA: John Wiley & Sons, Inc., 2002.
- [10] David M Pozar, *Microwave Engineering*, 3rd ed. Amherst, Massachusetts: John Wiley & Sons, Inc., 2005.
- [11] R. Gold, "Optimal Binary Sequences for Spread Spectrum Multiplexing," *IEEE Transactions on Information Theory*, pp. 619-621, October 1967.
- [12] Robert J Fontana and Steven J Gunderson, "Ultra-Wideband Precision Asset Location System," *IEEE Conference on Ultra-Wideband Systems and Technologies*, May 2002.
- [13] Solomon W Golomb, *Shift Register Sequences*. San Francisco: Holden-Day, Inc., 1967.
- [14] Constantine A Balanis, *Antenna Theory: Analysis and Design*, 3rd ed. Hoboken, New Jersey, USA: John Wiley & Sons, Inc., 2005.

[15] Michał Odyńiec, Ed., *RF and Microwave Oscillator Design*. Norwood, MA: Artech House, Inc., 2002.

[16] Ulrich L Rohde, *Digital PLL Frequency Synthesizers: Theory and Design*. Englewood Cliffs, New Jersey: Prentice-Hall, Inc., 1983.